Cellular mechanisms underlying

mast cell - memory T cell interactions in chronic

type IV allergic skin inflammation in mice

Inaugural-Dissertation

to obtain the academic degree

Doctor rerum naturalium (Dr. rer. nat.)

Submitted to the Department of Biology, Chemistry and Pharmacy

of Freie Universität Berlin

by

Vladimir Andrey Gimenéz Rivera

from Bogotá, D.C. (Colombia)

2014

I completed my doctoral studies from November 01, 2010 to November 11, 2014 under the supervision of Prof. Dr. M. Maurer at the Department of Dermatology and Allergy, Charité-Universitätsmedizin Berlin.

1st Reviewer: Prof. Dr. Rupert Mutzel

2nd Reviewer: Prof. Dr. Marcus Maurer

Date of defense: 10th of February 2015.

Acknowledgement

$$“E = mc^2”$$

Albert Einstein
(German-American. *physicist, 1921 Nobel prize for Physics, 1879 - 1955).*

Table of contents

1 Abstract

Allergic contact dermatitis (ACD) is a T cell-mediated chronic inflammatory skin condition. ACD is one of the most common occupational diseases worldwide and causes severe quality of life impairment. Mast cells (MCs) are key players in chronic inflammation and involved in the regulation of immune homeostasis and immunosurveillance in various tissues including the skin. As of now, the role of MCs in the chronification of ACD is poorly understood. To address this, we induced chronic contact hypersensitivity (CCHS) to oxazolone (OXA), a contact allergen, in mice as a model for human ACD. Using different murine models, we investigated the role of MCs in CCHS. Mice deficient for MCs or treated with the MC inhibitor cromolyn developed exacerbated CCHS reactions and the reconstitution of MCs in MC-deficient mice prevented this. This exacerbation of inflammation and the protective effects of MCs in CCHS were both restricted to skin sites that had previously been exposed to the allergen, suggesting that MCs control CCHS inflammatory reactions by effects in local skin T cell populations. In support of this, skin areas pre-exposed to allergen showed more tissue resident memory (TRM) CD8β^+ T cells in MC-deficient mice. These T cells were found to produce the cytokine interferon gamma (IFNγ), and this pro-inflammatory cytokine was increased in the inflamed skin during CCHS responses in MC-deficient mice. The reduction of TRM CD8β^+ T cells in MC-deficient mice prevented the exacerbation of inflammatory CCHS responses.

In conclusion, these findings demonstrate that MCs protect from exacerbated inflammatory responses in CCHS by controlling the accumulation of local cutaneous TRM CD8β^+ T cell populations.

2 Zusammenfassung

Die allergische Kontaktdermatitis (*allergic contact dermatitis* (ACD)) ist eine chronische Hauterkrankung, die auf Reaktionen gegen Kontaktallergene in sensibilisierten Patienten besteht. Sie ist eine der häufigsten berufsbedingten Krankheiten weltweit und führt zu schwerer Beeinträchtigung der Lebensqualität. Mastzellen (MZ) spielen eine zentrale Rolle bei andauernden Entzündungen und sind an der Regulation des immunologischen Gleichgewichts und an der Immunkontrolle in verschiedenen Geweben, einschließlich der Haut, beteiligt. Dennoch ist die Funktion von MZ in der Entwicklung der ACD kaum verstanden.

Um dies zu untersuchen, haben wir als Model für humane ACD in Mäusen wiederholt Kontakthypersensitivitätsreaktionen (*chronic contact hypersensitivity* (CCHS)) gegenüber Oxazolon, einem Kontaktallergen, ausgelöst. Unter Verwendung verschiedener Mausmodelle wurde die Beteiligung von MZ bei der CCHS untersucht. Mäuse ohne MZ, sowie Mäuse, die mit dem Mastzell-Blocker cromolyn behandelt wurden, entwickelten eine deutlich stärkere CCHS Reaktion. Das Wiedereinsetzen von MZ in MZ-defizienten Mäusen beugte der Entwicklung stärkerer CCHS-Antworten vor. Der schützende Effekt von MZ war auf Hautstellen beschränkt, die vorher dem Allergen ausgesetzt waren. So vermuteten wir, dass MZ CCHS-assoziierte Entzündungsreaktionen durch Effekte auf das lokale Immunsystem der betroffenen Hautpartien kontrollieren und dass die MZ-bedingten Veränderungen für die Schwere der Entzündungen in CCHS-Antworten verantwortlich sind. Wir fanden heraus, dass CCHS-Hautareale eine erhöhte Anzahl an Hautgedächtnis- (tissue resident memory (TRM)) CD8β$^+$ T-Lymphozyten aufweisen. Diese TRM CD8β$^+$ T-Zellen produzierten Interferon-gamma (IFNɣ), ein pro-entzündliches Zytokin und Mäuse ohne MZ zeigten während CCHS Reaktionen eine vermehrte IFNɣ-Produktion. Die Reduktion von Haut-TRM CD8β$^+$ T-Zellen mittels depletierender Antikörperbehandlung führte zu einer Normalisierung der entzündlichen CCHS Reaktionen in MZ-defizienten Mäusen. MZ schützen also vor überschießenden inflammatorischen CCHS-Reaktionen, indem sie die Anzahl von Haut-TRM CD8β$^+$ T-Zellen in Hautarealen reduzieren, welche zuvor mit dem Allergen in Kontakt gekommen sind.

Zusammenfassend zeigen diese Ergebnisse, dass MZ durch die Kontrolle der Haut-TRM CD8β$^+$ T-Zellen in Hautregionen, die dem Kontaktallergen ausgesetzt waren, vor schweren entzündlichen CCHS Reaktionen schützen.
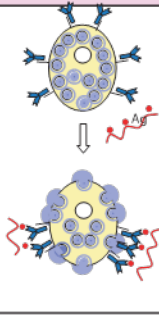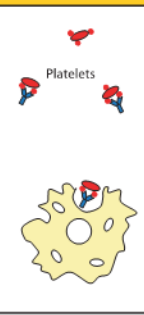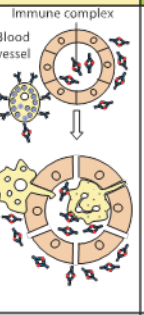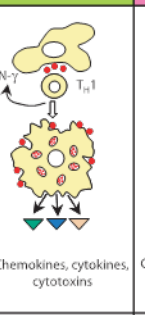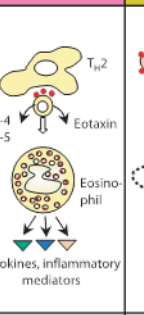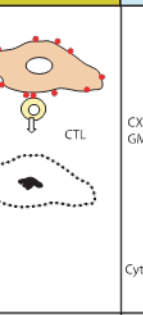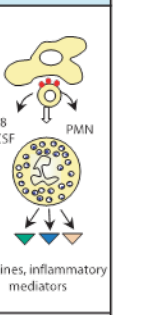
3 Introduction

3.1 Allergic contact dermatitis and chronic contact hypersensitivity

3.1.1 Pathogenesis

Allergic contact dermatitis (ACD) is a chronic inflammatory skin disease caused by repeated exposure to contact allergens. The clinical picture of ACD is characterized by eczematous lesions appearing after cutaneous exposure to a contact allergen in individuals sensitized to this allergen. Common contact allergens are drug derivatives, transition metals and fragrances (Martin, 2012, Jack *et al.*, 2013). ACD lesions typically appear between 24 to 72 hours after allergen contact. In the early stages of ACD, the skin shows redness, papules and vesicles. In contrast, late lesions are characterized by skin peeling, scaling and thickening with appearance of linear fissures (Skotnicki-Grant, 2008). It is estimated that ACD represents about 20% of occupational skin disorders. It often starts at a young age with a prevalence of 15% in 12 to 16 year old individuals (Peiser *et al.*, 2012). The treatment of ACD is the avoidance of relevant allergens and the use of topical steroids and immunosuppressive drugs, e.g. calcineurin inhibitors (Alase and Wittmann, 2012). However, the difficulties in avoiding widespread allergens, e.g. Nickel, and the low efficacy and side effects from long-term use of pharmacological treatments, call for the development of new therapeutic strategies.

Immunologically, ACD is a type IV hypersensitivity according to the classification of Gell and Coombs (Texbook of immnunology, 1963). Type IV hypersensitivities are characterized by a delayed inflammatory onset and by a dependence on T cells. This is in contrast to type I hypersensitivity, which is an immediate inflammatory allergic response mediated by humoral immunity, i.e. IgE antibodies (Fig. 1), (Mal'tsev *et al.*, 2012).

	Type I	Type II	Type III	Type IVa	Type IVb	Type IVc	Type IVd
Immune reactant	IgE	IgG	IgG	IIFN-γ, TNF-α (T_H1 cells)	IL-5, IL-4/IL-13 (T_H2 cells)	Perforin/ granzyme B (CTL)	CXCL8, GM-CSF (T cells)
Antigen	Soluble antigen	Cell- or matrix-associated antigen	Soluble antigen	Antigen presented by cells or direct T-cell stimulation	Antigen presented by cells or direct T-cell stimulation	Cell-associated antigen or direct T-cell stimulation	Soluble antigen presented by cells or direct T-cell stimulation
Effector	Mast cell activation	FcR+ cells (phagocytes, NK cells)	FcR+ cells Complement	Macrophage activation	Eosinophils	T cells	Neutrophils
Example of hypersensitivity reaction	Allergic rhinitis, asthma, systemic anaphylaxis	Hemolytic anemia, thrombocytopenia (e.g., penicillin)	Serum sickness, Arthus reaction	Tuberculin reaction, contact dermatitis (with IVc)	Chronic asthma, chronic allergic rhinitis Maculopapular exanthema with eosinophilia	Contact dermatitis Maculopapular and bullous exanthema Hepatitis	AGEP Behçet's disease

Figure 1. Classification of hypersensitivity reactions. Cellular and soluble immune components implicated in hypersensitivity responses. _Abbreviations_: IgE - Immunoglobulin E, IgG - Immunoglobulin G; IL- Interleukin, IFNγ - Interferon-gamma, TNFα - tumor necrosis factor-alpha, NK - natural killer, T_H1 - T helper 1, T_H2 - T helper 2, CTL - cytotoxic T lymphocytes, CXCL8 - CXC ligand 8, GM-CSF - Granulocyte-macrophage colony-stimulating factor, AGEP - Acute generalised exanthematous pustulosis (Modified from Pichler 2013).

Since ACD is a T cell-mediated response, the lesional skin of ACD patients contains infiltrating T cells that produce pro-inflammatory mediators (Yawalkar _et al._, 2001, Bangert _et al._, 2003, Dyring-Andersen _et al.,_ 2013). The sensitizing effect of all contact allergens, _also called_ haptens, depends on their capacity to bind autologous proteins within the tissue. Hapten-protein binding interactions lead to changes in the structure of the targeted protein, which allows the immune system to recognize the hapten-protein complexes as foreign antigens. In order to generate hapten-specific T cells, the antigen presenting cells (APC) migrate to the draining lymph nodes (dLNs) and present the modified protein to naive T cells. Thus, the development of ACD requires a previous sensitization step before the appearance of clinical symptoms upon reexposure. Sensitization results in the generation of T cells that respond

specifically to the relevant hapten-protein complex. This feature distinguishes ACD from irritant contact dermatitis, which does not require sensitization to induce cutaneous eczematous lesions (Skotnicki-Grant, 2008).

The physicochemical properties of contact allergens/haptens usually do not allow an efficient antibody response, but antibodies against haptens can be found in some ACD patients (Thierse *et al.*, 2005, Seier *et al.*, 2010). Generally, responses to contact allergens require direct and specific T cell recognition (Moed *et al.*, 2005).

Haptens can be divided into three categories (Fig. 1): 1) Derived from pro-haptens, i.e. substances that become immunogenic only after they are metabolized, e.g. urushiol, the allergenic essence of the North American poison ivy. 2) Transition metals such as chromium, beryllium or nickel. These haptens are able to form non-covalent bonds with proteins (Thierse *et al.*, 2005). 3) Low molecular chemicals such as oxazolone and other experimental haptens, which covalently bind to proteins (Thierse *et al.*, 2005, Martin and Jakob, 2008). The percutaneous penetration of haptens is facilitated by their low molecular weight, which is a common trait of contact allergens (Nosbaum *et al.*, 2009).

3.1.2 Contact hypersensitivity (CHS)

Contact hypersensitivity (CHS) is defined as a type IV hypersensitivity reaction elicited by a topical application of experimental haptens, e.g. DNFB, TNCB, oxazolone or FITC, in sensitized animals (Honda *et al.*, 2013). CHS is commonly used as a model to investigate the immunologic mechanisms of ACD (Friedmann and Pickard, 2014). The use of CHS as a model in mice has made it possible to identify three distinct phases, i.e. sensitization, elicitation and resolution.

3.1.2.1 The sensitization phase of CHS

During the sensitization phase of CHS, when the mice are exposed for the first time to the hapten, the contact allergen penetrates the skin and forms complexes with proteins in the extracellular matrix. These hapten-protein complexes are recognized by dendritic cells (DCs) and processed for antigen presentation. DCs migrate to the dLNs and present the hapten-protein complexes to naive T cells (Fig. 2), (Honda *et al.*, 2013). This process induces hapten-specific T cells to proliferate and then

6

migrate to peripheral organs such as the blood and the spleen (Saint-Mezard *et al.*, 2004).

One of the primary events during the sensitization phase is the activation and chemical destruction of keratinocytes inflicted, for example, by the acidic properties of some haptens (Fig. 2, step 1). As a consequence, keratinocytes release pro-inflammatory mediators including tumor necrosis factor α (TNFα), IL-1β and prostaglandin E2 (Cumberbatch and Kimber, 1995, Cumberbatch *et al.*, 1997, Kabashima *et al.*, 2003).

In addition, activated keratinocytes also release danger signals such as Reactive-Oxigen-Species (ROS) that subsequently induce the degradation of hyaluronic acid and other components of the extracellular matrix. The degradation products of these components bind to Toll-like receptor 4 (TLR-4) present on DCs, mast cells (MCs) and other cells, which induces the activation of these cells (Martin and Jakob, 2008). Inhibition of the degradation of hyaluronic acid impairs the sensitization process (Fig. 2, step 2), (Honda *et al.*, 2013).

The activation of the TLR2/4 pathway as well as the inflammasome pathway plays a central role in the activation, migration and maturation of DCs during the sensitization phase of CHS (Arthur *et al.*, 2010, Kimber *et al.*, 2012, Peiser *et al.*, 2012). Several subtypes of DCs are present in the skin. They can be divided into Langerhans cells (LCs) and dermal dendritic cells (dDCs). Within dDCs there are functional differences found between CD207^{+} and CD207^{-} cells. CD207^{+} dDCs are thought to be the main subtype responsible for sensitization after hapten contact (Fig. 2, step 3), (Kissenpfennig *et al.*, 2005, Bursch *et al.*, 2007, Xu *et al.*, 2008). However, LCs can compensate for this in the absence of CD207^{+} dDCs (Honda *et al.*, 2010b, Noordegraaf *et al.*, 2010). In contrast, some authors have suggested that LCs have a immunosuppressive effect in CHS by producing IL-10 during the sensitization phase (Igyarto *et al.*, 2009).
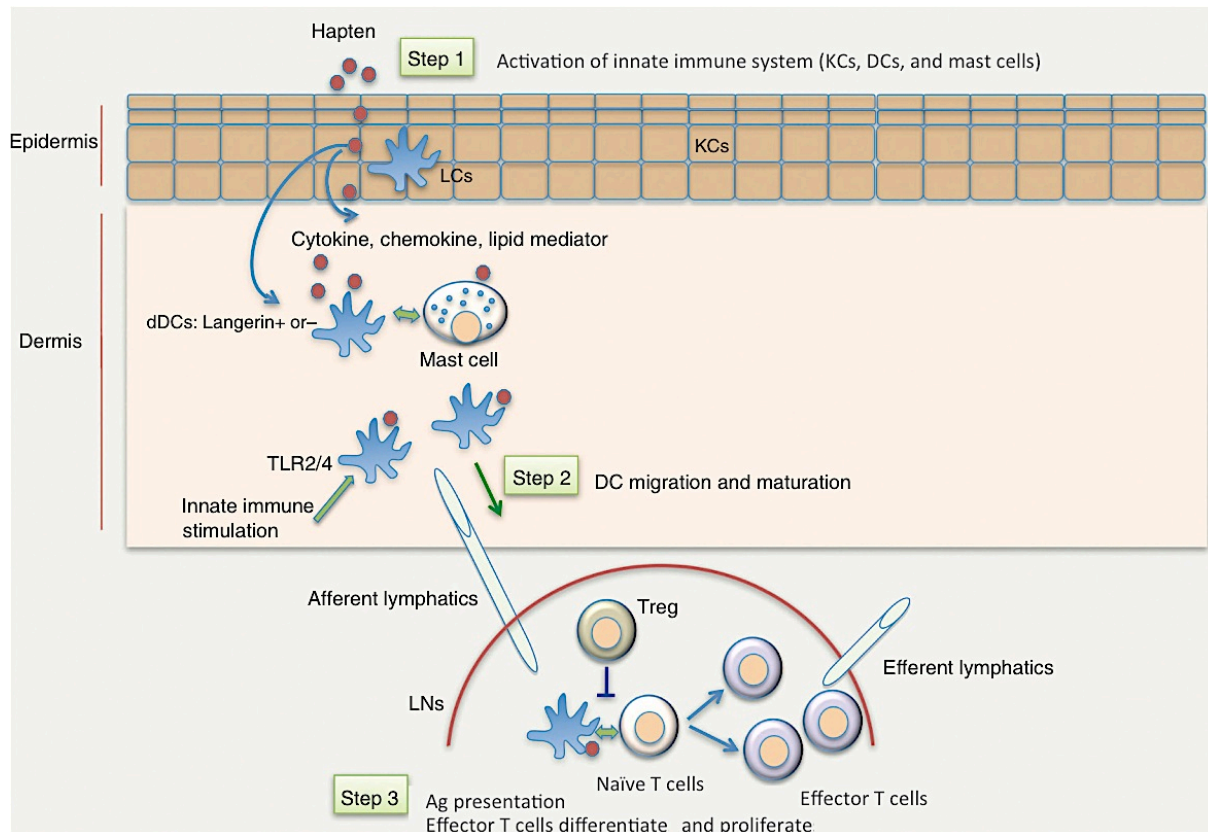
Figure 2. The sensitization phase of CHS. Immunologic steps during the sensitization phase of CHS. The hapten penetrates the skin barrier and forms complexes with autologous proteins. The contact with the hapten activates the innate immune system, e.g. KCs, MCs and DC (1). Activated DC maturate and migrate towards dLN carrying the protein-hapten complexes (2). T cells that specifically recognize the hapten-protein complexes presented by DC, differentiate to effector T cells followed by its clonal expansion (3). _Abbreviations_: dDC - dermal DC, dLN - draining lymph nodes, LC - Langerhans cell, LN - lymph node, Tc - T cytotoxic, Th - T helper, Treg - regulatory T cell, KCs – keratinocytes (Modified from Honda _et_ al. 2013).

3.1.2.2 The elicitation phase of CHS

As early as five to seven days after sensitization, a secondary contact to the hapten results in the elicitation of skin inflammatory reactions. The elicitation phase of CHS is characterized by extensive crosstalk between cells of the innate and adaptive immune system of the skin, which is responsible for the cutaneous inflammatory responses to the allergen. The tissue damage induced by the hapten triggers the release of local danger signals, which attracts innate immune cells, e.g. leukocytes (He _et al._, 2009). Hapten-specific T cells migrate to the allergen challenged skin sites, because of chemotactic signals provided by tissue cells and innate immune cells. This is crucial for CHS inflammatory responses, as only sensitized animals with

allergen specific T cells, but not non-sensitized animals show CHS inflammatory responses (Akiba *et al.*, 2004). This demonstrates the importance of T lymphocytes during the elicitation phase (Fig. 3. Step 1), (Wang *et al.*, 2000). The time required for the migration of effector T cells and the production of pro-inflammatory molecules by these hapten-specific T cells is responsible for the delayed onset of inflammation at up to 24 hours after the contact to the hapten, a common feature of contact hypersensitivity reactions (Fig. 3. Step 2). The inflammation can persists 24 to 72 hours and decreases gradually over the next 5-10 days. The time of recovery depends on the dose and the experimental model (Bacci *et al.*, 1997).

The relevance of alpha-beta T cells, i.e. CD4$^+$ and CD8$^+$ T cells, in the context of CHS responses was demonstrated by experiments with mice lacking either one or both alpha-beta T cell populations. In the absence of alpha-beta T cells, mice did not show inflammation during the elicitation phase of CHS (Wang *et al.*, 2000).

The injection of antibodies that deplete either CD8 or CD4 positive cells in WT mice, demonstrated different roles of these T cell populations. CD8$^+$ T cells play a pro-inflammatory role in CHS, whereas a sub-population of CD4$^+$ T cells, the CD4$^+$ T helper 2 (Th2) cells contribute to down regulate CHS inflammatory responses. These findings were verified in T cell-deficient mice reconstituted with either CD8$^+$ or CD4$^+$ T cells (Gocinski and Tigelaar, 1990, Bour *et al.*, 1995).

However, Wang an coworkers in 2000 showed that the pro-inflammatory role of CD8$^+$ T cells, in animals lacking these cells, can be assumed by a sub-population of pro-inflammatory CD4$^+$ T cells, i.e. the CD4$^+$ T helper 1 (Th1) cells, which revealed cellular compensatory mechanisms in the alpha-beta T cell compartment in CHS reactions (Fig. 3, step 1). Additionally, Bacci and coworkers in 1997 demonstrated that CD4$^+$ T cells collaborate with CD8$^+$ T cells during the effector phase of CHS in order to mount normal inflammatory responses.

Invariant natural-killer T (iNKT) cells, in particular IL-4-derived iNKT cells, control the CD8$^+$ T cell population by reducing the production of IFNɣ in the dLNs during the sensitization and elicitation phase of CHS (Goubier *et al.*, 2013). Gamma-delta T cells were reported to assist alpha-beta T cells in the elicitation of CHS to the hapten paraphenylene-diamine (Yokozeki *et al.*, 2001).

Among T cell-derived products, both type 1 and type 2 cytokines can be found in challenged areas. CD8^{+} T cells produce IFNɣ, whereas IL-4 and IL-10 are produced by CD4^{+} T cells (Fig. 3, step 2), (Xu *et al.*, 1996). Depending on the immunogen the inflammation can be driven by IFNɣ or IL-4 (Grabbe and Schwarz, 1996). A subpopulation of IL-17 expressing CD4^{+} T cells also appears to be important for the induction of CHS. Animals that lack IL-17 expression display a reduced inflammatory outcome and reconstitution of these animals with IL-17^{+}CD4^{+} T cells restores normal CHS responses (Peiser, 2013).
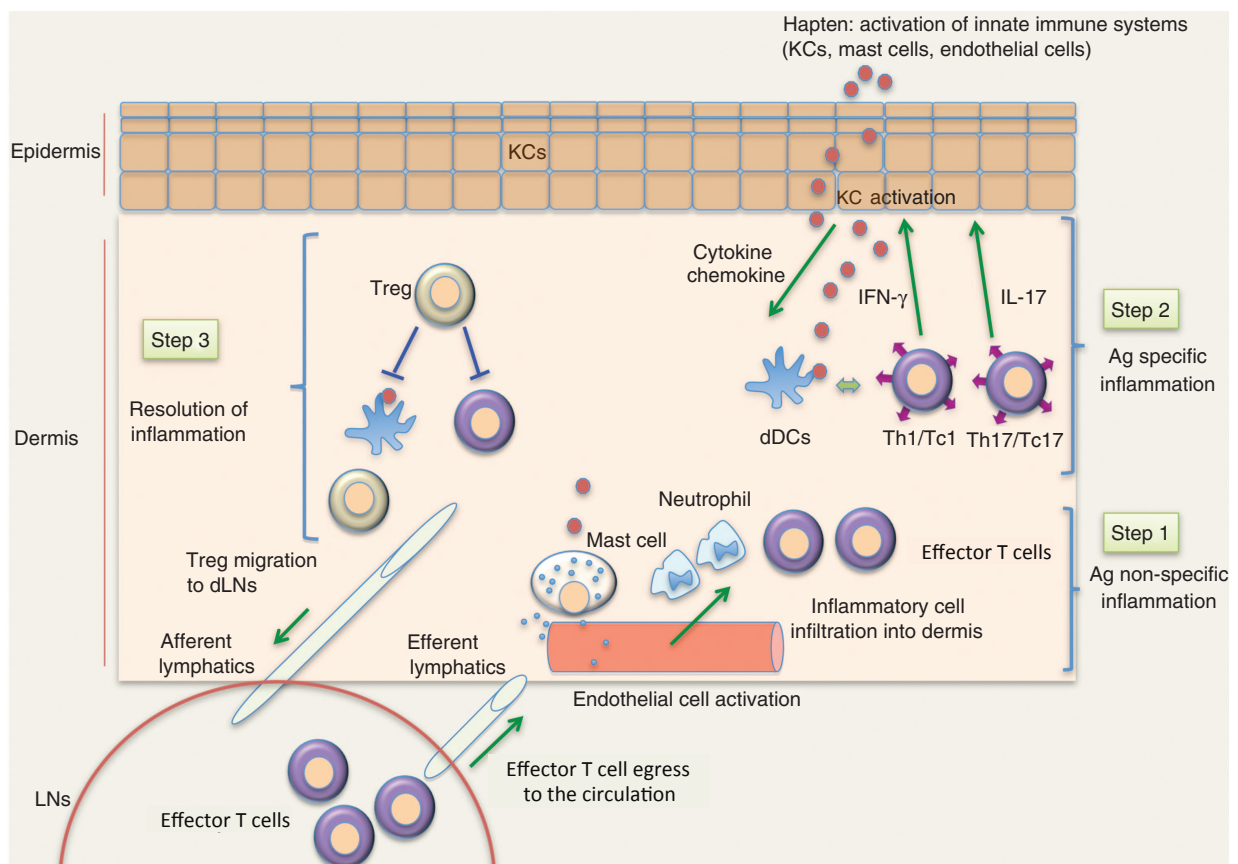
Figure 3. The elicitation and resolution phases of CHS. Immunologic steps during the elicitation phase and the resolution phase of CHS. The hapten penetrates the skin barrier and forms complexes with autologous proteins (1). The contact with the hapten activates the innate immune system, which attracts neutrophils and T cells. The combination of pro-inflammatory mediators released by hapten-specific effector T cells and by innate immune cells, e.g. dDCs, result in signs and symptoms of CHS inflammation (2). T regulatory cells migrate to the site of inflammation and constrain the pro-inflammatory activity of hapten-specific effector T cells and innate immune cells. This results in the resolution of inflammation (3). *Abbreviations*: Ag – antigen, dDC - dermal DC, dLNs - draining lymph nodes, LC - Langerhans cell, LN - lymph node, Tc - T cytotoxic, Th - T helper, Treg - regulatory T cell, KCs - keratinocytes (Modified from Honda *et* al. 2013).

During the elicitation phase of CHS the infiltration of the allergen-challenged tissue by hapten-specific T cells is crucial. Animals sensitized with a given hapten do not cross-react, when challenged with an unrelated hapten (Baker *et al.*, 1991, Asherson and Dieli, 1992, Okazaki *et al.*, 2002). The recruitment of hapten-specific T cells to the area of allergen challenge requires previous steps, i.e. inflammasome activation, activation of TLR4 expressing cells, DC migration towards dLNs (Honda *et al.*, 2013) and recruitment of neutrophils to the site of allergen challenge through the secretion of chemokines by keratinocytes and MCs (Fig. 3, step 1), (Kneilling *et al.*, 2009). Mast cell (MC)-derived histamine can also contribute to the attraction of neutrophils (Dudeck *et al.*, 2011). Honda and coworkers in 2013 suggested that IL-1β and TNFα-mediated the activation of the endothelium leads to the expression of adhesion molecules such as ICAM-1, P/E-selectins, which allows the migration of T lymphocytes to the challenged skin. This may be potentiated by neutrophils, because the depletion of neutrophils inhibits the inflammatory response in CHS through the inhibition of CD8$^+$ T cell recruitment (Dilulio *et al.*, 1999, Engeman *et al.*, 2004).

3.1.2.3 The resolution phase of CHS

The resolution phase of CHS is the time following maximum inflammation to its complete resolution. The cellular and molecular mechanisms that contribute to the resolution of inflammation in CHS are largely unknown. During the resolution phase of CHS, interleukin 10 (IL-10) contributes to the suppression of the activation of leukocytes, which reduces the duration of inflammatory CHS responses (Lehtimäki *et al.*, 2012). MCs and T regulatory cells (Treg), i.e. CD4$^+$ CD25$^+$FoxP3$^+$, located in the inflamed area, are a source of this cytokine (Grimbaldestone *et* al., 2007, Honda *et al.*, 2010a, Ring *et al.*, 2011). Although it is not clear the time when exactly these cells release IL-10, their mRNA levels peak locally within the first 24 hours after the elicitation of inflammation and are abrogated after 48 hours (Lehtimäki *et al.*, 2012). During the resolution phase, Treg also suppress leukocyte activation and recruitment through the local release of adenosine in the inflamed skin (Fig. 3, step 1) (Ring *et al.*, 2011). Honda and coworkers in 2013 postulated that the remigration of Treg from the skin to the dLNs after challenge is another mechanism that contributes to the resolution of CHS.

3.2 Mast cells (MCs)

3.2.1 Background

Mast cells (MCs) were described for the first time by Paul Ehrlich in 1877. He used Aniline Blue/Methyl Blue staining and described highly granulated cells present in the intestinal mucosa (Ehrlich, 1877). Ehrlich also discovered that these cells increase in pathological conditions involving chronic inflammation (Ehrlich, 1878). In 1966 Enerbäck characterized two different types of murine MCs: 1) Mucosal tissue MCs "MMCs", e.g. MCs in the gut. 2) Connective tissue type MCs "CTMCs", e.g. skin MCs. This classification is still used and is based on the tissue localization, size and features of their secretory granules (Enerbäck, 1966). In MMCs, the granules contain Chondroitin E, whereas CTMCs granules contain Heparin (Bienenstock *et al.*, 1982). The most important difference between MMCs and CTMCs, which is also related to their functions, is the protease composition of the granules. According to their proteolytic activity, MC proteases are subdivided in three major groups, i.e. tryptases, chymases and carboxypeptidases. Mast cell proteases contribute to the elimination of extracellular pathogens and to the inactivation of hazardous bioactive products, e.g. toxins, venoms and cytokines. CTMCs express one α-chymase, the MC protease 4 (MMCP-4), one β-chymase the MMCP-5, two tryptases MMCP-6 and -7, and the carboxypeptidase A3 (CPA3). MMCs express two β-chymases, i.e. MMCP-1 and -2, but do not express tryptases or carboxypeptidases (Pejler *et al.*, 2007).

MCs are derived from $CD34^+$ myeloid pluripotent progenitors (MCPs) in the bone marrow (Kirshenbaum *et al.*, 1991, Gurish and Boyce, 2006). The specific factors responsible for the differentiation to CTMCs or MMCs are largely unknown. The initial differentiation of $CD34^+$ progenitors to MCs is dependent on Stem Cell Factor (SCF) (Kirshenbaum *et al.*, 1991). Mice caring loss of function mutations in the receptor for SCF (cKit) are devoid of MCs (Jarboe and Huff, 1989). In humans, a gain of function mutation in the same receptor is positively correlated with mastocytosis, a disease characterized by increased numbers of MCs in different organs (Kristensen *et al.*, 2011).

In mice, interleukin-3 represents a maturation factor necessary for the complete development from MCPs to mature MCs (Razin *et al.*, 1981, Lantz *et al.*, 1998, Ord

et al., 2012). In humans, this function appears to be covered by interleukin-4 (Toru *et al.*, 1998). There are many unresolved questions regarding the development, proliferation and migration of MCs in physiological as well as in pathological conditions.

3.2.2 MC activation and products

MCs express a wide variety of receptors such as for immunoglobulins, complement, cytokines, neuropeptides and toll-like receptors (Table 1) (Marshall, 2004).

Immunoglobulin E (IgE) crosslinking is the most studied mechanism of MC activation. It represents the backbone of type I immediate hypersensitivity reactions. This activation mode is selective, because IgE recognizes only relevant allergens. MCs release pro-inflammatory mediators by degranulation two to five minutes after allergen binding and IgE crosslinking. The primary contact to a relevant allergen induces the production of allergen-specific IgE antibodies by B cells. The high affinity IgE receptor (FceRI), expressed on the membrane of MCs, binds the antigen-specific IgE. MCs reside in the interphase between internal and external environment, e.g. skin, gut and lungs. At these sites, MCs "armed" with IgE will get activated upon new encounter with the relevant allergen. When the allergen binds two or more IgE simultaneously (crosslinking), a signaling cascade initiated by a delta sub-unit of the $Fc_\varepsilon RI$ evolves and leads to an increase of intracellular calcium influx, which results in: 1) MC degranulation, 2) Synthesis of eicosanoids, i.e. prostaglandins and leukotrienes, from the metabolism of arachidonic acid and 3) *De novo* production of cytokines motivated via activation of Ras and NF-kB (Gilfillan and Tkaczyk, 2006, Kalesnikoff and Galli, 2008).

Table 1. Mediators released by MCs. (Modified from Marshall, 2004)

Mediators	Examples of function
Granule-associated	
Histamine and serotonin	Alter vascular permeability
Heparin and/or chondroitin sulphate peptidoglycans	Enhance chemokine and/or cytokine function and angiogenesis
Tryptase, chymase, carboxypeptidase and other proteases	Remodel tissue and recruit effector cells
TNF, VEGF and FGF2	Recruit effector cells and enhance angiogenesis
Lipid-derived	
LTC_4, LTB_4, PGD_2 and PGE_2	Recruit effector cells, regulate immune responses, and promote angiogenesis, edema and bronchoconstriction

Platelet-activating factor	Activates effector cells, enhances angiogenesis and induces physiological inflammation
Cytokine	
TNF, IL-1α, IL-1β, IL-6, IL-18, GM-CSF, LIF, IFNα and IFNβ	Induce inflammation
IL-3, IL-4, IL-5, IL-9, IL-13, IL-15 and IL-16	Functions of T helper 2-type cytokines
IL-12 and IFNγ	Functions of T helper 1-type cytokines
IL-10, TGF-β and VEGF	Regulate inflammation and angiogenesis
Chemokine	
CCL2, CCL3, CCL4, CCL5, CCL11 and CCL20	Recruit effector cells, including dendritic cells, and regulate immune responses
CXCL1, CXCL2, CXCL8, CXCL9, CXCL10 and CXCL11	Recruit effector cells and regulate immune responses
Other	
Nitric oxide and superoxide radicals	Bactericidal
Antimicrobial peptides	Bactericidal

The release of MC granules occurs within minutes after the IgE crosslinking. Once the granules are discharged to the extracellular medium, changes in the pH allow the release of the bioactive molecules from the proteoglycan granule matrix (Ruoss *et al.*, 1991). In the granules, not only proteases but also biogenic amines, lysosomal enzymes and cytokines can be found (*see* table 1), (Lundequist and Pejler, 2011). A key factor for the pro-inflammatory effects of MC degranulation is histamine, a mediator of allergic symptoms *par excellence* due to its effects on immune cells, blood vessels and nerve endings (Gri *et al.*, 2012). MC-proteases are essential for the inactivation of poisons (Akahoshi *et al.*, 2011), the killing of extracellular parasites (Anthony *et al.*, 2007) and the induction of tissue remodeling (Galli and Tsai, 2008). Pre-stored cytokines such as TNFα and IL-4 are also released during MC degranulation, whereas de novo synthesis and release of cytokines after MC activation through IgE/allergen takes several hours to occur and several days to subside (Marshall, 2004).

Another well-studied mechanism of MC activation is through scavenger receptors, e.g. Toll-like receptors (TLR). TLRs can sense microenvironmental danger signals and get activated when the homeostasis of the tissue is disturbed. For example, most subtypes of MCs express TLR-2 and -4 (Varadaradjalou *et al.*, 2003), which are responsible for lipopolysaccharides (LPS) binding in Gram-negative bacteria. After binding of LPS, MCs start to produce and release cytokines but do not degranulate (Sandig and Bulfone-Paus, 2012). In humans, one of the most prominent contact

sensitizers, Nickel, binds and activates TLR-4 (Rothenberg, 2010). Human MCs express all known TLRs, i.e. 1 - 10, except for TLR-8 (Chen *et al.*, 2011).

3.2.3 Immune crosstalk of MCs in the skin

In the skin MCs are located strategically in the dermis and subcutis. The most likely explanation for this distribution is that this tissue is a primary target site for pathogens (Metz *et al.*, 2007). Within the skin, MCs are found in the vicinity of nerve fiber bundles near the hair follicles (Fig. 4), (Hendrix *et al.*, 2008, Harvima and Nilsson, 2012). Under both immunologic and physical stress the sensory C-nerve fibers release neuropeptides, e.g. VIP and Substance P, which are sensed by MCs. In response, MCs degranulate and activate the nerve fibers through the release of histamines and tryptases (Kleij and Bienenstock, 2005, Harvima *et al.*, 2010). Hair follicles are rich in sensory nerves and express and release hormones, and MCs also contain receptors for hormones, e.g. Corticotropin-realising hormone receptor (CGRP), (Botchkarev *et al.*, 1997). The crosstalk between MCs and hair follicles appears to be relevant in neurogenic inflammation (Naukkarinen *et al.*, 1993, Harvima *et al.*, 2010).

Another location within the skin where MCs are commonly found, is around blood and lymph vessels (Fig. 4), (Marshall, 2004). MCs can activate the endothelium through the release of pro-inflammatory mediators (Gerritsen, 1996). For example, MCs can also control the migration of leukocytes into inflamed areas by modulating the expression of leukocyte-adhesion molecules in the vasculature, e.g. MC-derived TNFα, interleukin-1 and -6 as well as histamine and tryptase (Kunder *et al.*, 2011). The MC-vessels proximity allow MCs to release bioactive molecules to the bloodstream following their activation and degranulation, e.g. during anaphylactic responses to bee sting (Marichal *et al.*, 2013). MCs contribute to edema formation, by changing the endothelium permeability, for example, by releasing histamine and eicosanoids (Bellanti, 2012). Another advantage of MCs being next to the vasculature is the capacity to extend cytoplasmic protrusions through the vessel fenestration in order to catch IgE circulating in the blood (Cheng *et al.*, 2013). MC-vessel proximity is important for the recovering and *de novo* generation of vessels. For example, Crivellato and coworkers reported that MC-derived mediators can

induce angiogenesis as well as lymphangiogenesis in the skin, e.g. interleukins -1, -6 and -8 as well as TNF, VEGF, bFGF and TGFβ (Crivellato *et al.*, 2008).

In the skin, MCs also interact with dendritic cells (DC), for example during the sensitization to allergens, which indirectly control the development of adaptive responses, i.e. the generation of effector and memory T cells. In this context, a study show the capacity of MCs to potentiate the emigration of Langerhans cells (LCs) from the epidermis to the dLNs in response to infection with pathogens or after skin exposure to the contact allergen oxazolone (Bryce *et al.*, 2004). In other settings MCs induce the migration of LCs to the dLNs upon IgE stimulation (Jawdat *et al.*, 2004). MC-derived TNFα also potentiates the migration of CD11c$^+$ DC to the dLNs in a contact hypersensitivity (CHS) model elicited with fluorescein isothiocyanate (FITC), (Suto *et al.*, 2006).

MC-derived mediators also affect the maturation and activation state of DC, e.g. MC-derived histamine enhances the expression of MHC-II and co-stimulatory molecules in DC *in vitro* (Caron *et al.*, 2001b), and histamine and prostaglandins induce DC to promote Th2 immunity (Caron *et al.*, 2001a, Faveeuw *et al.*, 2003, Gosset *et al.*, 2003).

MCs also interact with skin structural cells such as fibroblast and keratinocytes. Skin MCs can produce diverse fibroblast growth factors, e.g. FGF-10 and -7, and induce fibroblasts to produce other growth factors, e.g. FGF-2, in a histamine-dependent mechanism (Artuc *et al.*, 2002). Keratinocytes act as immune sensors during different physiologic and pathologic conditions (Nestle *et al.*, 2009). MCs respond to IL-1, IL-33 and vitamin D stimulation (Biggs *et al.*, 2010) and the main source of these products in the skin are activated keratinocytes (Albanesi *et al.*, 2005, Nestle *et al.*, 2009, Ziegler and Artis, 2010, Hart *et al.*, 2011). MCs can also induce the production of antimicrobial peptides in keratinocytes through the release of histamine and prostaglandin D2 (Ishikawa *et al.*, 2009, Kanda *et al.*, 2010).

Skin MCs can reportedly contribute to responses of dLNs by delivering their granular content to dLNs through lymphatic vessels and by directly migrating into these organs (Hershko *et al.*, 2011, Liu *et al.*, 2013). Nanoparticles carrying TNFα have been shown to be released upon MC degranulation and to travel through the

lymphatics to reach and activate the dLNs (Kunder *et al.*, 2009, Gunzer, 2012, St John *et al.*, 2012).
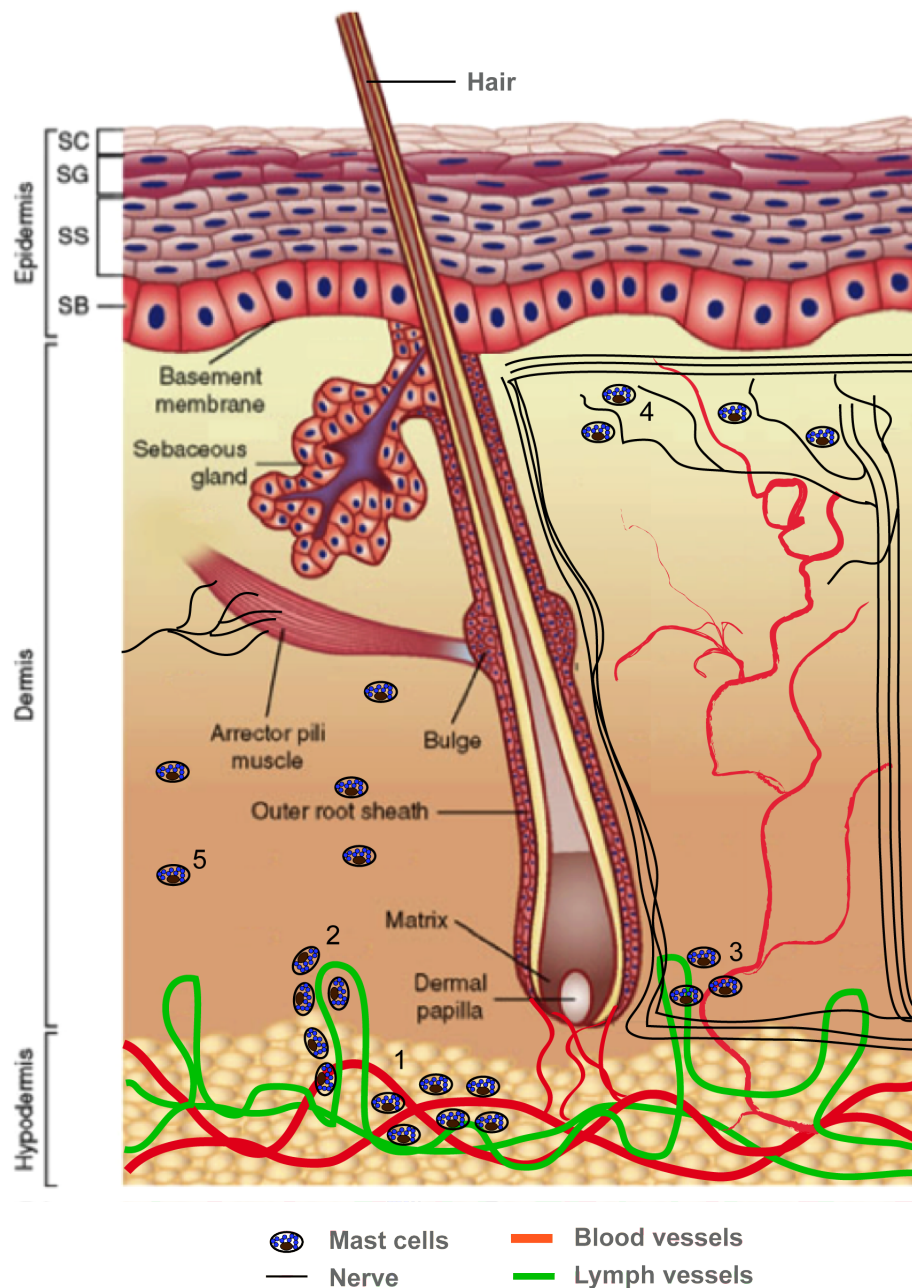
Figure 4. Skin localization of mast cells. (1) Mast cells can be found in surrounding blood (1) and lymphatic vessels (2), next to the hair follicle and subcutaneous nerve plexus (3) and close to dermal nerve sensory fibers (4). Mast cells can eventually be found arbitrarily in the skin (5). *Abbreviations*: SC - stratum corneum, SG - stratum granulosum, SS - stratum spinosum, SB - stratum basale (Modified from Wong DJ, Chang HY., 2008-2009).

Hershko and coworkers show that MC migration to dLNs and spleen is required to control inflammation in a model for chronic CHS. In this study, they show that after

repeated hapten-challenge MCs migrate from the skin to dLNs and from dLNs to the spleen. They also demonstrated that the migration of MCs to lymphoid organs was accompanied by increased levels of interleukin 2 in those organs, i.e. a growth factor for T cells, which was required to control the degree of inflammation (Hershko *el al.,* 2011).

3.2.4 Murine models for MC deficiency

To study the role of MCs *in vivo*, the use of MC-deficient mouse models is crucial. The available MC-deficient mouse models can be classified in Kit-dependent and Kit-independent mouse models.

The stem cell factor (SCF), which is the ligand of the Kit receptor, is expressed by various structural cells in hematopoietic organs, e.g. fibroblasts, endothelial cells, etc., as well as by immune cells and structural cells during inflammatory conditions in the skin and lungs (Reber *et al.*, 2006, Kent *et al.*, 2008, Metz *et al.*, 2007). SCF is the main growth factor for MCs, promoting their generation from $CD34^+$ progenitor cells (Nakahata and Toru, 2002).

The term "mast-cell deficient mouse" was used for the first time in 1970 (Mayer, 1970) to describe mice containing naturally occurring mutations at the *Dominant white Spotting* (W) locus on chromosome 5 (Kit^W/Kit^{W-v} mice). This is a loss-of-function mutation, which affects the SCF receptor named Kit (CD117). The direct consequences of that mutation are the lack of melanocytes (white coat color) and profound deficiency of MCs in all examined organs (Grimbaldeston *et al.*, 2005).

A second Kit-dependent MC-deficient strain was reported for the first time in 1982 (Lyon and Glenister, 1982) and characterized in detail by Galli and coworkers in 2005. This strain, named Kit^{W-sh}/Kit^{W-sh}, has a genomic mutation that hits the same target gene as in Kit^W/Kit^{W-v} mice. As a consequence, both Kit^{W-sh}/Kit^{W-sh} mice and Kit^W/Kit^{W-v} mice share the MC deficiency and the lack of melanocytes (white coat color) (Grimbaldeston *et al.*, 2005). However, some disparities between Kit^W/Kit^{W-v} and Kit^{W-sh}/Kit^{W-sh} remain unexplained. Kit^W/Kit^{W-v} mice are neutropenic, whereas Kit^{W-sh}/Kit^{W-sh} mice have increased numbers of neutrophil-like cells named myeloid-derived suppressor cells (MDSC) (Michel *et al.*, 2013). The mutation in Kit^{W-sh}/Kit^{W-sh} consists in a genomic inversion. This genomic inversion truncates the final product of

the gene *corin*. The protein *Corin* is important for the myocardial cells. Kit^{W-sh}/Kit^{W-sh} mice have cardiomegaly and thrombocytosis, i.e. the presence of high platelet counts in the blood. In Kit^{W-sh}/Kit^{W-sh} mice the cardiomegaly compensates for the loss-of-function of *Corin* and the thrombocytosis compensates for their cardiomegaly (Nigrovic *et al.*, 2008).

The Kit-independent mouse models can be further subdivided in Cre dependent and Cre independent. Cre dependent MC-deficient mouse strains were developed with the Cre-Lox technology (Matthaei, 2007, Smith, 2011).

MC deficient mice having Cre under the control of the Mcpt5 promoter are presented in two modalities, the constitutive, i.e. Mcpt5-Cre x R-DTA, and the inducible, i.e. Mcpt5-Cre x iDTR. Those models result from the crossbred of two knockout mouse lines, the MCPT5-Cre with the R-DTA, and the MCPT5-Cre with the iDTR respectively (Dudeck *et* al. 2011). For this study we only used the Mcpt5-Cre x iDTR inducible model.

Mast cell protease 5 (Mcpt5) is expressed exclusively in connective tissue type mast cells (CTMCs), but not in mucosal MCs (MMCs) or in other cell types in the skin (Scholten *et* al. 2008). The MCPT5-Cre mice express the Cre-recombinase protein (Cre) under the control of the MCPT5 promoter. The Cre protein recognizes and cleaves DNA regions surrounded by a specific nucleotide sequence called LoxP, e.g. 5' LoxP – Gene X – LoxP 3'.

iDTR mice have a modified version of the gene encoding for the human diphtheria toxin receptor (DTR) under the control of the ROSA26 promoter. The ROSA26 promoter is ubiquitously distributed in the murine genome and it is constitutively active.

The gene encoding for DTR contains a 5' LoxP – Stop codon – LoxP 3' construct, which prevents the transcription of its functional proteins. Consequently, Cre expressing cells, i.e. CTMCs, delete the stop codon and allow the expression of DTR in the Mcpt5-Cre x iDTR mice.

Mcpt5-Cre x iDTR mice are called inducible, because a treatment with diphtheria toxin (DT) is required to deplete the CTMCs from the system. Because murine cells

are naturally protected from the effects of DT, the other cells of the animal are minimally affected by the DT treatment (Scholten *et al.*, 2008, Reber *et al.*, 2013).

Additional MC-deficient mouse models are available, but they are not used in this study. Two of them are based on the expression of Carboxypeptidase A3 (Cpa3) (Feyerabend *et al.*, 2011, Lilla *et al.*, 2011). There is also a Kit-independent and Cre independent mouse model named Mas-TRECK, and it is based on the expression of IL-4 by MCs (Otsuka *et al.*, 2011).

3.3 MC involvement in CHS responses

The role of MCs in CHS is controversial. In some studies, MC-deficient Kit^W/Kit^{W-v} mice exhibit reduced inflammation to TNCB-induced CHS (Askenase *et al.*, 1983; Biedermann *et al.*, 2000). The report of Askenase and coworkers shows that MCs contribute to CHS during the elicitation phase, suggesting that MC-derived vasoactive mediators allow T cells to leave the intravascular space, enter the tissue, and become activated by the hapten. Biedermann and collaborators concluded that MCs modulate TNCB-induced CHS by controlling T cell–dependent neutrophil recruitment through two mediators, tumor necrosis factor (TNF) and the CXC chemokine macrophage inflammatory protein 2 (MIP-2). In contrast to these reports, two studies show undiminished CHS responses induced by OXA or by DNFB in Kit^W/Kit^{W-v} mice (Galli and Hammel, 1984; Mekori and Galli, 1985). Galli and Hammel reported that neither infiltrated cells nor swelling responses were altered in the ears of sensitized Kit^W/Kit^{W-v} mice challenged with OXA as compared to wildtypes. Mekori and Galli confirmed that MCs are not critical in DNFB-induced CHS inflammation or in the gain of tolerance after supraoptimal sensitization with DNFB in this CHS model. In 2007, Grimbaldeston *et al.* using Kit^W/Kit^{W-v} mice and Kit^{W-Sh}/Kit^{W-Sh} mice, reported that MCs have regulatory effects in CHS and that they limit and reduce CHS responses through the production of IL-10. They came to this conclusion, because MC-deficient mice as well as MC-deficient mice reconstituted with MCs that lack IL-10 exhibited increased DNFB-induced CHS as compared to wildtype mice or MC-deficient mice reconstituted with wildtype MCs (Grimbaldeston *et al.*, 2007). Dudeck et al., who used different MC-deficient mouse models, i.e. MCPT5-Cre x iDTR and MCPT5-Cre x R-DTA mice, did not reproduce the results from Grimbaldeston and coworkers. Dudeck *et al.* described that mice depleted of MCs exhibited reduced

CHS inflammation to DNFB and to OXA. They attributed the detrimental contribution of MCs to CHS to MC-derived adjuvant effects occurring after challenge, e.g. release of histamine. In addition, the deletion of MC-derived IL-10 did not result in exacerbated CHS inflammation in this study (Dudeck *et al.*, 2011). Employing Mas-TRECK mice, i.e. another MC-deficient mouse model, Otsuka and coworkers found a pro-inflammatory contribution of MCs in CHS reactions to FITC and to OXA. In this report, they concluded that MCs improve the migration and maturation of skin DC during the sensitization phase, which facilitates the efficient generation of hapten-specific T cells. Additionally, they show that MC-DC interactions were exerted via ICAM-1, lymphocyte function-associated antigen 1 and by membrane-bound TNFα in MCs (Otsuka *et al.*, 2011).

To date, the reasons for these discrepancies remain unclear, but several lines of evidence point to differences in the experimental settings as a possible explanation. For example, Askenase *et al.* in 1983, Biedermann *et al.* in 2000, Galli and Hammel in 1984, and Mekori and Galli in 1985 used the same MC-deficient mouse model in their studies, i.e. Kit^{W}/Kit^{W-v} mice, but employed different haptens and hapten concentrations. Of note, CHS reactions to TNCB, DNFB and OXA are similar, but not identical. For example, 49% of the up-regulated gene expression profile after DNFB sensitization differs from that after OXA sensitization (Saito *et al.* 2013). Furthermore, unlike CHS to TNCB, CHS to OXA results in long-term accumulation of T lymphocytes in the challenged skin (Rana *et al.* 2008). On the other hand, responses to haptens are dose-dependent. Norman *et al.* show that low dose OXA challenge results in diminished CHS responses in Kit^{W}/Kit^{W-v} mice, whereas high dose OXA challenge show severe CHS responses (Norman *et al., 2008*). In addition, because of the congenital absence of MCs in Kit-dependent MC-deficient mouse models, a compensatory mechanism may exist, such as neutropenia in Kit^{W}/Kit^{W-v} mice and increased numbers of neutrophil-like cells named myeloid-derived suppressor cells (MDSC) in Kit^{W-sh}/Kit^{W-sh} mice (Michel *et al.*, 2013). In Mas-TRECK mice the depletion of MCs also involves reduction in a sub-population of basophils as reviewed elsewhere (Reber *et al.* 2012). Basophils may have a role in CHS, as basophil-derived Amphiregulin, i.e. a growth factor for T regulatory cells, is essential for Ultravioulet-B irradiation-induced immune suppression in a model of CHS to DNFB (Meulenbroeks *et al.,* 2014). Another explanation for the discrepancies in previous

reports about the role of MCs in CHS may be that MC-deficient mouse models, which relay on the deletion of these cells, have variable depletion efficiencies. For example, MCPT5-Cre x iDTR mice show an average of 89% skin MC reduction after diphtheria toxin treatment, whereas Kit^W/Kit^{W-v} mice and Kit^{W-Sh}/Kit^{W-Sh} mice are above 97% deficient in MCs as compared to WT mice (Reber *et al.* 2012). It is possible that MCs contribute to CHS responses as a sum of forces. This means that the quantity of MCs in the skin is proportional to their contribution in the CHS inflammatory outcome. Consequently, the combination of MC-deficient mouse models, which contain different numbers of MCs, makes it difficult to draw conclusions about the real role of MCs by hindering the discrimination of their contribution from strain-specific effects. Further studies that compare CHS responses in different MC-deficient mice subjected to the same CHS protocol are needed.

3.4 Skin tissue resident memory (TRM) T cells

Effector T cells are released to the circulation after their clonal expansion in the dLNs, i.e. antigen specific proliferation in secondary lymphoid organs. Thereafter, these cells recirculate between the blood and secondary lymphoid organs. Without further stimulation, effector T cells survive between 5 to 7 days after their generation (Hand and Kaech, 2009). Effector T cells that find their relevant antigen and become activated survive longer and produce a specific mediator-profile depending on their sub-phenotype, e.g. Th1, Th2, Th17, Tc1, Tc2, Treg. Antigen-specific memory T lymphocytes are generated in a similar way as effector T lymphocytes, but survive for longer time periods (months to years) without requiring contact to the antigen (Kaech *et al.*, 2002). Antigen-specific memory T lymphocytes are subdivided in central memory T cells (T_{CM}), effector memory T cells (T_{EM}) and tissue resident memory (TRM) T cells. This classification is based on the tissue localization and gene profiling (Gebhardt and Mackay, 2012). In chronic inflammatory conditions, e.g. chronic infection, autoimmune diseases and chronic skin diseases, certain populations of long living memory T lymphocytes increase, survive and proliferate in the inflamed tissues. These memory T lymphocytes are known as TRM T cells (Kaech *et al.*, 2002, Shin and Iwasaki, 2013). In the skin, the TRM T cell populations are important players in skin viral infections and chronic skin diseases such as psoriasis (Boyman *et al.*, 2004, Verjans *et al.*, 2007). However, the contribution of TRM T cells in the

development of skin allergy is largely unknown and highly speculative (Islam and Luster, 2013).

TRM T cells were discovered in a mouse model of herpes simplex virus infection. In this model, they show that TRM CD8^{+} T cells are more efficient in the elimination of this infection in comparison with T_{CM} (Gebhardt and Mackay, 2012). Other reports showed similar populations of TRM T cells in the brain and submandibular glands after viral infection (Hawke *et al.*, 1998, Wakim *et al.*, 2010, Hofmann and Pircher, 2011).

Skin TRM T cells are positive for CD103, CD69 and CD127, and highly positive for CD44. CD103 is the alpha subunit of the $\alpha_E\beta7$ integrin, and it is responsible for their permanence in the skin. CD69 and CD127 are responsible for TRM T cells survival and proliferation, and CD44 is a memory marker responsible for tissue permanence and migration. In addition, TRM CD8^{+} T cells produce high amounts of IFNɣ upon stimulation (Masopust *et al.*, 2001, Gebhardt and Mackay, 2012). As for now, nothing is known about the involvement of TRM T cells in contact hypersensitivity reactions, and the present study is pioneer in this regard.

3.5 Aim of the study

The main goal of this project was to explore the role and relevance of MCs in a chronic mouse model for ACD focusing on the crosstalk between MCs and memory T cells.

Initially we established an experimental murine model representing the chronic features of ACD in patients, called chronic contact hypersensitivity (CCHS). After inducing CCHS inflammation in MC-deficient mice and WT mice treated with a MC-inhibitor, we ascertained whether MCs represent a detrimental or a beneficial factor in CCHS induced inflammation. Since chronically affected skin sites of ACD patients show a remarkable accumulation of MCs (Wolverton and Gada, 2013), we verified this observation in our CCHS model. Subsequently, we investigated whether the MC contribution in this model was extended systemically or it was restricted to skin sites of frequent hapten exposure.

Since ACD is a memory T cell mediated disease (Islam and Luster, 2012, Schnuch *et al.*, 2009, Honda *et al.*, 2012), a secondary goal of this study was to identify and characterize the memory T cell population responsible for CCHS inflammation. Therefore, we determined whether the activity of the relevant memory T cell population was extended systemically or it was restricted to skin sites of frequent hapten exposure.

The study achieved its main aim of identifying a protective role of MCs in CCHS by controlling the accumulation of allergen-specific tissue resident memory CD8β^+ T cells.

4 Materials and methods

The appliances, chemicals, antibodies, media, buffers, kits and disposables used during this study are listed below. The concentrations and specific applications of the listed materials are specified in the corresponding method section.

4.1 Appliances

All the appliances and instruments used for this study are listed in table 2.

Table 2. List of appliances employed for this study

Appliance	Model	Distributor
Autoclave		MELAG, Berlin, Germany
Caliper (micrometer)	Series No 547,7300	Mitutoyo, Japan
Cell sorter	FACS ARIA II	Becton Dickinson, Germany
Centrifuge	Megafuge 1.0 ST R	Heraeus, Hanau, Germany
Chirurgic instruments	Different scissors and forceps	Aesculab B. Braun, Tuttlingen, Germany
CO2-incubator	HeraCell 150	Heraeus, Hanau, Germany
Confocal microscope	FV-1000 MPE	Olympus, Hamburg, Germany
Draying cabinet	Hera Cell	Heraeus, Hanau, Germany
Electronic pipette boy	Handy Step®	Brandt GmbH & Co, Wertheim, Germany
Electronic weighing machine	LA 4200 und PT120	Sartorius, Göttingen, Germany
Flow cytometer	MACSquant Analyzer	Miltenyi Biotec, Bergisch Gladbach, Germany
Inverted microscope	CKX 41	Olympus, Hamburg, Germany
Multi channel pipette	5µl - 50µl, 50µl - 300µl	Eppendorf, Hamburg, Germany
Neubauer chamber	Deep 0.1 mm; Big square 1 mm2	Marienfeld, Lauda Königshofen, Germany
pH-Meter	PB-11	Sartorius, Göttingen, Germany
Pipettes	2µl, 10µl, 20µl, 100µl, 200µl, 1000µl	Brandt GmbH & Co, Wertheim, Germany; Eppendorf, Hamburg, Germany; Gilson, Middleton, USA
Plate reader	VICTOR X	PerkinElmer, Rodgau
Platform Shaker	VIBRAMAX 100	Heidolph, Schwabach, Germany
Power Supply	Power Pac 300	BioRad, München, Germany

Suctions bulb	pipetus®	Hirschmann® Laborgeräte, Eberstadt, Germany
Thermomixer	Thermomixer R	Eppendorf, Hamburg, Germany
Tissue embedding machine	Shandon CitadelTM 1000	Thermo Fisher Scientific, Walldorf, Germany
Vortexer	Model 72020	NeoLab, Heidelberg, Germany
Water bath	WBT 222	Medingen, Dresden, Germany

4.2 Chemicals

The chemicals and reagents used for the development of this doctoral thesis are listed alphabetically in table 3.

Table 3. List of chemicals employed for the study

Chemicals/Reagents	Distributor
1-Fluoro-2,4-dinitrobenzene (DNFB)	Sigma-Aldrich, Steinheim, Germany
4-Ethoxymethylene-2-phenyl-2-oxazolin-5-one (Oxazolone)	Sigma-Aldrich, Steinheim, Germany
4',6-Diamidino-2-Phenylindole, Dihydrochloride (DAPI)	Roche, Mannheim, Germany
Aqua ad iniectabilia	Braun, Melsungen, Germany
Bovines Serum Albumin (BSA)	Serva, Heidelberg, Germany
Bromphenolblau	Merck, Darmstadt, Germany
D-biotinyl-ε-aminocaproic acid-N-hydroxysuccinimide ester (Biotin)	Roche, Mannheim, Germany
Dimethylsulfoxid (DMSO)	Sigma-Aldrich, Steinheim, Germany
Ethylendiamintetraessigsäure (EDTA)	Merck, Darmstadt, Germany
Isofluran (Forene)	Abbott, Baar, Schweiz
Liberase TL	Roche, Mannheim, Germany
MACSFlow	Miltenyi Biotec, Bergisch Gladbach, Germany
Methanol	Merck, Darmstadt, Germany
Natriumhydroxid (NaOH)	Merck, Darmstadt, Germany
Paraformaldehyd	Sigma-Aldrich, Steinheim, Germany
PBS w/o Ca2+ and Mg2+	PAA, Pasching, Österreich
Proteinase K (x10)	DAKO, Hambug, Germany
Streptavidin-FITC	DAKO, Hambug, Germany
Streptavidin-TexasRed	Roche, Mannheim, Germany

Tris-buffer saline (x10)	Sigma-Aldrich, Steinheim, Germany
Trypan blue-Solution (0,4 %)	Sigma-Aldrich, Steinheim, Germany
Tween-20	Sigma-Aldrich, Steinheim, Germany
H_2O, steril	Braun, Melsungen, Germany
α-Monothioglycerol	Sigma-Aldrich, Steinheim, Germany
1-Fluoro-2,4-dinitrobenzene (DNFB)	Sigma-Aldrich, Steinheim, Germany
4-Ethoxymethylene-2-phenyl-2-oxazolin-5-one (Oxazolone)	Sigma-Aldrich, Steinheim, Germany

4.3 Antibodies

The antibodies listed below (Table 4) were used for flow cytometric analyses or/and for whole mount immunohistology studies of skin samples. The Isotypes were used as background controls (Table 5). The Fc-lock reagent was included in each staining to reduce the unspecific background (Table 5).

Table 4. List of antibodies employed for the study

Antigen	Isotype	Clone	Dilution	Conjugate	Distributor
CD103	Armenian Hamster IgG	2,00E-07	1:200	Fluorescein (FITC)	Biolegend, London, United Kingdom
CD117	Rat IgG2b	2B8	1:300	APC-Cy7	eBioscience, Frankfurt, Germany
CD3	Armenian Hamster IgG	145-2C11	1:50	PerCP-Cyanine5.5 (PerCP-Cy5.5)	eBioscience, Frankfurt, Germany
CD4	Rat IgG2b	GK1.5	1:200	Allophycocyanin (APC)	Biolegend, London, United Kingdom
CD44	Rat IgG2b	IM7	1:300	APC-Cyanine7 (APC-Cy7)	Biolegend, London, United Kingdom
CD45	Rat IgG2b	30-F11	1:300	PE-Cy7	Biolegend, London, United Kingdom
CD45.1	Mouse (A.SW) IgG2a	A20	1:50	PE	eBioscience, Frankfurt, Germany
CD8α	Rat IgG2a	2.43	per mg	Unconjugated	Donated by Prof. Blankenstain
CD8β	Rat IgG2b	YTS156.7.7	1:300	Phycoerythrin (PE)	Biolegend, London, United Kingdom

Fc-Block	Rat IgG2a, λ	93	1:100/ 1:50	Unconjugated	Biolegend, London, United Kingdom
FcεR1	Armenian Hamster IgG	mar-01	1:200	FITC	Biolegend, London, United Kingdom
IFNγ	Rat IgG1	R4-6A2	1:50	Biotin	Biolegend, London, United Kingdom
IL-4	Rat IgG1	BVD6-24G2	1:50	Biotin	eBioscience, Frankfurt, Germany
TCRβ	Armenian Hamster IgG	H57-597	1:50	PerCP-Cy5.5	Biolegend, London, United Kingdom

Table 5. List of isotype controls and Fc-block

Isotype	Clone	Conjugate	Distributor
Armenian Hamster IgG	eBio299Arm	FITC/ PerCP-Cy5.5	eBioscience, Frankfurt, Germany
Rat IgG1	R3-34	Biotin	BD Pharmingen, Heidelberg, Germany
Rat IgG2a, κ	R35-95	PE	BD Pharmingen, Heidelberg, Germany
Rat IgG2b	A95-1	PE/ APC/ APC-Cy7/ PE-Cy7	BD Pharmingen, Heidelberg, Germany

4.4 Media and buffers

The components used to set up the media and buffers employed in the study are listed in table 6. The list of media and buffers are arranged in table 7.

Table 6. List of isotype controls and Fc-block

Description	Distributor
Bovine serum albumin (BSA)	Sigma-Aldrich, Steinheim, Germany
FCS	Biochrom AG, Berlin, Germany
Mouse recombinant interleukin-3 (IL-3)	BD Pharmingen, Heidelberg, Germany
DMEM (with glucose)	Biochrom AG, Berlin, Germany
Penicillin/Streptomycin	Biochrom AG, Berlin, Germany

Table 7. List of media and buffer employed in that study

Medium/ Buffers	Components
Avidin mix buffer	DAPI (1:1000 dilution)
	Avidin-Texas Red or Avidin FITC (1:250 delution) in
	1x TBS
BMCMC culture medium	DMEM with
	10% FCS
	1% Pencicilin/Streptomycin
	0.002% α-Monothioglycerol
	IL-3 [10 ng/ml]
Digestion buffer (pH 7.5 – 7.7)	1x Proteinase K in
	0.05mol/L Tris-HCL
FACS washing buffer	1x PBS with
	0.01% EDTA
	1% Pencicilin/Streptomycin
	0.1% BSA
Flushing medium	DMEM with
	10% FCS
	1% Pencicilin/Streptomycin
	0.002% α-Monothioglycerol
Whole mount washing and staining buffer	1x TBS with
	0.1% BSA
RIPA buffer (x10)	Cell Signaling technology[®] Frankfurt am Main, Germany

4.5 Kits

A Cytokine detection kit was used for the quantification of cytokines in skin lysates (Table 8).

Table 8. Kits employed in the elaboration of that study

Kit description	Distributor
Multi-Analyte ELISArray Mouse (Th1/Th2/Th17) Kit	Quiagen, Hilden, Germany

4.6 Disposables

All disposables used in this study are listed below (Table 9).

Table 9. List of disposables used for the study

Material	Type	Distributor
96 well-plate Maxisorp®		NUNC, Wiesbaden, Germany
Coverslips	24 x 46 mm	Menzel GmbH, Braunschweig, Germany
Gloves	Nitril	verschiedene Hersteller
Needles	30/25G	Braun, Melsungen, Germany
Glass slides	Superfrost	Menzel GmbH, Braunschweig, Germany
Pipettes	5 ml in 1/10, 10 ml in 1/10, 25 ml in 2/10	BD FalconTM, Heidelberg, Germany; Sarstedt AG & Co., Nümbrecht-Rommelsdorf, Germany
Pipette tips	10µl, 20µl, 100µl, 200µl, 300µl, 1000µl	Sarstedt AG & Co., nerbe plus GmbH, STARLAB GmbH
Reaction tubes	500µl - 2000µl	Sarstedt, Applied Biosystems, Eppendorf
Reaction tubes	8-Tube Strips 0.2 ml	Kisker GbR, Steinfurt, Germany
Sytinges	10ml, 50ml	Braun, Melsungen, Germany
Cell culture plates	6, 24, 96 well plates	BD FalconTM, Heidelberg, Germany
Centrifuge vials	15 and 50ml	BD FalconTM, Heidelberg, Germany, Sarstedt AG & Co., Nümbrecht-Rommelsdorf, Germany; NUNC, Wiesbaden, Germany
Other vials	0.5, 1.5 and 2ml	BD FalconTM, Heidelberg, Germany, Sarstedt AG & Co., Nümbrecht-Rommelsdorf, Germany

4.7 Mouse strains

4.7.1 C57BL/6 mice

Four to eight weeks old C57BL/6 wildtype females from our own breeding colony were used as control animals and for experiments involving MC inhibitors, i.e. cromolyn.

4.7.2   C57BL/6-*Kit^{W-sh}/Kit^{W-sh}* mice (Sash)

Four to eight weeks old *Kit^{W-sh}/Kit^{W-sh}* (Sash) females with a C57BL/6 background from our own breeding colony were used as constitutive MC knockout mouse model (*see* introduction section 3.2.4). Sash mice lack 98 to 100% of MCs in all tissues examined (Grimbaldeston *et al.*, 2005).

4.7.3   MCPT5-Cre x iDTR mice

Four to eight weeks old MCPT5-Cre x iDTR females from our own breeding colony were used as inducible MC knock out mouse model (*see* introduction section 3.2.4). In 2011 Dudeck *et* al. reported that four intraperitoneal injections of DT administer weekly were required to obtain a reduction of 97.5% of the peritoneal MC population. An additional intradermal injection in the ears was required to get comparable depletion levels of skin MCs. This is the same protocol employed in this work (*see* methods section 4.8.3).

4.8   *In vivo* procedures

4.8.1   Maintenance of mice

All mice were kept under specific pathogen-free conditions in the animal facility of the Center for Cardiovascular Research, Charité-Universitätsmedizin Berlin or technical laboratory for Immunology, Cardiovascular and Renal Research of South-Denmark-University Odense, Denmark. The animals were subjected to a standard circadian cycles (12-hour light-dark), temperature, humidity and food. Hosted in type III cages filled with granulated straw and provided with nesting material, hiding places, water and pelleted dry food.

For all experiments, female mice were maintained in groups not bigger than 10 animals per cage. The starting age of the animals for the experiments was between 4 to 8 weeks. After the end of the experiments the animals were sacrificed by Isofluran overdose and cervical dislocation. All conditions and experiments were performed in accordance with the animal rights stipulated in the legislation stated by

"Landesamtes für Gesundheit und Soziales Berlin" (LaGeSo) and the Danish Animal Experiments Inspectorate.

4.8.2 Contact hypersensitivity models

The concentrations and vehicles employed to prepare the haptens are listed below (Table 10).

4.8.2.1 Conventional contact hypersensitivity (CHS)

Sensitization: The corresponding dose of hapten for the sensitization (Table 10) was pipetted on the abdominal skin (Belly) on day -5. During the next ten seconds after hapten application, the animal was maintained under sedation leading the evaporation of the vehicle (acetone).

Challenge: The corresponding dose of hapten for the challenge (Table 10) was pipetted on the left ears on day 0 and the opposite ears were treated with vehicle (acetone). During the next ten seconds after hapten application, the animal was maintained under sedation leading to the evaporation of the vehicle.

The concentrations and vehicle employed to prepare the haptens are listed below (Table 10).

Table 10. List of haptens employed for that study

Hapten	Vehicle	Sensitization area	Challenge area	Sensitization dose	Challenge dose	Volume
OXA	Acetone	Abdomen	Abdomen or ears	1% to 6% w/v	0.4 to 0.6% w/v	20 µl
DNFB	Acetone	Abdomen	Ears	0.3 to 0.5% v/v	0.1 to 0.2% v/v	20 µl

OXA (oxazolone): 4-Ethoxymethylene-2-phenyl-2-oxazolin-5-one
DNFB: 1-Fluoro-2,4-dinitrobenzene

4.8.2.2 Chronic contact hypersensitivity (CCHS)

For the induction of CCHS, the animals were sensitized and challenge with OXA as described in figure 5.
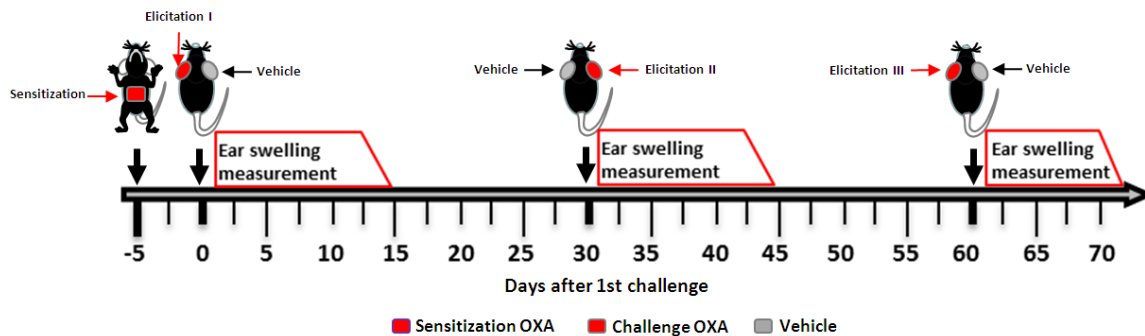
Figure 5. Experimental design of CCHS. The mice were sensitized with OXA at day -5 (belly) and challenged with the same hapten on day 0 (left ears), day 30 (right ears) and day 60 (left ear). The opposite ear was painted with acetone (vehicle). The ear thickness was measured daily starting before every challenge and until 7 to 15 days after every challenge. *Abbreviations*: OXA - oxazolone, CCHS - chronic contact hypersensitivity.

4.8.2.3 Modifications of the challenging pattern in CCHS

In order to study different aspects of the reaction, some steps were modified as follows:

Modification 1 ("left ear–belly–ears" approach): On the 2nd challenge, the hapten was applied on the belly and the vehicle was applied on the left ear (Fig. 6). The rest of the protocol was the same as for the CCHS "left-right-left" approach.
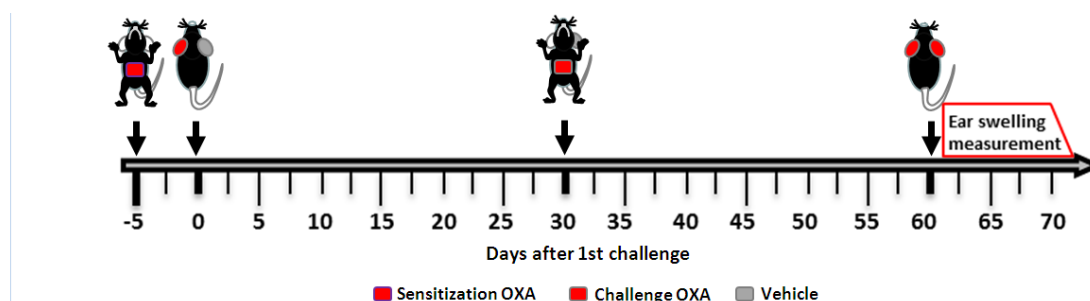
Figure 6. Modification 1. The sensitization and 1st challenge were performed exactly as described in figure 5. On the second challenge the animals received the challenging dose on the belly and vehicle on the left ear. For the 3rd challenge both ears were provoked with the hapten. *Abbreviations*: OXA - oxazolone.

33

Modification 2 ("belly–belly–ears" approach): For the 1st and 2nd challenge, the mice were elicited in the belly and the vehicle was applied on both ears. The 3rd challenge consisted in a topical application of the hapten on both ears. The rest of the protocol was the same as for the CCHS "left-right-left" approach.

Modification 3 ("ears–belly–ears" approach): For the 1st and 3rd challenges, the hapten was applied on both ears and the vehicle was applied on the belly. The 2rd elicitation consisted in a topical application of the hapten on the belly. The rest of the protocol was the same as for the CCHS "left-right-left" approach.

Modification 4: Twenty-five days after the 3rd challenge with oxazolone (day 85 of the whole CCHS protocol), the mice were sensitized with 1-Fluoro-2,4-dinitrobenzene (DNFB) on the belly and 5 days after DNFB sensitization the mice were challenged with oxazolone on the left ears and with DNFB on the right ears (Fig. 7). The concentrations and vehicle employed to prepare the haptens are listed in table 10.
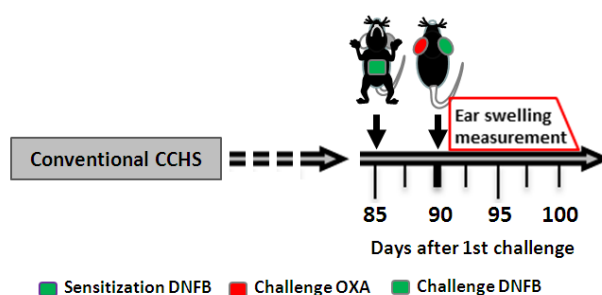
Figure 7. Modification 4. The sensitization and challenges with OXA were performed exactly as described in figure 5 (basic method of CCHS). 85 days after the 1st challenge with OXA all the mice were sensitized with DNFB and 5 days before challenged with the same hapten on the right ears. The left ears were challenged with OXA. Ear swelling measurements were performed before the challenge and daily the subsequent 7 days after challenge. *Abbreviations*: OXA - oxazolone, CCHS - chronic contact hypersensitivity, DNFB - 1-Fluoro-2,4-dinitrobenzene.

4.8.3 Depletion of MCs with diphtheria toxin treatment

Four weeks old MCPT5-Cre x iDTR female mice were treated weekly for 4 weeks with an intraperitoneal (i.p.) injection of diphtheria toxin [25 ng/ gr bodyweight in saline] before the hapten-sensitization. Two days before the hapten sensitization an intradermal (i.d.) injection of 40 µl of DT [5 ng/ gr bodyweight in saline] was practiced in the ear pinnae of those animals. To maintain the MC depletion during the induction

of chronic inflammation, further i.p. injections of DT [25 ng/ gr bodyweight in saline] were administered weekly during the next 90 days after the 1st challenge with oxazolone.

4.8.4 Depletion of CD8+ T cells with anti-CD8 antibody

On day 5 and 6 after the 1st challenge with oxazolone, a single i.p. injection of 0.250 mg diluted in 500 µl of PBS of anti-CD8 antibody (clone 2.43) was applied to the mice.

4.8.5 Treatment with Sodium Cromoglycate (Cromolyn)

Wildtype animals were injected i.p. with cromolyn (25µg/ gr bodyweight) diluted in 500 µl of saline. The cromolyn treatment was performed at 0 hours, 24 hours and 48 hours after every challenge, i.e. days 0,1, 2, 30, 31, 32, 60, 61 and 62 in the CCHS protocol.

4.8.6 Reconstitution of MCs in the ears of Sash mice

Four weeks old, bone marrow cultured derived MCs (BMCMCs) were centrifuged and resuspended ($2x10^6$ cells/ 40µl of saline). The purity of the cells was assessed by Kimura staining and by the expression of cKit and $Fc_\varepsilon RI$ that was analyzed by flow cytometry. Sash mice (4 to 6 weeks old) were sedated with Isofluran/O_2 mixture. Using a 30g needle and 1 ml syringe, an i.d. injection of 40µl of cell suspension was performed in the ear pinnae of those mice. Four to six weeks after the MC reconstitution the animals were used for the CCHS protocol.

4.8.7 Adoptive transfer of total lymphocytes

Donor Ly5.1 mice as well as recipient animals, i.e. Sash and WT mice, were sensitized (day -5) and challenged (day 0) with oxazolone on the same day.
On day 6 the draining lymph nodes (dLN) as well as total blood of donor animals were collected. The organs were passed through a 70 µm cell strainer and washed with PBS to bring it to cell suspension. Blood was depleted of erythrocytes by using an erythrocyte lysis buffer and a lymphoprep centrifugation gradient (conditions specified by the provider). The cellular suspension rich in lymphocytes was washed

twice with PBS and pelleted by standard centrifugation, i.e. 300g for 10 min at 4 °C. The cell-suspension from both organs was pooled and centrifuged once more. The cells were incubated with anti-CD8β-PE antibody for 20 min, 20g in ice. Afterwards, the cells were washed with FACS-buffer and pelleted by standard centrifugation. Next, the cells were resuspended in PBS 0.1% BSA in a concentration of 10^7 cells/ml. Subsequently, the CD8β$^+$ cells were purified (> 90% purity) by FACS sorting. The positive fraction was washed and pelleted with FACS-buffer. The resultant pellet was resuspended in 400 µl of PBS to $2x10^7$ cells and kept on ice prior to injection. 200 µl of the cell suspension was injected in the tail vein of each recipient mouse.

Two days after the adoptive transfer of CD45.1$^+$CD8β$^+$ T cells, the ears and dLNs of WT and Sash recipient mice were harvested as described above in this section and the composition and number of CD45.1$^+$CD8β$^+$ T cells expressing the TRM markers were analysed by flow cytometry.

4.9 *In vitro* procedures

4.9.1 Culture and enrichment of bone marrow derived MCs

The bone marrow was obtained from C57BL/6 female animals that were between 4 to 6 weeks old. For the isolation of the bone marrow the femur and shinbone were cleaned from the surrounded tissue and separated from the rest of the animal. The bone marrow was retrieved by cutting the bone ends and flushing the medullary cavity of the femur and shinbone with a 30g needle and a 10 ml syringe filled with flushing medium. Subsequently, the bone marrow was collected in a petri dish. The resultant cell suspension was transferred to a 50 ml falcon tube and pelleted by standard centrifugation. The resuspension of the pellet was performed in culture medium. The cell suspension was cultured for 4 weeks renewing the media every 7 days from the first 2 weeks and changing the half of the media in week 3 and 4 in the same time interval. After 4 weeks culturing, the purity of bone marrow derived MCs (BMCMC) was above 90%. The quantification of the purity was analyzed by Kimura staining (granularity) and flow cytometry (co-expression of cKIT and Fc$_\varepsilon$RI; Fig. 8).
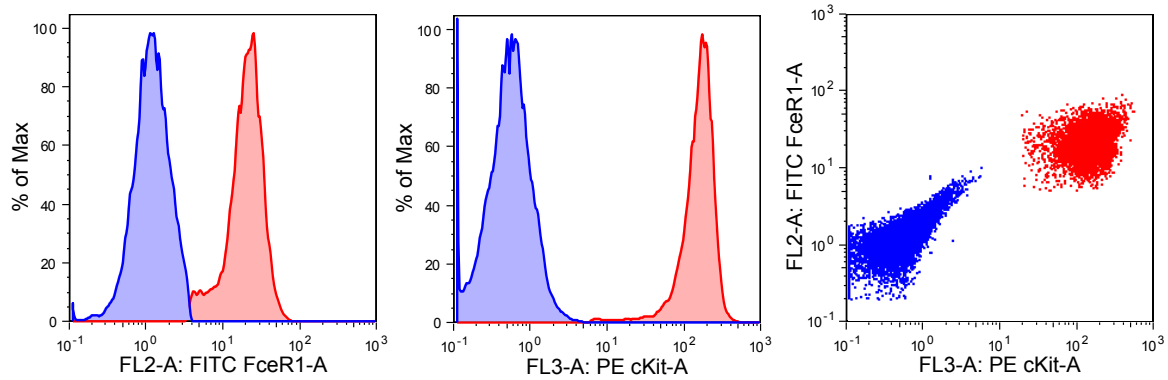
Figure 8. Expression of Fc$_\varepsilon$RI and CD117 (cKit) in bone marrow cells cultured in presence of IL-3. The bone marrow was cultured in presence of IL-3 for four weeks and then stained with anti-cKIT and anti-Fc$_\varepsilon$RI antibodies prior flow cytometric analysis. The left picture shows the expression of Fc$_e$RI against the isotype control. The center panel shows the expression of cKit in the same population compared with the isotype control. The right panel shows the co-expression of both cell surface-markers compared with their respective isotype controls. *Abbreviations*: FL - Fluorescence channel, FITC - fluorescein isothiocyanate, FceR1 - Fc epsilon receptor 1, PE - phycoerythrin, IL-3 - Interleukine-3.

4.9.2 Isolation of infiltrating immune cells from the skin

After euthanizing the mice their ears were collected and weighed. The ventral and dorsal sides of each ear were separated from each other and placed in 1.5 ml vial containing 0.2 mg/ml of Liberase TL diluted in RPMI and Streptomycin/Penicillin 1% (300 µl of solution per ear). By using scissors the ears were cut in small pieces in a 1.5 ml vial and incubated in a thermomixer at 37 °C and 650 rpm with constant shaking. The reaction was stopped after 45 minutes by adding 500 µl of RPMI with 10% FCS v/v. To bring the tissue to a cellular suspension, the digested tissue was passed through a 100 µm cell strainer, pressed with a 10 ml syringe-plunger and washed with ice cold PBS. To clean the cellular suspension from epidermal conglomerates, the fluid was passed through a 40 µm cell strainer and collected in a 50 ml falcon tube. The cell suspension was pelleted by standard centrifugation and resuspended in a staining master mix containing the selected antibody mixture coated to different fluorochromes.
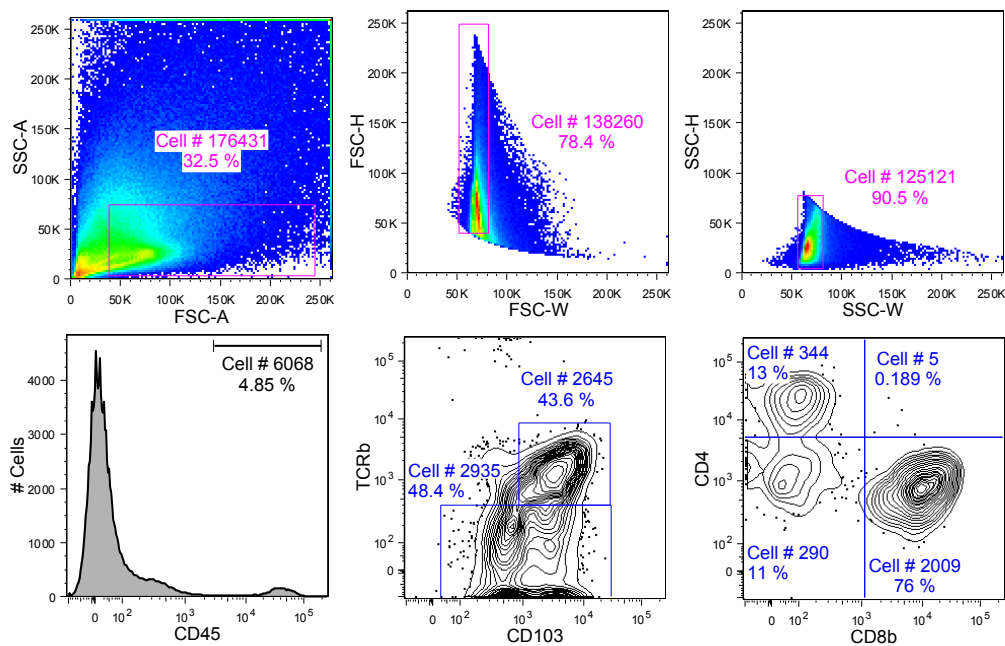
Figure 9. Gating strategy and analysis of skin lymphocytes. Using the forward and side scatter the lymphocytic gate was employed to exclude non-lymphocytic populations (upper left panel). The single cells were selected using the FSC-W/FSC-H and SSC-W/SSC-H (upper center and left). Next, the CD45 marker was used to exclude non-immune cell-populations (lower left). From CD45$^+$ cells the TCRβ and CD103 double positive population was gated (lower center panel). The subpopulation of CD45$^+$TCRβ$^+$CD103$^+$ cells was then displayed in terms of CD8β$^+$ and CD4$^+$ expression (lower right panel). The total cell counts and percentages were used as comparative variables. _Abbreviations_: FSC - forward scatter, SSC - side scatter, TCRβ - T cell receptor β.

The cell staining was incubated for 30 min on ice and while mixed at 250 rpm. The cells were washed once with ice cold PBS and centrifuged as described previously, before cell-sorting. T cells were resuspended in 0.1% BSA in PBS and kept on ice until cell-sorting. Cell sorting was performed according to the following criteria (Fig. 9): FSC-A/SSC-A gate (Lymphocyte gate), SSC-A/SSC-H (Singlet gate), CD45+ cells, CD4+ or CD8β+ cells. Some other makers were employed in specific conditions for sorting and will be specified at the corresponding section.

4.10 Cell biological methods

4.10.1 Flow cytometry and cell sorting

Flow cytometry is a method for analysis of fluorescence labeled particles. Specific sensors (photomultiplier tubes) installed in the machine are able to collect information about the particles, when those particles (cells) are excited by lasers beam (Fig. 10A). The information collected from the lasers can be divided in three categories, size (detected by the forward scatter "FSC"), complexity or/and granularity (detected by the side scatter "SSC") and the fluorescence intensity, which is detected by different filters installed in the appliance.

The fluorescent information varies depending of the excitation and emission wavelengths of the fluorescence and the exiting laser beam. Normally, fluorescent particles are coated to antibodies, which recognize specific cell-markers, e.g. anti-CD117 coated to phycoerythrin (αCD117-PE). The cytometer detects cells-binding fluorescent antibodies as events. The cytometer-compute such parameters for each analyzed cell and represents it in a two-dimensional plot on the screen. That plot representation enables the user to select the population of interest by so-called population gating (Fig. 10B). The gating of a specific cell-population can inform us about the percentage of that particular population proportionally to other cells within the cell mixture as well as the expression levels of the specific markers in the population of interest (Fig. 10B and C).

Some cytometers are equipped with a sorting system and therefore also called cell-Sorters. Cell sorters apply an electric charge to selected cells that after getting charged, a magnetic field located at the end of the flow system can change the trajectory of the charged cells towards a separated collector tube (Fig. 10A4). Consequently only charged cells will end together in one tube obtaining a pure population.

A.

B.

C.
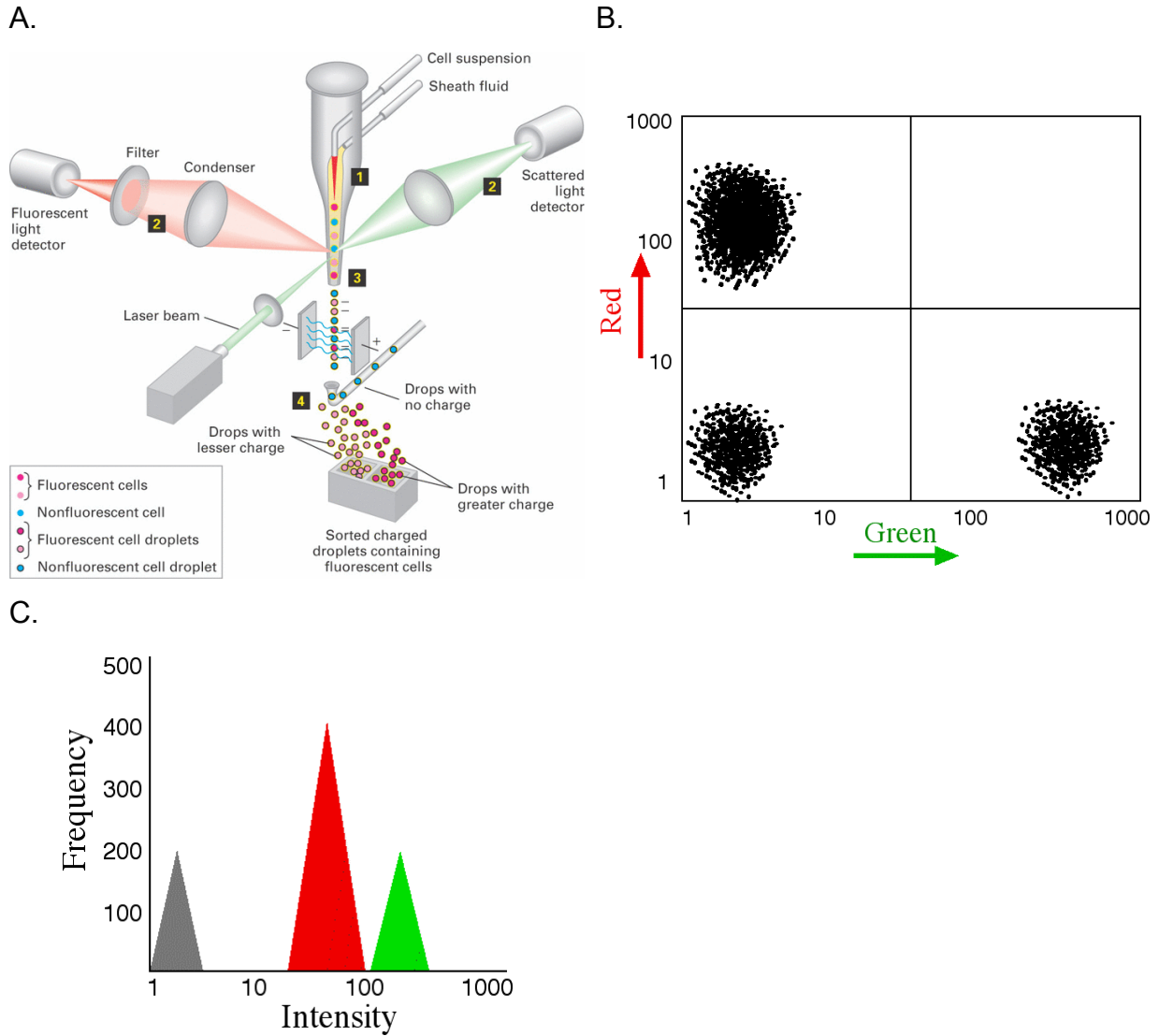
Figure 10. Principles of FACS analysis and cell sorting technology. Cells in suspension are socked and transported through a capillary system in stream (Panel A1). Single cells go through the laser detector-system. In that place is where the lacers-beam scans the cells. The light diffraction and the fluorescence emitted by the cells are collected by the scatters and photomultiplier tubes (Panel A2). The retrieved information (fluorescence intensity, size and granularity) is processed by the CPU and represented in a two-dimensional dot-plot (Panel B). By using the dot-plot representation it is possible to gate the population of interest, according to the parameters previously described, and indicate to the sorter-unity which population of cells need to be sorted out of the cell mixture. The selected cells will be electrically charged and passed through an electric field that will alter their trajectory towards a collector tube (Panel A3 and A4). Panel C shows the schematic representation of a two-dimensional plot in which it is possible to distinguish the cells in terms of the frequency within the cell mixture and the relative expression of a specific marker measured in terms of the fluorescence intensity. (Pictures adapted from: http://www.bio.davidson.edu/genomics/method/FACS.html, http://www.studyblue.com/notes/note/n/unit-1-chapters-1-3-9-10/deck/3412445)

4.11 Histological methods

4.11.1 Ear whole mount for confocal analysis

4.11.1.1   Tissue preparation

Before harvesting the ears, an intradermal injection of 80 µl of TBS 1x was practiced on the ears. The ears were then fixed in TBS containing 4% PFA for 20 minutes and at room temperature. The excess of PFA was washed by submerging the ears in 1x TBS. Next, the ventral and dorsal sides of each ear were separated from each other and incubated for 1 hours at 37 °C in digestion buffer (700 µl / Ear in a 1.5 ml vial) and constant shaking (900 RPM). The ear sides were then washed in 1x TBS once and incubated with Avidin mix diluted in 1x TBS for 15 minutes at 37 °C and constant shaking (900 RPM). To remove the excess of Avidin the ear-sides were submerged once in 1x TBS. The tissue was blocked with 1x Biotin block for 15 minutes at 37 °C and constant shaking (900 RPM). Afterwards, the tissue was washed twice for 5 minutes in 1x TBS. Subsequently, the tissue was incubated with antibody mix diluted in 1x TBS and 0,5% BSA for 1h at 37 °C and constant shaking (600 RPM). After incubation, the tissue was washed twice for 5 minutes in 1x TBS, which induced the spontaneous separation the epidermal layer from the dermis. The dermal layer and epidermal layer were mounted in bi-distillated water and prepared for confocal imaging.

4.11.1.2   Confocal imaging

The imaging was performed with an Olympus FV1000 MPE Confocal and Multiphoton Laser Scanning Microscope. The lasers used according each type of fluorochrome are listed in the table 11.

Table 11. List of lasers and its corresponding fluorochromes.

Laser	Fluorochrome detection
405	DAPI
488	Alexa 488 / FITC
559	Rhodamine/ Texas red
635	Alexa 647/ APC

Five consecutive microscopic fields of a 63X magnification objective were imaged in a Z-stack format. The imaged area corresponded with the area of the ear swelling measurements. For visualization, 50 μm of the Z-axis, were scanned with 10 intervals of 5 μm between every picture (Fig. 11A). The imaging was performed with a single photon setting.

Imaging analysis type 1 (MC counting): 5 Z-stacks were imaged per ear. The Z-stacks containing the maximal number of MCs within each ear were selected to represent this ear. The numbers of MCs were counted in the representative Z-stacks (Fig. 11B).

Imaging analysis type 2 (Cytokine quantification): For cytokine semi-quantitative analysis, all collected Z-stacks were processed as for type 1 analysis. In this particular case the channel used for cytokine analysis was imaged alone. Using a pixel quantification method, as explained in section 4.13.1.2, the concentrations of extracellular and intracellular cytokines were analyzed (Fig. 11D).
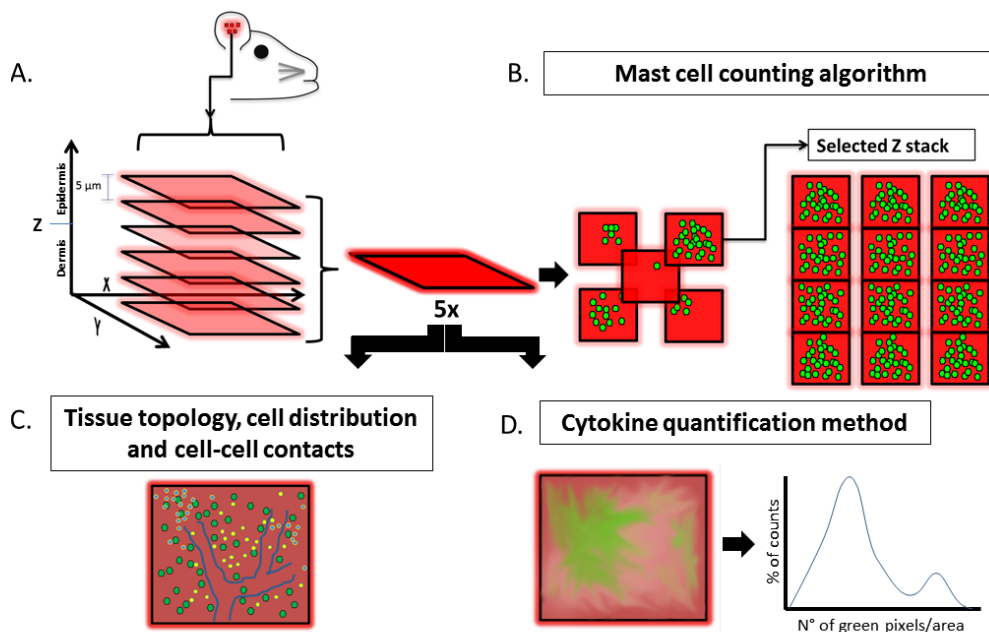
Figure 11. Analysis of ear whole mount. (A) After whole mount staining, 5 microscopic fields within the swelled area were imaged in a Z-stack format. Every Z-stack was transformed to a maximal projection and used for cell counting, cell topology and cytokine quantification. (B) The microscopic field showing the higher number of MCs in each ear was selected as representative of that ear and displayed in a stripe together with other representative microscopic fields. (C) Cells were imaged and analyzed in terms of numbers; cell-cell contact and position respect the challenged area and the

central vessels rood. (D) Cytokine concentration was estimated by the amount of florescence represented in form of pixel count within every Z-stack collected.

4.12 Molecular biological methods

4.12.1 Isolation of total protein of skin lysates

Biopsies of 4 mm of diameter were taken from the central part of the ear lobule and storage dry in 0.5 ml vial at -80 °C. Prior to analysis the biopsies from each group were pooled and weighed. After, the samples of each group were collected in 1.5 ml vial and cut in small pieces while digested with 1x RIPA buffer for 20 min at room temperature. Using a glass douncer the proteins were further extracted from the tissue. The protein lysate was collected and stored in -80 °C until its analysis.

4.12.2 Multiple Enzyme-Linked ImmunoSorbent Assay (Multi-ELISA)

Two hundred microliters of protein lysate extracted from ear-skin was transferred to selected wells in a 98-well plate platform in order to perform a Multi-ELISA assay. The procedure was followed as specified by the provider. The optical density measured the concentration of cytokines, based on the radish peroxidase activity on the colored subtract. Because the absence of a standard it was not possible to assess the absolute concentration of cytokines in the samples, but the kit contained a positive and a negative control to verify the functionality of the test

4.12.3 Trypan blue staining

To determine the cell numbers and viability of the cells 10 µl of the cell suspension were mixed 1:2 in 0.4% trypan blue. Since dead cells lose membrane integrity, the blue dye is able to diffuse into the cells. The stained and unstained cells were counted using a Neubauer counting chamber. Taking into account the dilution factor of the Chamber, the cell number was determined as followed:

- Unstained cells x 10^4 (chamber factor) x dilution = number of viable cells per ml.
- Stained cells x 10^4 (chamber factor) x dilution = number of dead cells per ml.

4.12.4 Kimura staining

To check the MC purity 10 µl of the cell suspension were mixed 1:2 with a Kimura solution163. Kimura dye turns the proteoglycans in MC granules purple. Using a Neubauer counting chamber all stained and unstained cells were counted. Taking into account the dilution factor of the chamber, the number of MCs was determined as follows:

- Stained cells x 10^4 (chamber factor) x dilution = number of MCs per ml.
- Unstained cells x 10^4 (chamber factor) x dilution = number of non-MCs per ml.

4.13 *In silico* methods

4.13.1 Imaging analysis of confocal microscopy

All pictures, Z-stacks and videos obtained by confocal microscopy were analyzed with the open-software FIJI (ImageJ).

4.13.1.1   Automatic cell counting

For automatic cell counting the whole Z-stack was transformed to a 16-Bit pixel picture and flattened with the *Z-project* tool for *Maximal intensity*. Next, the *3D object counter* tool was employed to perform the automatic count (Threshold: 30000-60000, filter size: 30 to 200 pixels). The *Surface map* and *Object map* output were used to perform the counting. The counting was validated manually.

4.13.1.2   Cytokine quantification in whole mount samples

The Z-stack was flattened with a *Z-project* tool for *Maximal intensity* and transformed to an RGB format. Next, the colored pixels were calculated using the *Color histogram* tool. The values per unit area were normalized and the area under the curve calculated using the software GraphPath Prism. The mean and the standard deviation were taken as reference values to prepare the histograms (Fig. 12).
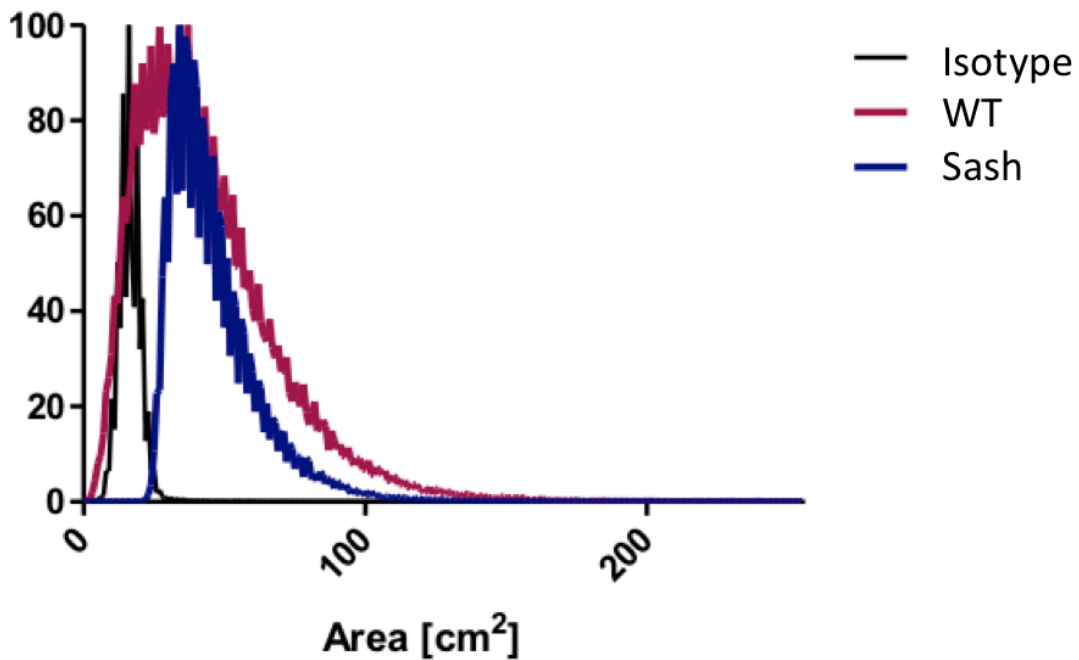
Figure 12. Graphic of pixel count and distribution in whole mount of ears used for cytokine analysis. The histogram is showing the pixel distribution along of a Z-stack, which correlates with the relative amount of cytokine within this Z-stack. *Abbreviations and legend description*: Isotype - ears stained with Isotype control, WT - ears of wildtype mice stained with anti-IL-4 antibody, Sash - ears of C57BL/6-Kit^{W-Sh}/ Kit^{W-Sh} mice stained with anti-IL-4 antibody.

4.14 Statistical analysis

One-tailed/two-tailed student's T-test for independent samples or Mann–Whitney *U* test was employed to compare means in regular bases. Exceptional cases, requiring other statistical tests, are specified in the corresponding section.

The statistical analysis was performed with the software GraphPath Prism (Version 6.1.1). For the selection of the representative Z-stacks used to count MCs in the skin, an algorithmic selection was used (Fig. 11B).

5 Results

5.1 Effects of MCs in chronic contact hypersensitivity (CCHS)

5.1.1 Genetically MC-deficient Sash mice show exacerbated CCHS reactions

The role of MCs in CCHS induced by multiple subsequent challenges with the contact allergen oxazolone (OXA) was assessed by comparing the ear swelling of genetically MC-deficient C57BL/6-Kit^{W-Sh}/Kit^{W-Sh} (Sash) mice with the ear swelling of control wildtype (WT) mice. To this end, the ears of mice were challenged with OXA 3 times, on day 0, day 30 and day 60, using the "left-right-left" approach (*see* methods section 4.8.2.2). To compare CCHS responses of Sash mice and WT mice, the area under the curve (AUC) was calculated for each animal using the ear swelling measurements performed during eight days after each challenge (AUC$^{initial\ day\ -\ end\ day}$).

After the 1st challenge with OXA, i.e. during acute CHS, WT mice as well as Sash mice showed maximum inflammation on day 2, and inflammatory responses subsided around day 8 after the challenge (Fig. 13A, CHS area). After the 1st challenge the ear swelling did not show significant differences between Sash mice and WT mice (AUC$^{1-8}$: Sash = 275.2±91.1, WT = 203.9±47.2; n.s.).

After the 2nd challenge with OXA, both Sash and WT mice showed maximum inflammation on day 1 after its elicitation. In the WT group, the inflammatory responses were completely resolved by day 7 after this challenge (day 37), whereas in the Sash group the inflammation required more than 8 days to disappear completely (Fig. 13A). The ear swelling responses after the 2nd challenge with OXA in Sash mice were 2.1 fold higher than those in their WT control littermates (AUC$^{30-38}$: Sash 512.6±374.8, WT = 244.3±109.6; p-value < 0.01).

A

B

C
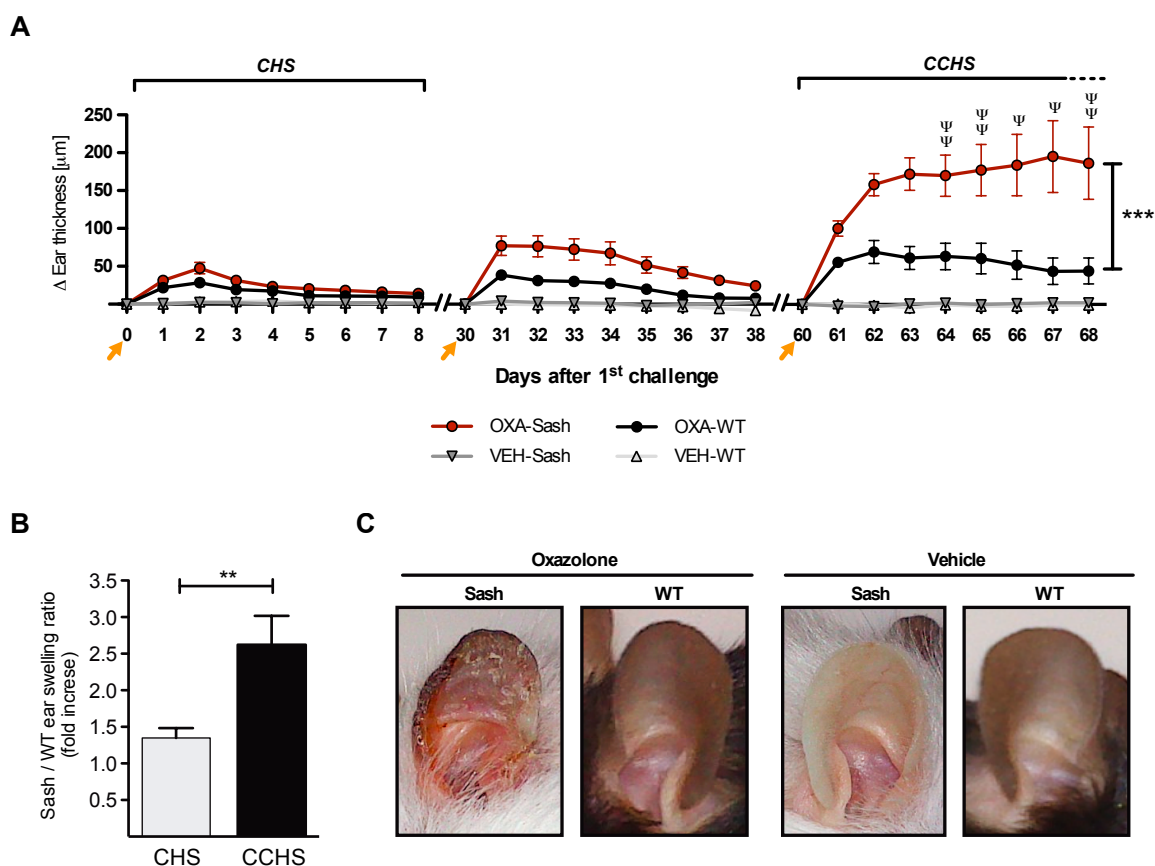
Figure 13. Genetically mast cell-deficient Sash mice exhibit exacerbated inflammation during chronic contact hypersensitivity (CCHS) reactions to oxazolone (OXA). Animals were sensitized by a topical application with OXA on day -5 (belly) and inflammation was elicited by topical application (challenge) with OXA at day 0 (left ears), day 30 (right ears) and day 60 (left ears). The opposite ears were treated with vehicle (acetone) as control. (A) Ear swelling responses after each OXA challenge (Orange arrows) in mast cell-deficient mice (Sash) and WT mice. Data are shown as means of pooled values of n = 4 experiments, error bars indicate ±SEM of 20 animals per group. Statistical significance calculated with Mann–Whitney *U* test. P-value < 0.001 (***) compares OXA-challenged ears of Sash mice (OXA-Sash) versus OXA-challenged ears of WT mice (OXA-WT) after the 3rd challenge. (B) Fold increase in ear swelling of Sash mice after CHS (following the 1st challenge) and CCHS (following the 3rd challenge). (C) Ears of Sash mice and WT mice 8 days after the induction of CCHS (day 68 in A). Each image was chosen as representative of the group. *Abbreviations and legend description*: CHS - Conventional contact hypersensitivity, CCHS - chronic contact hypersensitivity, Δ Ear thickness - ear swelling obtained after the subtraction of ears thickness baseline, Ψ - indication when an individual Sash mouse ear became necrotic, ↗ - indication when mice were challenged on the ears with OXA, OXA-Sash - ears of C57BL/6-Kit^{W-Sh}/Kit^{W-Sh} mice challenged with oxazolone, OXA-WT - ears of C57BL/6-Kit^+/ Kit^+ mice challenged with oxazolone, VEH-Sash ears of C57BL/6-Kit^{W-Sh}/Kit^{W-Sh} mice treated with vehicle, VEH-WT ears of C57BL/6-Kit^+/ Kit^+ mice treated with vehicle, MC - mast cell, OXA - oxazolone.

After the 3rd challenge with OXA, the WT group showed maximum inflammation 2 days after its elicitation. In contrast, the inflammatory response in Sash mice increased gradually and reached its maximum 7 days after challenge. After this challenge, neither Sash mice nor WT mice ears thickness returned to baseline values during the observation period. The ear swelling responses after the 3rd challenge with OXA in Sash mice were 2.6 fold higher than those in their WT control littermates (AUC^{60-68}: Sash = 1355±865.7 versus WT = 516.7±526.4, p-value < 0.001; Fig. 13A the CCHS peak).

Next, we compared the inflammatory responses elicited by OXA after the 1st challenge (CHS) to those after the 3rd challenge (CCHS). The difference in the inflammation of the OXA-treated ears in Sash mice compared with that in WT mice was higher during CCHS than during CHS (p-value < 0.01; Fig. 13B). Furthermore, the visual examination of the ears revealed that around 25% of Sash mice developed scaling and necrosis of the ears that received a 3rd challenge with OXA (*see* Ψ symbol in Fig. 13C). Necrosis was not observed in WT mice after the 1st, 2nd or 3rd challenge or in Sash mice after the 1st or 2nd challenge (Fig. 13C).

These findings show that genetically MC-deficient Sash mice exhibit uncontrolled CCHS inflammation upon repeated exposure to OXA. We, therefore, hypothesized that MC can protect from exacerbated inflammation during CCHS responses.

5.1.2 Genetically MC-deficient mice exhibit increased skin levels of pro-inflammatory cytokines in CCHS

IFNɣ as well as other pro-inflammatory cytokines (i.e. IL-17 and IL-4) are up regulated within the inflamed area after single exposure to OXA in sensitized mice (Ulrich *et al.*, 2001). Additionally, the inflammation associated with CHS responses to OXA are driven by IFNɣ$^+$ effector T cells (Ku *et al.*, 2009). We, therefore, measured the levels of IFNɣ, IL-23, IL-17 and other cytokines in the ears of mice subjected to CCHS using a multiple Enzyme-linked immunosorbent assay (*see* methods section 1.12.2).
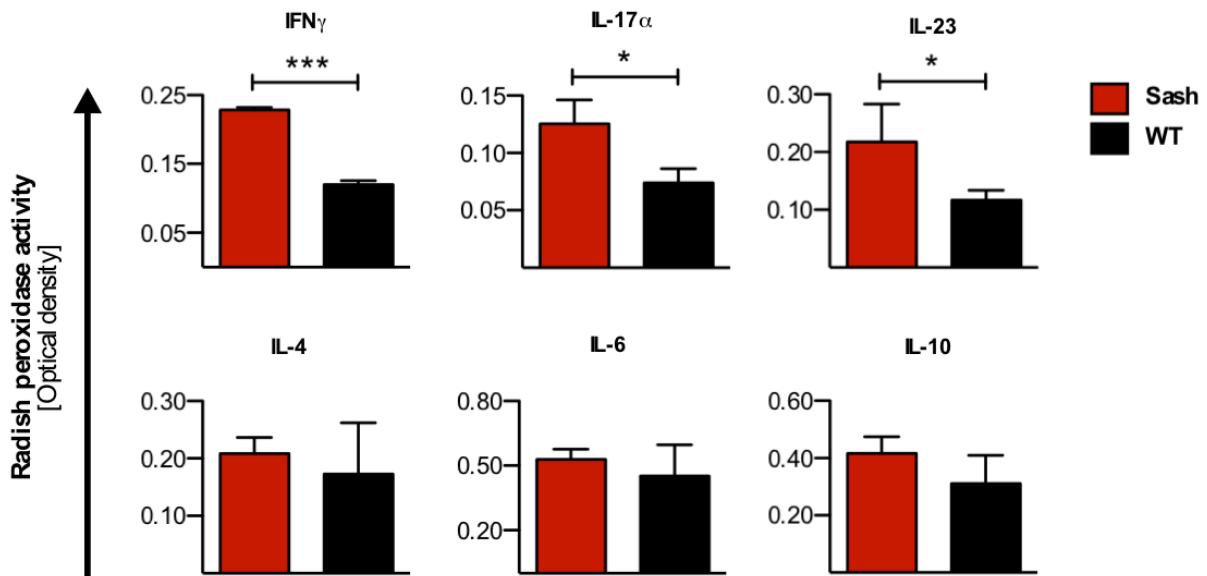
Figure 14. The pro-inflammatory cytokines IFNγ, IL-17 and IL-23 are increased at skin sites of CCHS reactions in genetically mast cell-deficient Sash mice. Cytokines levels of ear-skin were measured by ELISA 24 hours after the 3rd challenge with OXA (day 61). Data are shown as the mean of pooled values of n = 3 experiments, error bars indicate ±SEM of 9 animals per strain. Statistical significance calculated with Student's t-test. *Abbreviations and legend description*: IFNγ - interferon gamma, IL - Interleukin, p-value < 0.001 (***), p-value < 0.05 (*), Sash - ears of C57BL/6-Kit^{W-sh}/Kit^{W-sh} mice challenged with OXA, WT - ears of Wildtype mice challenged with OXA, CCHS - chronic contact hypersensitivity, MC - mast cell, OXA - oxazolone.

As early as 24 hours after the 3rd challenge with OXA, the levels of the cytokines IFNγ, IL-17 and IL-23, but not of the cytokines IL-4, IL-6 or IL-10, were significantly higher in the ears of Sash mice than in the ears of WT control mice (IFNγ p-value < 0.001; IL-17 and IL-23 p-value < 0.05; Fig. 14). These results indicate that in CCHS, exacerbated inflammation observed in Sash mice is accompanied by increased skin-levels of certain pro-inflammatory cytokines.

5.1.3 Local MC reconstitution in genetically MC-deficient Sash mice reduces CCHS-associated inflammatory reactions

To test whether the exacerbated inflammation seen in Sash animals in CCHS to OXA is due to the lack of MCs and not due to other abnormalities present in these mice, we reconstituted the ears of Sash mice with bone marrow derived cultured MCs (Sash-Ear^+BMCMC) six weeks before sensitization with OXA (*see* methods section 4.8.6).

After the 3rd challenge with OXA, maximum ear swelling of WT mice, Sash mice, and Sash-Ear[+BMCMC] mice was observed at 24 hours, 48 hours, and 24 hours, respectively. In contrast to the WT group, ear swelling responses in Sash mice and Sash-Ear[+BMCMC] mice did not resolve during the first 8 days after challenge.

Sash-Ear[+BMCMC] mice exhibited reduced inflammation after the 3rd challenge with OXA as compared to Sash mice (AUC[1-8]: Sash-Ear[+BMCMC] = 476.7±268.4 versus Sash = 926.3±375.4, p-value < 0.001; Fig. 15A). Sash-Ear[+BMCMC] mice did not show scaling or necrosis, whereas 4 out of 15 Sash mice developed scaling and necrosis of OXA-treated ears during CCHS inflammation (Fig. 15A, *see* scaling or necrosis symbol "Ψ"). CCHS ear swelling responses in MC-reconstituted Sash mice were similar to those in WT mice in their kinetics and extent, although statistically significantly stronger mice.
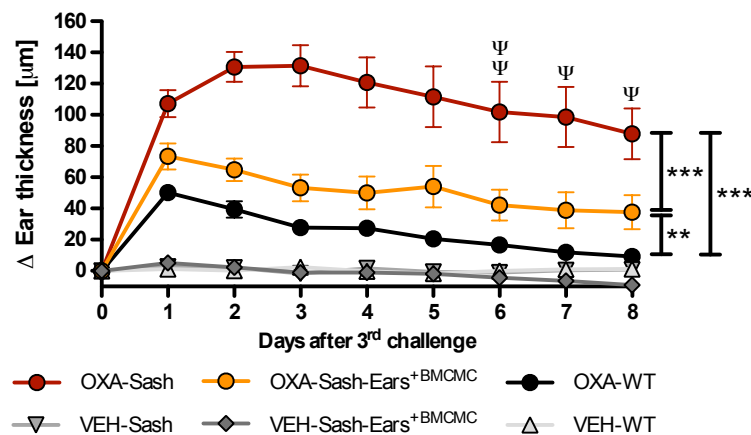
Figure 15. Reconstitution of mast cells (MCs) in the ears of genetically mast cell-deficient Sash mice protects from exacerbated inflammation during CCHS reactions to OXA. Ear swelling responses after the 3rd challenge with OXA in Sash mice, WT mice and Sash mice locally reconstituted with MCs in the ears (Sash-Ears[+BMCMCs] mice). Data are shown as means of pooled values of n = 4 experiments, error bars indicate ±SEM of 15 animals per group, Statistical significance calculated with Mann–Whitney *U* test. *Abbreviations and legend description*: Ψ - indication when an individual Sash mouse ear became necrotic, Δ Ear thickness - ear swelling obtained after the subtraction of ears thickness baseline, p-value < 0.001 (***), p-value < 0.01 (**), OXA-Sash - left ears of C57BL/6-*Kit[W-Sh]/Kit[W-Sh]* mice challenged with oxazolone, OXA-Sash-Ears[+BMCMCs] - left ears of C57BL/6-*Kit[W-Sh]/Kit[W-Sh]* mice reconstituted with BMCMCs in the ears and challenged with oxazolone, OXA-WT - left ears of Wildtype mice challenged with oxazolone, VEH-Sash - right ears of C57BL/6-*Kit[W-Sh]/Kit[W-Sh]* mice treated with vehicle, VEH-Sash-Ears[+BMCMCs] - right ears of C57BL/6-*Kit[W-Sh]/Kit[W-Sh]* mice reconstituted with BMCMCs in the ears and treated with vehicle, VEH-WT - right ears of Wildtype

mice treated with vehicle, MCs - mast cells, CCHS - chronic contact hypersensitivity, OXA - oxazolone, BMCMCs - bone marrow derived mast cells.

Taken together, the skin reconstitution of Sash mice with MCs protects from the exacerbation of CCHS inflammatory responses in this mice. Restoring the MC population in the ears of Sash mice not only abrogates the appearance of necrosis during CCHS responses to OXA, but also reduces the degree of inflammation to a level that falls between that of Sash mice and WT mice.

These results led us to conclude that exacerbated inflammation in MC-deficient Sash mice is largely due to their lack of cutaneous MCs.

5.1.4 Depletion of skin MCs results in an increased CCHS associated inflammation

Sash mice contain aberrant immune cell populations, e.g. myeloid-derived suppressor cells (MDSC) (*see* introduction section 3.3.4). Interactions between reconstituted MCs and these aberrant populations could account for the lower response observed in Sash-Ear^{+BMCMC} mice during CCHS inflammatory responses to OXA, e.g. engrafted MCs could promote the suppressive activity of MDSC. We, therefore, made use of a *Kit*-independent MC-deficient mouse model, the MCPT5-Cre x iDTR mouse, to validate the results found in Sash mice. MCPT5-Cre x iDTR mice are conditional knockout animals and treatment with diphtheria toxin (DT) depletes their skin MCs (*see* methods section 4.8.3).

First, we assessed the MC numbers in the skin of DT-treated MCPT5-Cre^{+}iDTR^{+} (Cre^{+}) mice and of their control littermates, the DT-treated MCPT5-Cre^{-}iDTR^{+} (Cre^{-}) mice, before sensitization and after the 3rd challenge with OXA. DT treatment was started 4 weeks before sensitization with OXA. At that time point DT-treated Cre^{+} mice showed 90% reduction in skin MC numbers as compared to their DT-treated Cre^{-} littermates (Fig. 16A). This result was consistent with previously published reports on this mouse strain (Dudeck *et al.* 2011). After CCHS to OXA, the reduction of MCs in DT-treated Cre^{+} mice compared with their control littermates was 71.5% (Fig. 16B). This is in contrast to the situation observed in Sash mice after CCHS to

OXA, which show less than 3% of the skin-MCs numbers as compared with WT control mice (Fig. 16B).

A

Ears of unsensitized DT-treated mice
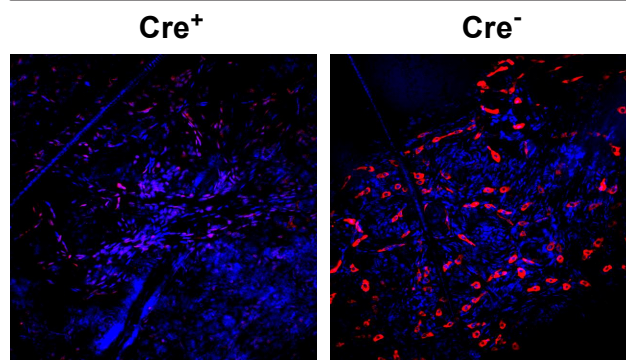
B
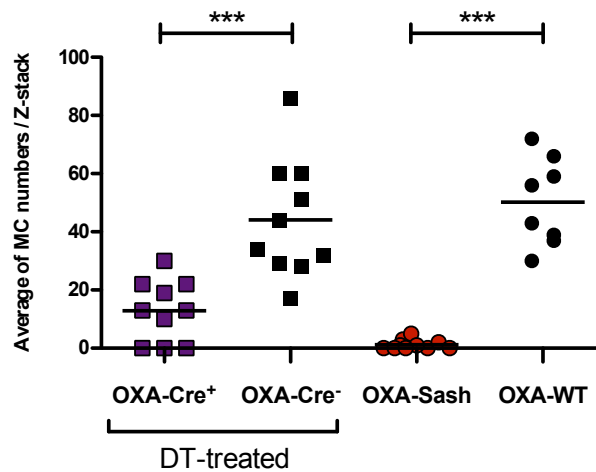
C
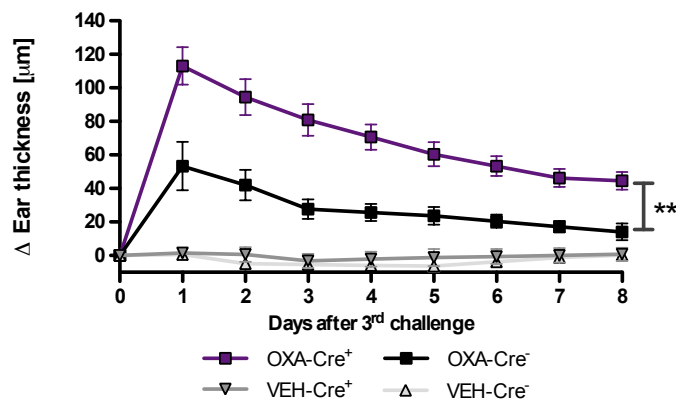
Figure 16. Mice depleted of MCs display increased inflammation during CCHS reactions to OXA. (A) Efficiency of mast cell depletion in MCPT5-Cre x iDTR mice before sensitization to OXA. Naive Cre[+] mice and their control littermates (naive Cre[-] mice) were treated weekly for 4 weeks with diphtheria toxin (DT). The pictures show MCs in a whole mount immunofluorescence staining of ear

skin. MCs were stained with Avidin-TR (red) and the nuclei were stained with DAPI (blue) as counterstain. The pictures show a confocal Z-stack of ear whole mounts at 40x magnification. (B) Quantification of MCs using whole mount immunofluorescence staining of ear skin one month after CCHS to OXA. All mice were sensitized with OXA on day -5 (belly) and challenged with the same hapten on day 0 (left ears), day 30 (right ears) and day 60 (left ear). The opposite ears were treated with vehicle (acetone) as control. Cre[+] and Cre[-] mice received weekly i.p. injections of DT starting 5 weeks before the 1st challenge with OXA until 4 weeks after the 3rd challenge with OXA. Ears of Cre[+], Cre[-], Sash and WT mice were harvested 4 weeks after the 3rd challenge and the numbers of MCs were determined by confocal microscopy. Data are shown as means of pooled values of n = 2 experiments. Statistical significance calculated with Student's t-test. (C) Ear swelling responses after the induction of CCHS in Cre[+] mice and Cre[-] mice. Mice were treated with DT and challenged with OXA as described in panel B. Data are shown as means of pooled values of n = 3 experiments, error bars indicate ±SEM of 12 animals per group. Statistical significance calculated with Mann–Whitney *U* test. *Abbreviations and legend description*: DT - Diphtheria toxin, Cre[+] - naive MCPT5-Cre[+] iDTR[+] mice, Cre[-] naive MCPT5-Cre[-] iDTR[+] mice, p-value < 0.001 (***), OXA-Cre[+] - left ears of MCPT5-Cre[+] iDTR[+] mice challenged with oxazolone, OXA-Cre[-] - left ears of MCPT5-Cre[-] iDTR[+] mice challenged with oxazolone, OXA-Sash - left ears of C57BL/6-*Kit[W-Sh]/Kit[W-Sh]* mice challenged with oxazolone, OXA-WT - left ears of Wildtype mice challenged with oxazolone, Δ Ear thickness - ear swelling obtained after the subtraction of ears thickness baseline, VEH-Cre[+] - right ears of MCPT5-Cre[+] iDTR[+] mice treated with vehicle, VEH-Cre[-] - right ears of MCPT5-Cre[-] iDTR[+] mice treated with vehicle, p-value < 0.01 (**), DAPI - 4' orto 6-diamidino-2-phenylindole, Avitin-TR - avidin coated Texas-red dye, MCs - mast cells, CHS - chronic contact hypersensitivity, OXA - oxazolone.

The maximal ear swelling of both, Cre[+] and Cre[-] mice was observed 24 hours after the 3rd challenge with OXA. In contrast to Cre[-] mice, ear swelling responses in Cre[+] mice did not subside within the first 8 days after this challenge.

Despite the failure of DT treatment to deplete MCs by more than 90% in Cre[+] mice, the ear swelling of DT-treated Cre[+] mice after the 3rd challenge with OXA was 2.01 fold stronger than that observed in Cre[-] control mice (AUC[1-8]: Cre[+] = 621.5±210.1, Cre[-] = 297.9±127.7; p-value < 0.001; Fig. 16C).

Both MC-deficient mouse models, i.e. DT-treated Cre[+] and Sash mice, displayed increased inflammation after CCHS to OXA compared with their respective control littermates (*see* results section 5.1.1), but the exacerbation of inflammation in Cre[+] mice was less pronounced compared to that in Sash mice (*compare* Fig. 15A to Fig. 16C). Furthermore, DT-treated Cre[+] animals subjected to CCHS did not show any signs of scaling or necrosis as was observed in Sash mice.

Together, these results confirm that cutaneous MCs play a protective role and control inflammatory responses during CCHS to OXA. In addition, the differences in the exacerbation of inflammation between Sash mice and DT-treated Cre[+] mice after CCHS to OXA suggests that the numbers of MCs in the challenged skin may influence the extent of the inflammatory response.

5.1.5 Cromolyn treatment results in increased CCHS associated inflammation

Here, we tested whether the treatment with cromolyn, which has been reported to inhibit selected MC functions, affects CCHS inflammatory responses in WT mice (*see* methods section 4.8.5).

As depicted in figure 17, mice treated with cromolyn (WT^{Cromolyn}) showed maximal inflammatory responses 48 hours after the induction of CCHS to OXA, whereas the maximum inflammation of control mice treated with Saline (WT^{Vehicle}) peaked much earlier (at 24 hours). In both groups, i.e. WT^{Cromolyn} and WT^{Vehicle}, the ear-thickness decreased gradually after the day of maximal inflammation, but it did not reach baseline values within the next 8 days after the 3rd challenge with OXA (Fig. 17).
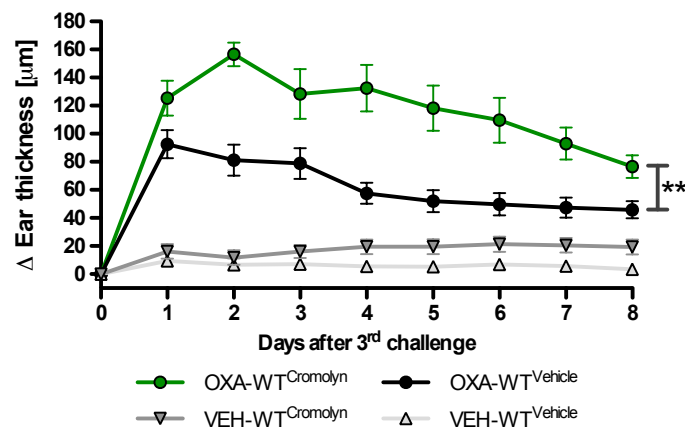
Figure 17. Systemic treatment with the mast cell-inhibitor cromolyn results in increased CCHS responses to OXA. Mice were sensitized with OXA on day -5 (belly) and challenged with OXA at day 0 (left ears), day 30 (right ears) and day 60 (left ears). The opposite ears were treated with vehicle (acetone) as control. Additionally, mice were treated with either cromolyn (WT^{Cromolyn}) or Saline (WT^{Vehicle}) at 0 hours, 24 hours and 48 hours after every challenge with OXA. Data are shown as means of pooled values of n = 4 experiments, error bars indicate ±SEM of 18 animals per group. Statistical significance calculated with Mann–Whitney *U* test. *Abbreviations and legend description*: (Δ Ear thickness - ear swelling obtained after the subtraction of ears thickness baseline, OXA-WT^{Cromolyn} - left ears of Wildtype cromolyn-treated mice challenged with oxazolone, OXA-WT - left ears of Wildtype

Saline-injected mice challenged with oxazolone, VEH-WT^{Cromolyn} - right ears of Wildtype cromolyn-treated mice painted with acetone, VEH-WT^{Vehicle} - right ears of Wildtype Saline-injected mice painted with acetone, p-value < 0.01 (**), i.p. - intraperitoneally.

The inflammation associated with CCHS in WT^{Cromolyn} mice was 1.74 fold stronger than that in WT^{Vehicle} mice (AUC$^{1-8}$: Cromolyn = 982.0±487.6, vehicle = 562.3±332.3; P-value < 0.01). This result suggests that MCs have a protective role in CCHS to OXA that can be inhibited through the pharmacological effects of cromolyn on MCs in WT animals, which proved that the increased CCHS inflammation is not restricted to MC-deficient mouse models.

Cromolyn was reported to inhibit MC degranulation in humans and rats (Ratner *et al.*, 2002, Santone *et al.*, 2008, Oka *et al.*, 2012, Vincent *et al.*, 2013, Yang *et al.*, 2014). We, therefore, tested whether cromolyn is also a MC inhibitor in mice, using MC degranulation induced by topical application of OXA as a model (*see* methods section 4.11.1.2). The ear skin of WT naive mice after single contact to OXA showed extensive MC degranulation, and this was not inhibited by treatment with cromolyn (Fig. 18).

Because treatment with cromolyn did not inhibit degranulation after OXA contact, we speculated that cromolyn inhibits MC cytokine release at sites of OXA exposure.
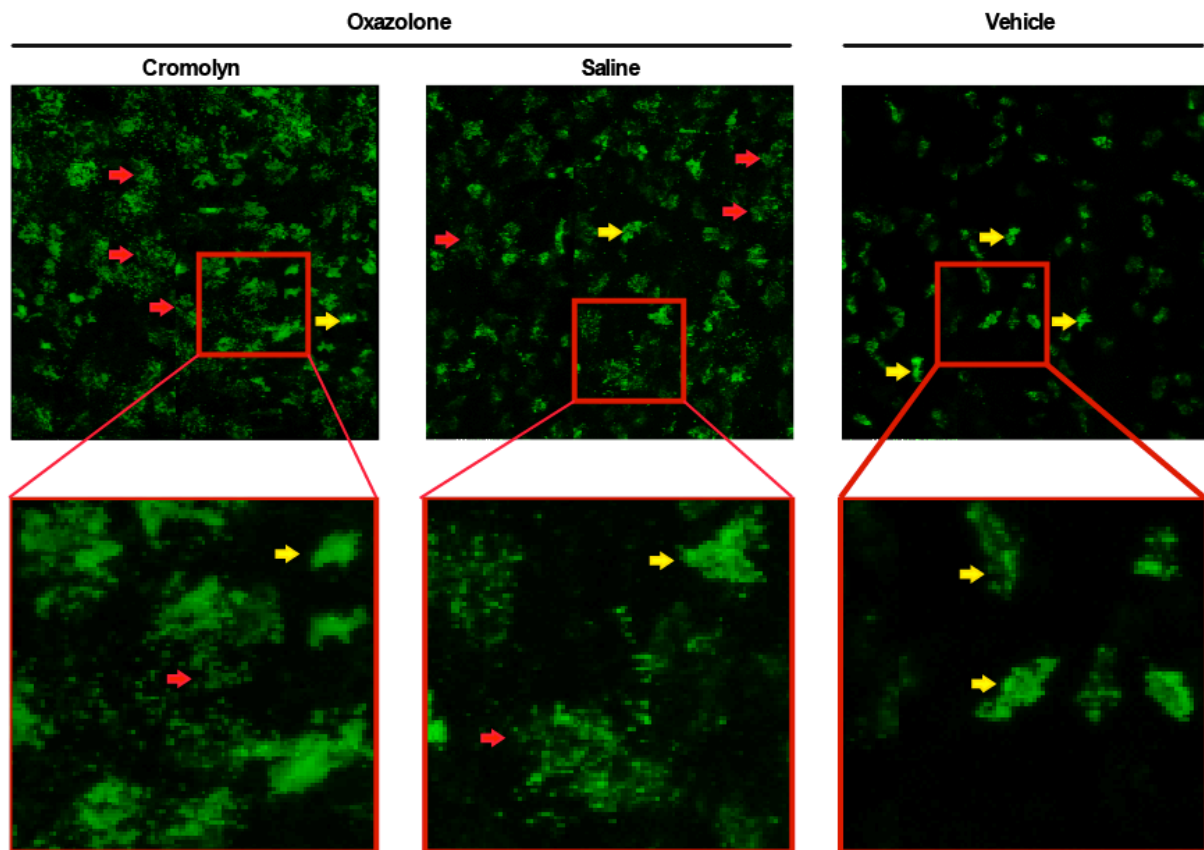
Figure 18. Cromolyn does not inhibit mast cell-degranulation induced by OXA. Naive WT mice were injected with either cromolyn or Saline (Vehicle) 30 minutes before OXA exposure on the ears. Ears painted with acetone (the vehicle of OXA) were used as control (right panel). 24 hours after hapten exposure the degranulation state of MCs within the ear skin was assessed by whole mount immunofluorescence staining using confocal microscopy (40x magnification). The Images show MC-granules stained with Avidin-TR (green). Yellow arrows indicate the granular content localized inside the cell. Red arrows indicate the granular content released from the cells to the extracellular matrix. _Abbreviations:_ MC - mast cell, OXA - oxazolone, WT - wildtype, TR - texas red.

Using confocal microscopy, the skin levels of Interleukin-4 (IL-4) were assessed in the ears of cromolyn- or vehicle-treated WT mice after the induction of CCHS responses to OXA as describe in figure 19 (*see* methods section 4.11.1.2). IL-4 was chosen as representative MC-derived cytokine, because it is produced *de novo* by skin MCs, stored in MC-granules (Fig. 19A right panel) and released upon MC activation (Gessner *et al.*, 2005).

A
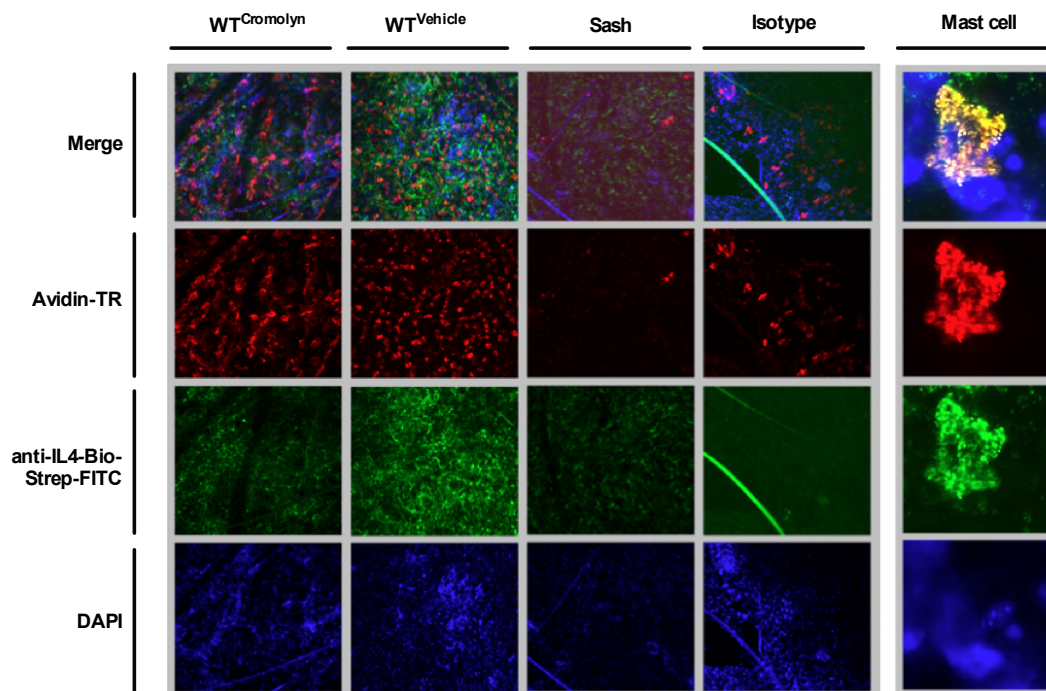
B
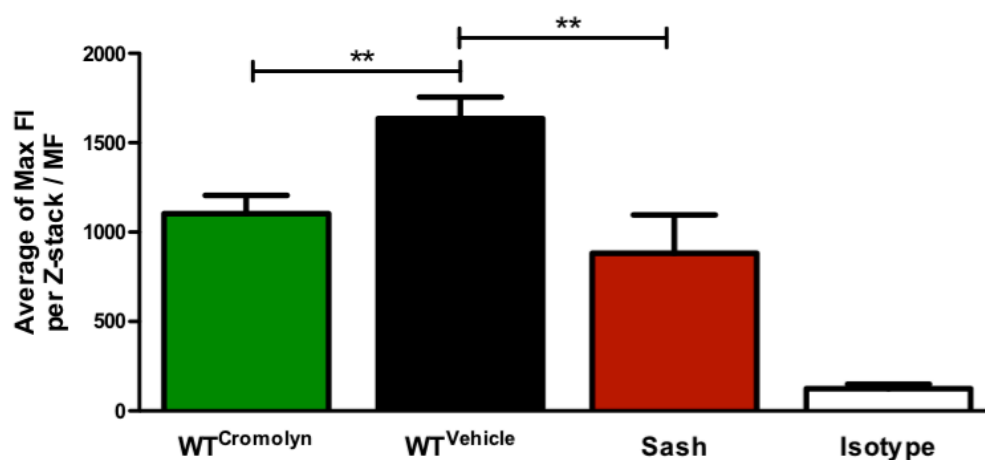
Figure 19. Cromolyn-treated WT mice exhibit reduced levels of IL-4 during the effector phase of CCHS to OXA. Mice were sensitized with OXA on day -5 (belly) and challenged with OXA at day 0 (left ears), day 30 (right ears) and day 60 (left ears). The opposite ears were treated with vehicle (acetone) as control. Additionally, mice were treated with either cromolyn (WT^{Cromolyn}) or Saline (WT^{Vehicle}) at 0 hours, 24 hours and 48 hours after every challenge with OXA. The ears of mice were prepared for whole mount immunofluorescence staining 12 hours after the 3rd challenge with OXA. Tissue levels of IL-4 on were assessed by confocal microscopy (40x magnification). The ear skin was stained with avidin-TR for MC-granules (Red), anti-IL-4-Bio-Strept-FITC (green) for IL-4 and DAPI (blue) for the nuclei. Isotype of anti-IL-4-Bio (IgG2b-Bio) was used in WT mice to control the background florescence. (A) Confocal images (40x magnification) showing the expression levels of IL-

4 in each group. The left panel displays representative images of WT^{Cromolyn} mice, WT^{Vehicle} control mice, Sash mice and Isotype control respectively. The right panel shows a high magnification (100x digital zoom) of a skin MC in a WT control positive for IL-4. (B) Quantification of the IL-4 levels in WT^{Cromolyn} mice, WT^{Vehicle} control mice and Sash mice 12h after the induction of CCHS. The calculation is based on the fluorescence intensity (FI) of the green channel (Anti-IL4-Bio-Strept-FITC). Data are shown as means of pooled values of n = 3 experiments, error bars indicate SD of 6 animals per group. Statistical significance calculated with Student's t-test. _Abbreviations_: WT^{Cromolyn} - ears of Wildtype cromolyn-treated mice, WT^{Vehicle} - ears of Wildtype vehicle-injected mice, Sash - ears of C57BL/6-Kit^{W-sh}/Kit^{W-sh} mice, TR - Texas red, Bio - Biotin, Strept – Streptavidin, FITC - Fluorescein isothiocyanate, DAPI - 4' orto 6-diamidino-2-phenylindole, FI - fluorescence intensity, p-value < 0.01 (**), IL - interleukin, CCHS - chronic contact hypersensitivity, OXA - oxazolone, MC - mast cell.

Twelve hours after CCHS induction, all groups, i.e. WT^{Cromolyn}, WT^{Vehicle} and Sash, showed IL-4 expression (Fig. 19A). WT^{Cromolyn} mice and Sash mice showed reduced levels of IL-4 as compared to WT^{Vehicle} mice (67.4%±12.4 and 53.9%±26.3 respectively). In addition, the majority of IL-4 was not found within the MC-granules but spread throughout the tissue (Fig. 19A, B), suggesting that the IL-4 was released by MCs upon OXA challenge.

This results showed that after the induction of CCHS inflammation the expression levels of IL-4 in WT^{Cromolyn} mice was similar to that of Sash mice, and clearly reduced as compared to WT^{Vehicle} mice, which make us suppose a possible MC-dependent effect on the expression levels of this cytokine. Since we found IL-4$^+$ MCs in the skin of this mice (Fig. 19), we wanted to study the effects of cromolyn treatment on the MC numbers after CCHS to OXA.

5.1.6 Cromolyn treatment inhibits MC accumulation during CCHS

To study, in more detail, the possible effect of cromolyn treatment on the cutaneous number of MCs, we quantified MCs in the ears of naive mice, of mice after CHS and of mice after CCHS treated with cromolyn or vehicle using confocal microscopy (_see_ methods section 4.11.1.2).
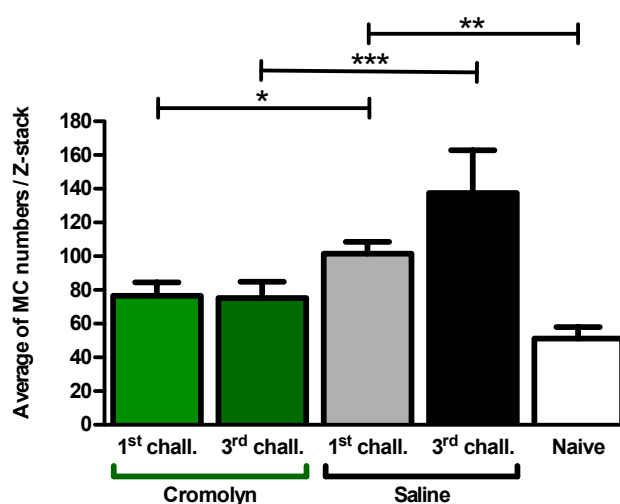
Figure 20. Cromolyn treatment prevents the increase of skin mast cell numbers associated with the application of OXA. Quantification of MCs in the ears of WT mice before and after challenge with OXA. Mice were treated with either cromolyn or Saline at 0 hours, 24 hours and 48 hours after each challenge. The ears were harvested 8 days after the 1st challenge or the 3rd challenge and the numbers of MCs were assessed by whole-mount immunofluorescence staining of ears using confocal microscopy. Data are shown as means of pooled values of n = 3 experiments, error bars indicate SD of 9 animals per group excepting for naive mice (1 animal per experiment). Statistical significance calculated with Student's t-test. _Abbreviations_: p-value < 0.05 (*), p-value < 0.01 (**), p-value < 0.001 (***), chall - challenge with oxazolone, OXA - oxazolone, i.p. - intraperitoneal, WT - Wildtype mice.

MC numbers, assessed by whole-mount immunofluorescence staining of ears, were increased after the first challenge with OXA, and subsequent OXA challenges induced further MC accumulation in the skin exposed to the hapten. The treatment with cromolyn prevented the occurrence of this phenomenon (Fig. 20). This experiment demonstrates that cromolyn reduces the accumulation of MCs associated with CHS and CCHS responses to OXA.

Taken together, two aspects of the effects of cromolyn on the CCHS responses to OXA were clarified with the previous experiments. (1) In WT mice, cromolyn treatment results in increased inflammation during CCHS responses to OXA. This observation is in accordance with the results obtained in MC-deficient strains in CCHS. (2) Challenge with OXA induces MC-accumulation in the exposed skin area and treatment with cromolyn impairs it.

Collectively, these results suggest that the inhibition of MC-accumulation by cromolyn is at least in part, responsible for its inhibitory effects on CCHS inflammation.

5.2 Mechanisms of MC control of inflammatory responses in CCHS

In this section we investigated the underlying mechanisms of the protective role of MCs in CCHS, especially the importance of previous local allergen contact.

5.2.1 MCs do not confer systemic protection from exacerbation of CCHS reactions

We investigated whether the protective role of MCs during CCHS inflammation involves systemic effects. To test this hypothesis, the initial "left-right-left" OXA challenge pattern was modified (*see* methods section 4.8.2.3), i.e. the 1st and 2nd challenges were done on the belly and the 3rd challenge on both ears (called "belly-belly-ears" approach; *see* methods section 4.8.2.3 modification 1). This experimental approach allowed us to study CCHS in previously unchallenged skin.

Using the "belly-belly-ears" approach, the inflammatory ear-skin responses in all experimental groups i.e. Sash, Sash-Ear$^{+BMCMCs}$, WT^{Cromolyn} and WT^{Vehicle}, peaked 24 hours after the 3rd challenge with OXA. The inflammation decreased slowly between days 2 to 8, but the ear thickness did not return to baseline values during the observation period (Fig. 21A). Inflammatory responses as assessed by AUC analysis did not show statistical differences between any of the experimental groups included in this experiment (AUC$^{1-8}$: WT^{Vehicle} = 390.4±94.2; WT^{Cromolyn} = 493.5±94,5, Sash = 447.0±86.3, Sash-Ear^{BMCMCs} = 483.3±83.2; n.s.).

These findings show that skin MCs protect from exacerbation of CCHS inflammation by effects in the skin during previous allergen exposure rather than by systemic effects.

5.2.2 Exacerbation of CCHS reactions is limited to sites of previous allergen contact

To further explore the relevance of site-specific effects in the protective role of MCs during CCHS responses to OXA, we next performed the 1st challenge on the left ears, the 2nd challenge on the abdominal skin and the 3rd challenge on both ears, i.e. a "left ear-belly-ears" approach (*see* methods section 4.8.2.3 modification 2). This experimental approach allowed for the assessment of MC-effects on OXA-induced

inflammation at sites that were previously exposed or not exposed to OXA within the same animal.

Using this "left ear-belly-ears" approach, the inflammatory responses in all experimental groups, i.e. Sash, WT^{Cromolyn} and WT^{Vehicle}, peaked 24 hours after the 3rd challenge with OXA. The inflammation decreased slowly between days 2 to 8 after challenge, but the ear thickness did not return to baseline during the observation period (Fig. 21B).

In the right ears, the degree of inflammation after the 3rd challenge with OXA was similar in all experimental groups (AUC$^{1-8}$: WT^{Vehicle}= 225.9±70.5, WT^{Cromolyn} = 341.8±56, Sash = 370.5±158.8; Fig. 21B, *see* dotted lines). In contrast, in the left ears, the degree of inflammation of Sash mice and WT^{Cromolyn} mice was clearly higher compared with that in the left ears of WT^{Vehicle} mice (AUC$^{1-8}$: WT^{Vehicle}= 474±99.9, WT^{Cromolyn} = 794.1±102.5, Sash = 1149±248.4; Fig. 21B, *see* continues lines).

This result indicates that the protective role of MCs during CCHS inflammation is limited to skin sites that had been pre-exposed to OXA. It also shows that skin pre-exposed to this hapten contains a sort of "local pro-inflammatory factors", because OXA pre-exposed skin sites (left ears) displayed stronger CCHS inflammatory responses than not pre-exposed skin sites (right ears).

To further explore the contribution of these "local pro-inflammatory factors", we modified the data obtain in experiment showed in figure 21B. By subtracting the ear swelling responses of the left ear from that of the right ear for each individual mouse, we obtained the Δ Local (Δ Local$_i$ = AUC$^{Left}_i$ − AUC$^{Right}_i$; The subscript "*i*" means each individual mouse). Δ Local give us information about the net contribution of MCs to the CCHS inflammatory response in OXA pre-exposed ears. Using a lineal regression analysis, we show that the mean values of ΔLocal in the Sash group and in the WT^{Cromolyn} group are statistically higher than that in the WT^{Vehicle} control group (Fig. 21C, p-value < 0.001 and <0.05 respectively). This result suggests that the protective effects of MCs in CCHS to OXA consist in controlling these "local pro-inflammatory factors", which are only present in OXA pre-exposed skin sites.
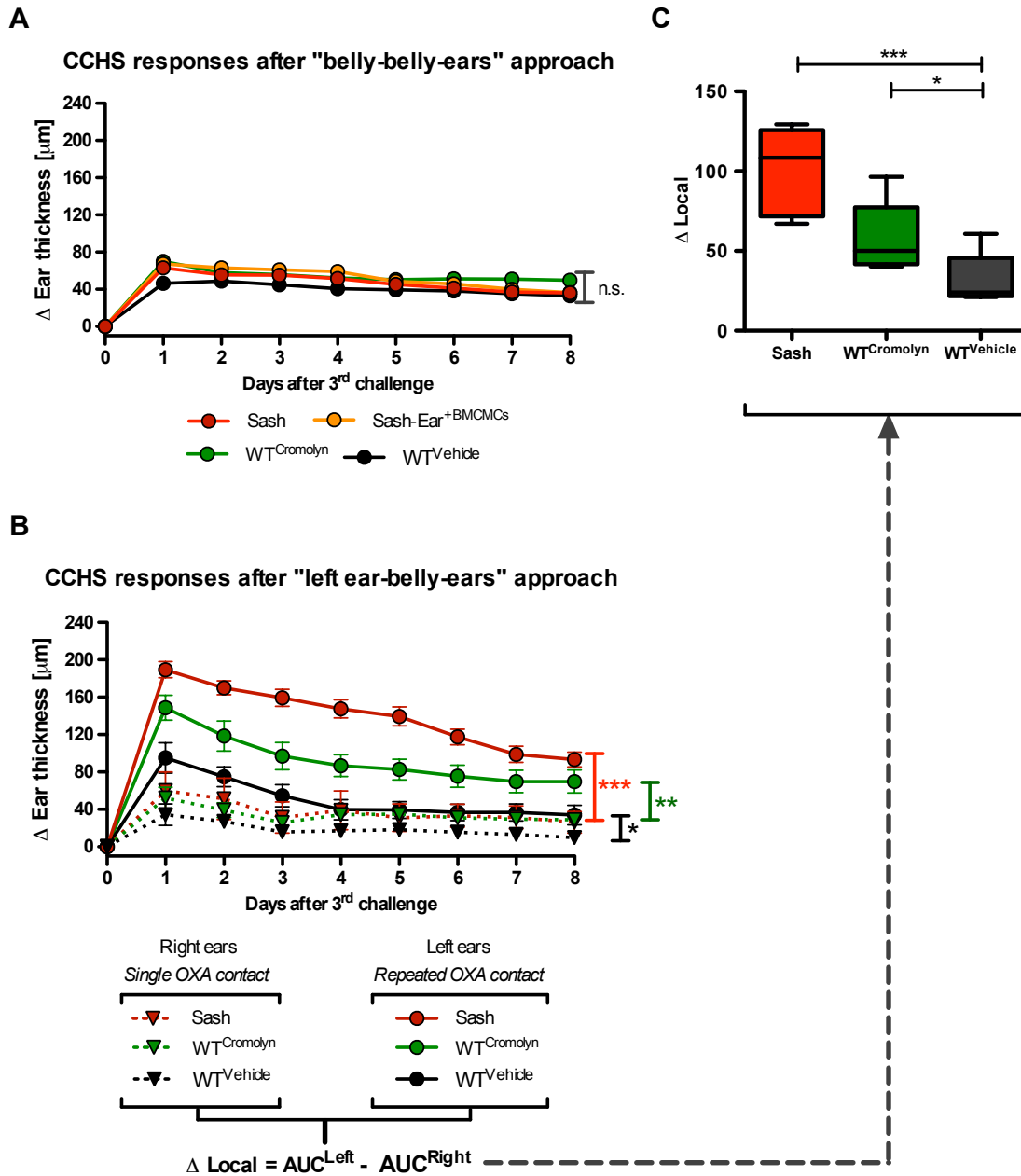
Figure 21. MCs provide local, but not systemic protection during CCHS inflammatory responses to OXA. (A) The *"belly-belly-ears" approach:* Ear swelling responses after 3rd challenge with OXA. Sash mice, Sash-EAR[+BMCMCs] mice, WT[Cromolyn] mice and WT[Vehicle] mice were sensitized with OXA on the abdominal skin (day -5) and challenged with the same hapten on day 0 (belly), day 30 (belly) and day 60 (both ears). Data are shown as means of pooled values of n = 4 experiments, error bars indicate ±SEM of 18 animals per group. Statistical significance was calculated with Student's t-test. (B) The "left ear-belly-ears" approach: Ear swelling after 3rd challenge with OXA. Sash mice, WT[Cromolyn] mice and WT[Vehicle] mice were sensitized with OXA on the abdominal skin (day -5) and challenged with the same hapten at day 0 (left ears), day 30 (belly) and day 60 (both ears). Right ears (inverted triangles), which received a single challenge with OXA, are plotted as dotted lines. Left ears (circles), which were formerly exposed to OXA in the 1st challenge, are plotted as continues lines. (C) Linear regression analysis of net ear swelling on the left ears. The AUC of each ear was calculated

from data of panel B. The plot compares Sash mice and WT^{Cromolyn} mice group versus WT^{Vehicle} mice. Data are shown as means of pooled values of n = 3 experiments, error bars indicate ±SEM of 12 animals per group. Statistical significance calculated with linear regression. *Abbreviations and legend description*: CCHS - chronic contact hypersensitivity, Δ Ear thickness - ear swelling obtained after the subtraction of ears thickness baseline, p-value > 0.05 (n.s.), Sash - ears of C57BL/6-*Kit^{W-Sh}/Kit^{W-Sh}* mice challenged with oxazolone, Sash-Ears$^{+BMCMCs}$ ears of C57BL/6-*Kit^{W-Sh}/Kit^{W-Sh}* mice reconstituted with BMCMCs in the ears and challenged with oxazolone, WT^{Cromolyn} - ears of C57BL/6-*Kit$^+$/Kit$^+$* cromolyn-treated mice challenged with oxazolone, WT^{Vehicle} - ears of C57BL/6-*Kit$^+$/Kit$^+$* Saline-injected mice challenged with oxazolone, p-value < 0.05 (*), p-value < 0.01 (**), p-value < 0.001 (***), OXA - oxazolone, AUC - area under the curve, n.s. - non-significant, Δ Local - average value obtained after the subtraction of left ears swelling from right ears swelling of each mouse.

5.3 Effects of MCs on the composition of the local immune compartment in CCHS

5.3.1 CD8β$^+$ T cell accumulation at sites of allergen challenge is increased in MC-deficient mice in CCHS

As demonstrated above, the MC-driven control of inflammation in CCHS to OXA is dependent on a previous OXA exposition in the same ears, presumably by controlling "local pro-inflammatory factors" present in OXA pre-challenged skin. Hence we hypothesized that MCs protect from exacerbated inflammation in CCHS to OXA by modulation of the local skin immune system.

Since contact hypersensitivity responses are mediated largely by T cells (Xu *et al.* 1996), we first examined OXA pre-exposed ears looking for changes within the T cell compartment one month after the 3rd challenge with OXA (CCHS ears), i.e. at a time when inflammatory responses after the 3rd OXA-challenge were already resolved.

First, we used WT mice and compared the composition of the T cell compartment in ear skin of naive mice with that in the skin of CCHS ears.

CCHS ears of WT mice showed significantly increased numbers of CD8β$^+$ T cells and CD4$^+$ T cells compared with WT naive mice (Fig. 22.), indicating that T cell accumulation in CCHS ears occurs as a consequence of challenge with OXA.
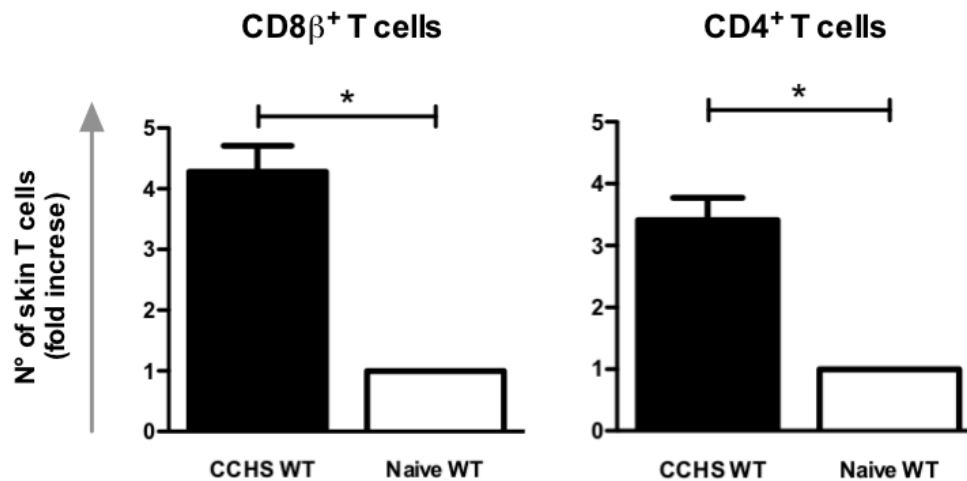
Figure 22. CCHS ears contain more CD8β^{+} T cells and CD4^{+} T cells, in their ears than naive mice. Quantification of skin resident T lymphocytes in CCHS ears and ears of naive mice. The ears of naive mice or of mice that were OXA-challenge on the ears for 3rd time for four weeks, were harvested and their T cell composition was analyzed by flow cytometry. Data are shown as means of pooled values of n = 3 experiments, error bars indicate ±SEM of 9 animals per group. Statistical significance calculated with non-parametric Wilcoxon test. *Abbreviations*: P-value < 0.05 (*), CCHS WT - ears of Wildtype mice challenged with oxazolone, Naïve WT - ears of Wildtype naive mice, CCHS - chronic contact hypersensitivity, OXA - oxazolone.

Next, we investigated whether the T cell composition in CCHS ears differs between Sash mice, WT[Cromolyn] mice and WT[Vehicle] control mice.

No differences were found between groups (Figure 23A) in the numbers of CD4^{+} T cells in CCHS ears. This result was verified in the MCPT5-Cre x iDTR strain, where both groups, Cre^{-} and Cre^{+} showed comparable numbers of CD4^{+} T cells in CCHS ears (Fig. 23B).

When we assessed CD8β^{+} T cells in CCHS ears, the Sash mice exhibit 3.8 [2.78 – 4.82] fold higher numbers as compared to their WT[Vehicle] control littermates (Fig. 23A). WT[Cromolyn] mice showed higher numbers of CD8β^{+} T cells in CCHS ears compared with WT[Vehicle] control mice, but this difference was not significant (Fig. 23A). This result was verified in the MCPT5-Cre x iDTR strain, where the numbers of CD8β^{+} T cells in CCHS ears of Cre[+] mice were 3.1 [1.23 – 4.97] fold higher than in those of their Cre[-] control littermates (Fig. 23B).
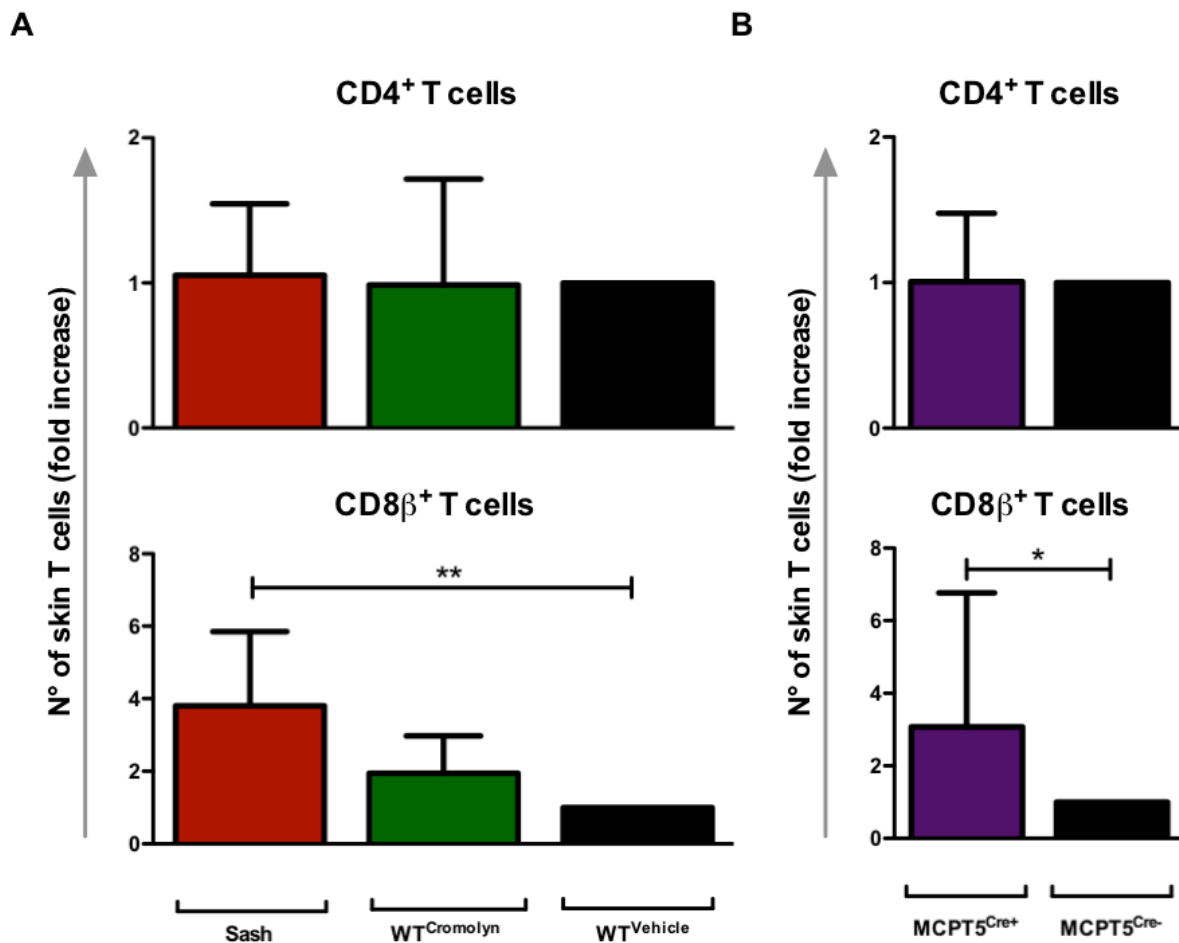
Figure 23. Mast cell-deficient mice show higher numbers of CD8β⁺ T cells, but not CD4⁺ T cells, in their ears after CCHS to OXA. Four weeks after the 3rd challenge with OXA the ear skin of mice was harvested and the T cell composition was analyzed by flow cytometry. (A) Quantification of skin resident T lymphocytes in Sash and WT mice. Upper bar diagram shows the n-fold change of CD4⁺ T cells of Sash mice, WT^{Cromolyn} mice in comparison to WT^{Vehicle} control mice. The lower bar diagram shows the same as the upper plot for CD8β⁺ T cells. (B) Quantification of skin resident T lymphocytes in MCPT5-Cre x iDTR strain one month after the 3rd challenge with OXA. Upper bar diagram shows the n-fold change of CD4⁺ T cells of Cre⁺ mice in relation to Cre⁻ control mice. The lower bar diagram shows the same as the upper plot for CD8β⁺ T cells. Data are shown as means of pooled values of n = 3 experiments, error bars indicate ±SEM of 9 animals per group. Statistical significance calculated with non-parametric Wilcoxon test. _Abbreviations_: P-value < 0.05 (*), p-value < 0.01 (**), Sash - ears of C57BL/6-Kit^{W-Sh}/Kit^{W-Sh} mice challenged with oxazolone, WT^{Cromolyn} - ears of Wildtype cromolyn-treated mice challenged with oxazolone, WT^{Vehicle} - ears of Wildtype Saline-injected mice challenged with oxazolone, Cre⁺ - ears of MCPT5-Cre⁺iDTR⁺ DT-treated mice challenged with oxazolone, Cre⁻ - ears of MCPT5-Cre⁻iDTR⁺ DT-treated mice challenged with oxazolone, MC - mast cell, CCHS - chronic contact hypersensitivity, OXA - oxazolone.

These experiments demonstrated that CD4$^+$ and CD8β$^+$ T lymphocytes accumulate in CCHS ears. CD8β$^+$ T cells but not CD4$^+$ T cells were markedly increased in the CCHS ears of MC-deficient mice.

5.3.2   Most CD8β$^+$ T cells at sites of allergen challenge in CCHS are tissue resident memory (TRM) T cells

Skin tissue resident memory (TRM) T cells are T lymphocytes that migrate to the skin, survive there for long periods of time *in situ*, and persist under non-inflammatory conditions.

TRM T cells are characterized by the additional expression of CD103 and CD44^{high} (Gebhardt and Mackay, 2012, Mackay *et al.*, 2013). In our settings, only CD8β$^+$ T cells were increased in the CCHS skin of MC-deficient mice. Hence, using FACS, we analyzed in detail the immunophenotype of the CD8β$^+$ T cell compartment in OXA-treated ears (*see* methods section 4.10.1).

When we assessed CD4, CD44, CD45, CD103 and TCRβ expression of CD8β$^+$ T cells in CCHS ears, we found that these CD8β$^+$ T cells in the ears of both, Sash mice and WT mice were negative for CD4, and positive for CD44, CD45, CD103 and TCRβ (Fig. 24).

The expression of CD103 together with the co-expression of high levels of CD44 confirmed that CD8β$^+$ T cells in CCHS ears are, by and large, TRM T cells.
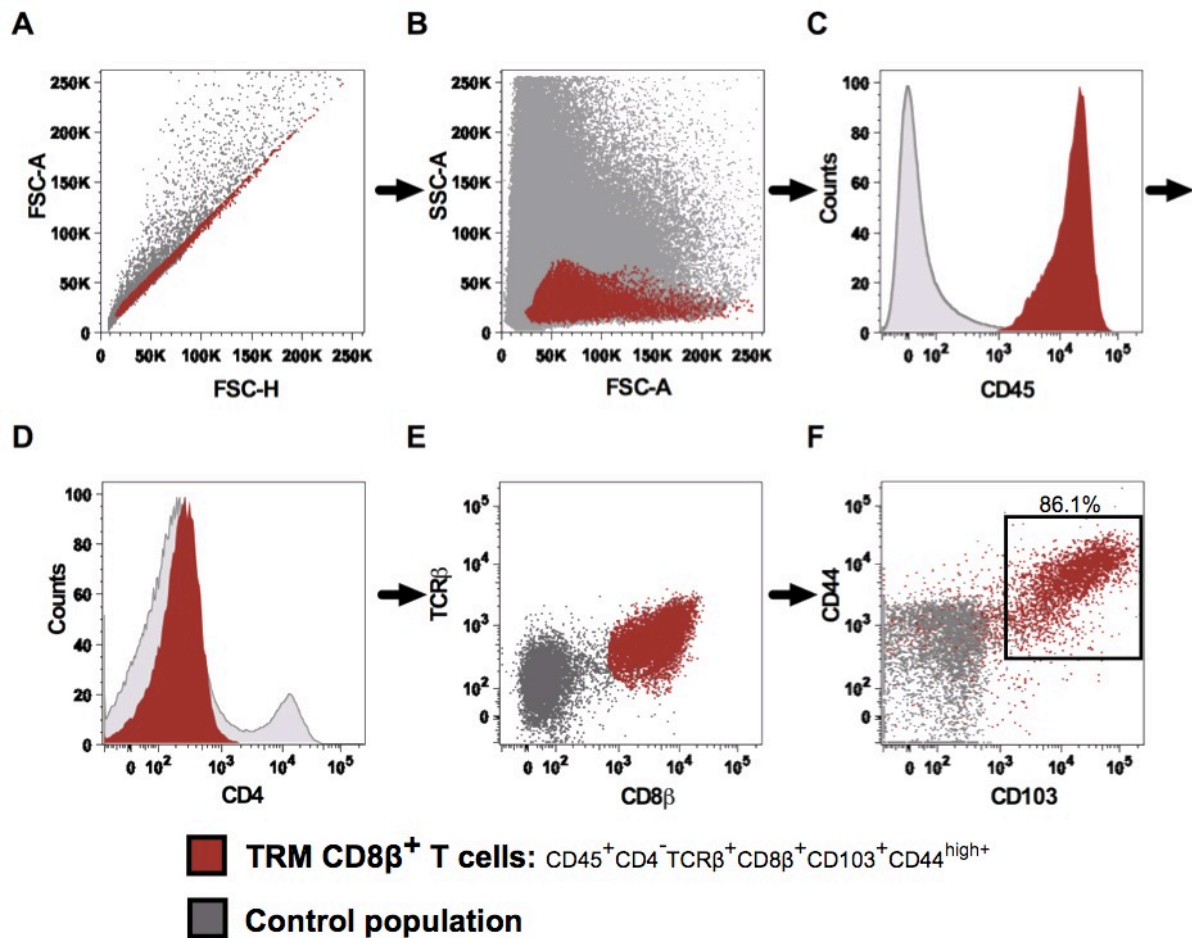
Figure 24. The phenotype of CD8β⁺ T cells in CCHS ears corresponds to the TRM T cell sub-type. Four weeks after the 3rd challenge with OXA the ear skin of mice was harvested and the immunophenotype of CD8β⁺ T cells was analyzed by flow cytometry. To achieve phenotypic characterization, the selected cells (red colored) were consecutively back gated from F to A. The gray dots from panel A to E represent the ungated population within the same cell suspension, whereas in figure F, the gray dots correspond to the isotype controls for CD44 and CD103. (F) 86.1% [82.1- 88.3] of the CD45⁺CD4⁻TCRβ⁺CD8β⁺ cells co-expressed CD44^{high} and CD103. _Abbreviations_: FSC - forward Scatter-Area, SSC - side scatter, TCRβ - T cell receptor beta subunit, TRM - tissue resident memory.

5.3.3 TRM CD8β⁺ T cells in CCHS OXA-challenged ear skin produce interferon gamma

One of the most important mediators of OXA-induced contact hypersensitivity reactions is IFNɣ (Ku _et al._, 2009). Additionally, previous results obtained in this study (_see_ results section 5.1.2) show that 24 hours after the 3rd challenge with OXA Sash animals exhibited enhanced levels of IFNɣ. We, therefore, analyzed TRM CD8β⁺ T cells for their IFNɣ production in CCHS responses.

Using whole mount immunofluorescence staining, we found that 24 hours after the 3rd challenge with OXA, the most prominent source of IFNɣ, in OXA-treated ears, was indeed CD8β$^+$ T cells (Fig.25), suggesting that MCs may protect from exacerbation of CCHS inflammatory responses by controlling the numbers of IFNɣ producing TRM CD8β$^+$ T cells. These findings reinforced the possible role of TRM CD8β$^+$ T in that model.
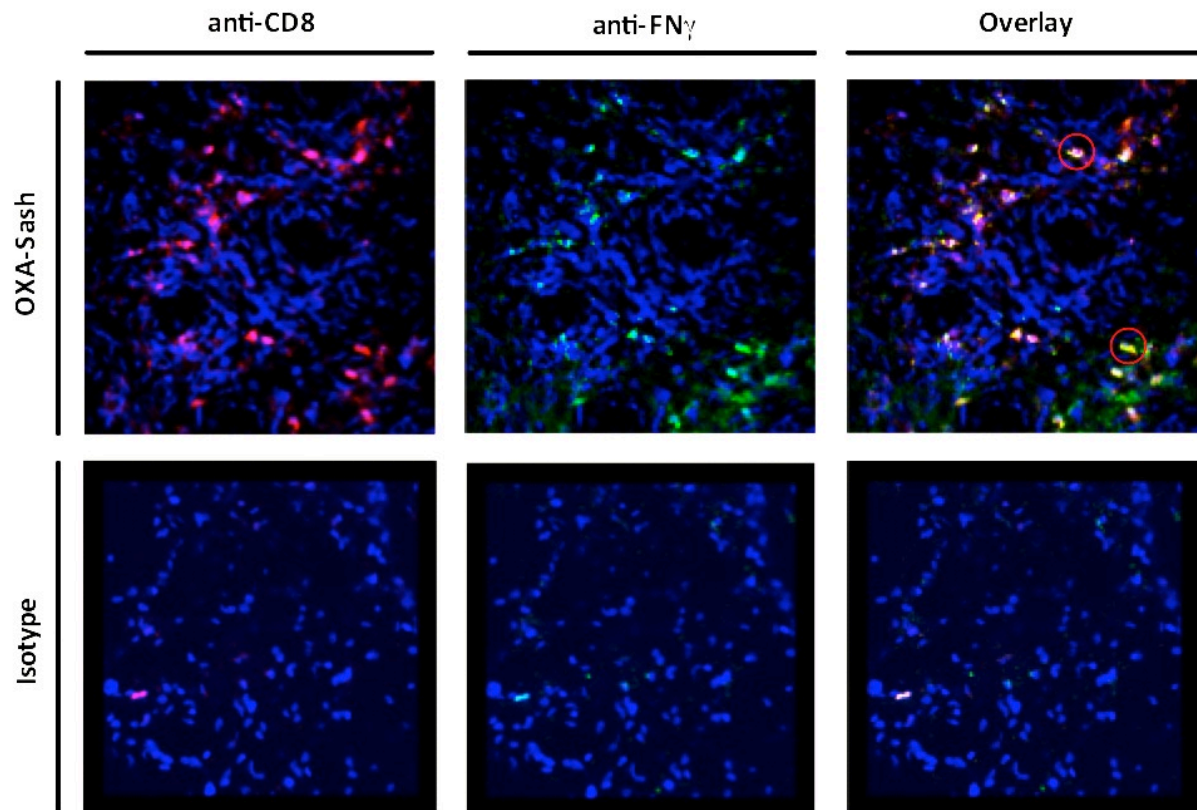
Figure 25. In CCHS, CD8β$^+$ T cells express IFNɣ upon OXA-contact *in situ*. The CCHS ears of Sash mice were harvested 24 hours after the 3rd challenge with OXA and prepared for whole mount immunofluorescence staining. The upper row shows ear skin stained with anti-CD8β-PE (red) and anti-IFNɣ-Bio-Strept-FITC (green). The opposite ear was stained with isotype control antibodies (lower row). In all the samples the nuclei was stain with DAPI (blue) as counterstaining. Red circles show examples of cells co-expressing CD8β and IFNɣ. The pictures show a confocal z-stack with a 40x magnification objective. *Abbreviations*: Anti-CD8 - antibody against CD8, Anti-IFNɣ - antibody against Interferon-gamma, OXA-Sash - ears of C57BL/6-*Kit*$^{W-sh}$/*Kit*$^{W-sh}$ after challenge with oxazolone, DAPI - 4' orto 6-diamidino-2-phenylindole, Bio - biotin, Strept - streptavidin.

5.3.4 Innate immune cells accumulation at sites of allergen challenge is increased in MC-deficient mice in CCHS

Next, we tested whether, in addition to TRM CD8β$^+$ T cells, innate immune cells numbers, e.g. DC, macrophages, neutrophils, are increased in CCHS ears of MC-deficient mice. Using flow cytometry, we gated out T cell populations from innate immune cell populations by selecting CD45$^+$CD3$^-$ cells, and assessed the numbers of these cells in the ears of mice one month later after the 3rd challenge with OXA (CCHS ears), i.e. at a time when inflammatory responses after the 3rd challenge were resolved.

The numbers of CD45$^+$CD3$^-$ cells in CCHS ears were 2.5 [2.25 – 2.75] fold higher in Sash mice as compared to their WT^{Vehicle} control littermates (Fig. 26A). WT^{Cromolyn} mice showed higher numbers of CD45$^+$CD3$^-$ cells compared with WT^{Vehicle} control mice, but this difference was not significant (Fig. 26A). In the MCPT5-Cre x iDTR strain, the numbers of CD45$^+$CD3$^-$ cells in CCHS ears were 3.3 [3.07 – 3.59] fold higher the Cre$^+$ mice compared with their Cre$^-$ control littermates (Fig. 26B).
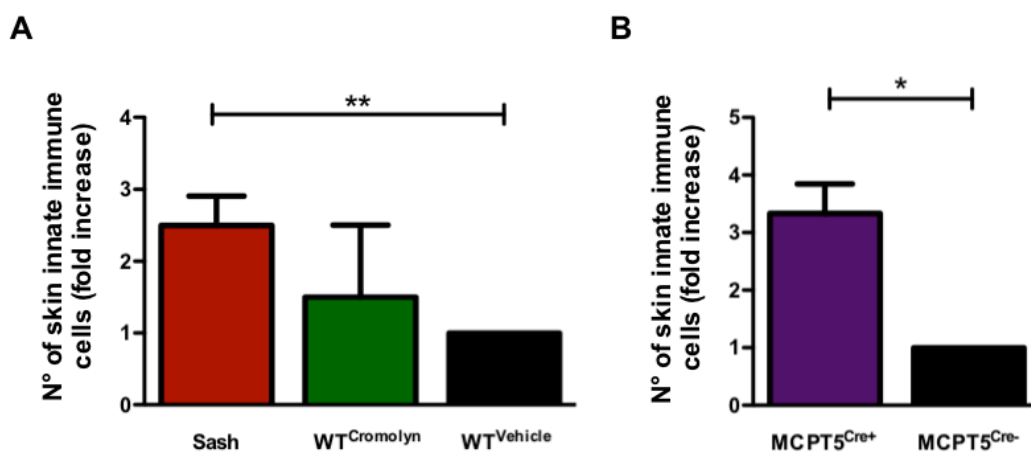
Figure 26. Innate immune cells are increased in the CCHS ears of mast cell-deficient mice. Four weeks after the 3rd challenge with OXA, CCHS ear skin of mice was harvested and the immune cell composition was analyzed by flow cytometry. (A) Quantification of skin CD45$^+$CD3$^-$ cells in Sash mice and WT mice. The bar graph shows the n-fold change of CD45$^+$CD3$^-$ cells of Sash mice and WT^{Cromolyn} mice in relation to WT^{Vehicle} control mice. (B) Quantification of skin CD45$^+$CD3$^-$ in MCPT5-Cre x iDTR strain, comparing Cre$^+$ mice and Cre$^-$ mice. Data are shown as means of pooled values of n = 3 experiments, error bars indicate ±SEM of 9 animals per group. Statistical significance calculated with non-parametric Wilcoxon test. _Abbreviations_: P-value < 0.05 (*), p-value < 0.01 (**), Sash - ears of C57BL/6-_Kit^{W-Sh}/Kit^{W-Sh}_ mice challenged with oxazolone, WT^{Cromolyn} - ears of C57BL/6-_Kit$^+$/Kit$^+$_ cromolyn-treated mice challenged with oxazolone, WT^{Vehicle} - ears of C57BL/6-_Kit$^+$/Kit$^+$_ Saline-injected

mice challenged with oxazolone, Cre$^+$ - ears of MCPT5-Cre$^+$iDTR$^+$ DT-treated mice challenged with oxazolone, Cre$^-$ - ears of MCPT5-Cre$^-$iDTR$^+$ DT-treated mice challenged with oxazolone, CCHS - chronic contact hypersensitivity, OXA - oxazolone.

This experiment demonstrated that in addition to TRM CD8β$^+$ T cells, innate immune cells are increased in the CCHS ears of MC-deficient mice.

5.4 Involvement of skin resident immune cells in the development of CCHS

The previous experiments showed that MC deficiency results in increased numbers of TRM CD8β$^+$ T cells and CD45$^+$CD3$^-$ innate immune cells at sites of CCHS responses. We, therefore, studied the relevance of both cell populations during the effector phase of CCHS.

5.4.1 The reduction of skin TRM CD8β$^+$ T cells in Sash mice abrogates the exacerbated inflammation during the effector phase of CCHS

We treated Sash animals with anti-CD8 antibody (Sash^{-CD8}) to reduce the skin numbers of CD8β$^+$ T cells. Subsequently, we compared the CCHS inflammatory responses of Sash^{-CD8} mice with these in Sash and WT control mice (see methods section 4.8.4).

The CHS ears of Sash^{-CD8} mice exhibited numbers of TRM CD8β$^+$ T cells that were very similar to these of WT mice (ratio Sash^{-CD8}/WT = 0.8 [0.7 – 0.9], n.s.) and clearly lower than those of Sash control mice (ratio Sash^{-CD8}/Sash = 0.43 [0.33 – 0.53], p-value < 0.01) 8 days after the 1st challenge with OXA (Fig. 27A). At this time, the numbers of TRM CD8β$^+$ T cells in the challenged ears of Sash mice were already markedly higher than in WT control mice (ratio Sash/WT = 1.73 [1.72 – 1.74], p-value < 0.01). In addition, treatment with anti-CD8 antibody reduced the expression levels of the CD8 molecule on the surface of TRM CD8β$^+$ T cells in the OXA-challenged skin of Sash^{-CD8} mice (Fig. 27B).

Next we examined the involvement of skin TRM CD8β$^+$ T cells in the inflammatory outcome of CCHS to OXA by applying the "ears-belly-ears" approach in Sash^{-CD8} mice and control mice (*see* methods section 4.8.2.3, modification 3).
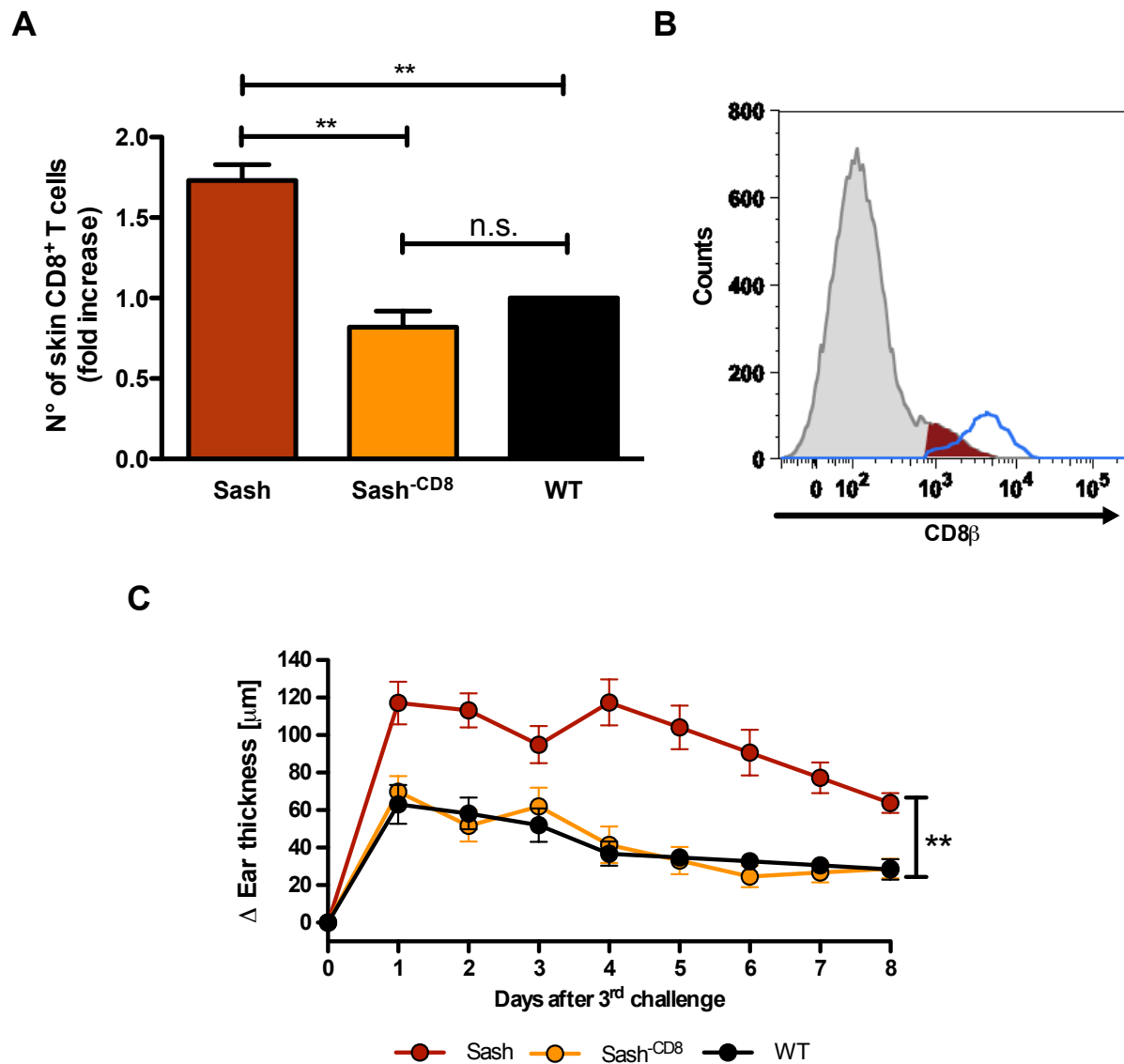
Figure 27. The reduction of skin TRM CD8β⁺ T cells in mast cell-deficient mice protects from CCHS exacerbated inflammation to OXA. Mice were sensitized with OXA on the belly (day -5) and challenged with the same hapten on day 0 (both ears). Additionally, on day 5 and 6 after the OXA-challenge some of the Sash mice were injected with anti-CD8 antibody (Sash^{-CD8}). Control mice were injected with Saline (Sash and WT). (A) Numbers of Skin TRM CD8β⁺ T cells after treatment with anti-CD8 antibody. Eight days after the 1st challenge with OXA, the ear skin was harvested and the numbers of TRM CD8β⁺ T cells were assessed by flow cytometry. One representative experiment of n = 3 independent repetitions. (B) FACS plot overlay showing the fluorescence intensity (FI) of cells quantified in panel A. Expression levels of CD8β in Sash^{-CD8} (red) are compared respect to their whole skin population (grey) and to the CD8β⁺ T cells from control Sash mice (blue line). (C) Ear swelling after the 3rd challenge with OXA in Sash mice, Sash^{-CD8} mice and WT mice. Animals were sensitized on abdominal skin (day -5) and challenged on days 0 (both ears), 30 (belly) and 60 (both ears). Additionally, on day 5 and 6 after the challenge with OXA some Sash mice were injected with anti-CD8 antibody (Sash^{-CD8}). Control mice were injected with Saline (Sash and WT). The figure shows the ear swelling response after the 3rd challenge with OXA. Data are shown as mean values of n = 4

experiments, error bars indicate ±SEM of 15 animals per group. Statistical significance calculated with Student's t-test. P-value < 0.01 (**) comparing Sash versus Sash^{-CD8} mice. *Abbreviations and legend description*: p-value < 0.01 (**), p-value > 0.05 (n.s.), Sash - ears of C57BL/6-*Kit*$^{W-Sh}$/*Kit*$^{W-Sh}$ mice challenged with oxazolone, Sash^{-CD8} - ears of C57BL/6-*Kit*$^{W-Sh}$/*Kit*$^{W-Sh}$ anti-CD8 antibody-treated mice challenged with oxazolone, WT - ears of C57BL/6-*Kit*$^{+}$/*Kit*$^{+}$ mice challenged with oxazolone, Δ Ear thickness - ear swelling obtained after the subtraction of ears thickness baseline, CCHS - chronic contact hypersensitivity, TRM - tissue resident memory, OXA - oxazolone.

All experimental groups, i.e. Sash, Sash^{-CD8} and WT, achieved the maximal inflammation 24 hours after the 3rd challenge with OXA. In none of the experimental groups did the average ear thickness return to the baseline values within the first 8 days after this challenge.

The degree of inflammation in the ears of Sash^{-CD8} mice was comparable to that in the ears of WT control mice, and clearly reduced compared with that in the ears of Sash mice (AUC$^{1-8}$: OXA-Sash = 826.6±230.9, OXA-Sash^{-CD8} = 404.1±193.8, OXA-WT = 402.9±136; Fig. 27C).

Taken together, these results indicate that the increase in TRM CD8β^{+} T cell numbers in the challenged skin is responsible for the exacerbated inflammation observed in MC-deficient mice during CCHS responses to OXA.

5.4.2 Exacerbation of inflammation in CCHS is antigen specific

Here, we tested whether exacerbated CCHS inflammation observed in CCHS ears of MC-deficient mice can be elicited after a challenge with a different contact allergen, i.e. whether the MC-dependent exacerbation of inflammation after CCHS is an antigen specific response.

One month after the 3rd challenge with OXA (day 85), the same mice used for the "ears-belly-ears" approach described in the previous experiments (results section 5.4.1), were sensitized with dinitrofluorobenzene (DNFB). Five days after DNFB sensitization (day 90), the right ears of these mice were challenged with DNFB, whereas their lefts ears were challenged, for a 4th time, with OXA for control purposes (*see* methods section 4.8.2.3, modification 4).

In all experimental groups, i.e. Sash, Sash^{-CD8} and WT, ear-swelling responses in DNFB-treated ears peaked at 48 hours after this challenge. In none of the experimental groups did the ear thickness returned to baseline values within the first 8 days after DNFB-challenge. Furthermore, the degree of inflammation in the DNFB-treated ears was comparable in all experimental groups (AUC$^{1-8}$: DNFB-Sash = 738±316.2, DNFB-Sash^{-CD8} = 628.5±408.6, DNFB-WT = 934.1±552; Fig. 28A).

As for OXA-treated ears, the Sash group achieved maximum inflammation about 8 days after the 4th challenge with OXA, whereas in the Sash^{-CD8} group and in the WT group, maximum inflammation was achieved 48 hours after this challenge. In contrast to Sash mice, which showed persistent inflammation, the ear thickness of Sash^{-CD8} mice and of WT mice slowly decreased and returned to baseline values during the next 8 days after the 4th challenge with OXA (Fig. 28B).

After the 4th challenge with OXA, the OXA-treated ears of Sash mice showed stronger degree of inflammation than those in Sash^{-CD8} mice and in WT mice (AUC$^{1-8}$: OXA-Sash = 1518±877.8, OXA-Sh^{-CD8} = 721.6±559, OXA-WT = 763.1±300.3; Fig. 28B). In addition, four out of ten Sash mice, but none of the Sash^{-CD8} mice or of the WT mice, developed necrosis preceded by scaling after this challenge (day 6 and 7; *see* Fig. 28B "Ψ").

Two conclusions arose from these experiments: (1) Since only OXA-challenged ears, but not DNFB-challenged ears, showed exacerbated inflammation in Sash mice compared with WT mice, we concluded that the exacerbated inflammation observed in MC-deficient Sash mice after CCHS is antigen specific. (2) As no differences were seen between Sash and Sash^{-CD8} in the swelling of DNFB-treated ears, we concluded that possible effects of anti-CD8 antibody treatment on innate immune skin resident cells, e.g. subpopulations of skin dendritic cells, cannot be relevant for the CCHS reactions.

Taken together, these results confirmed that increased skin numbers of antigen-specific TRM CD8β$^+$ T cells are responsible for the exacerbation CCHS inflammation at skin sites lacking MCs.

A

B

C

OXA-Sash **OXA-Sash^{-CD8}** **OXA-WT**
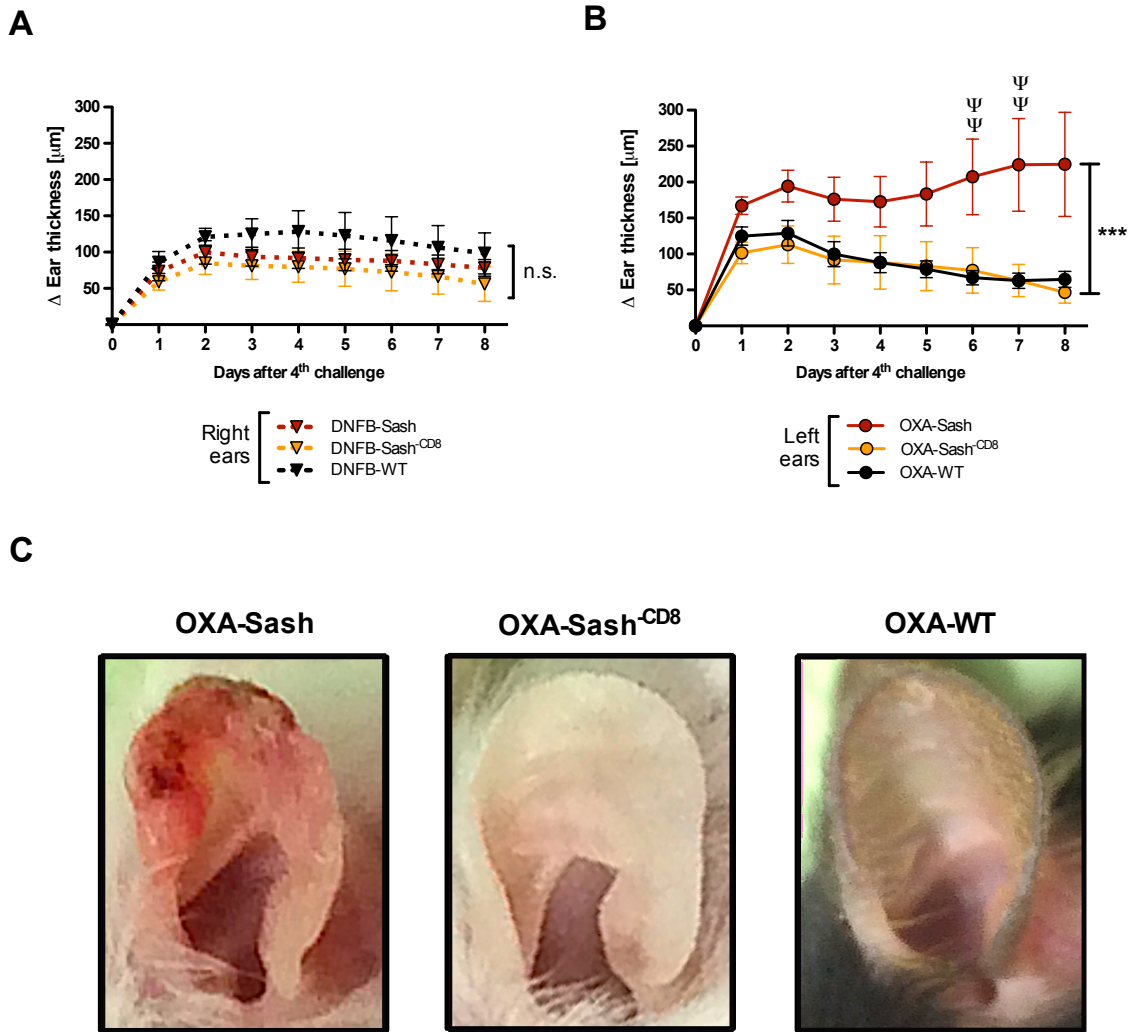
Figure 28. Mast cell-dependent exacerbation of CCHS inflammation is antigen-specific. The animals shown in Figure 27C were sensitized with a different hapten (DNFB) on the abdominal skin (day 85) and subsequently challenged at day 90 with DNFB on the right ears (panel A) and with OXA on the left ears (panel B). (A) Ear swelling on the right ears after the 1st challenge with DNFB. The figure shows the ear swelling responses after day 90 on the DNFB-treated ears. (B) Ear swelling on the left ears after the 4th challenge with OXA. The figure shows the ear swelling response after day 90 on the OXA-treated ears. (C) A representative left ear of OXA-Sash, OXA-Sash^{-CD8} and OXA-WT eight days after the 4th challenge with OXA. Data are shown as means of pooled values of n = 3 experiments, error bars indicate ±SEM of 10 animals per group. Statistical significance calculated with Student's t-test. *Abbreviations and legend description*: Δ Ear thickness - ear swelling obtained after the subtraction of ears thickness baseline, p-value > 0.05 (n.s.), DNFB-Sash - ears of C57BL/6-Kit^{W-Sh}/Kit^{W-Sh} mice challenged with 2,4-Dinitro-1-fluorobenzene, DNFB-Sash^{-CD8} - ears of C57BL/6-Kit^{W-Sh}/Kit^{W-Sh} anti-CD8 antibody-treated mice challenged with 2,4-Dinitro-1-fluorobenzene, DNFB-WT - ears of C57BL/6-Kit^{+}/Kit^{+} mice challenged with 2,4-Dinitro-1-fluorobenzene, OXA-Sash - ears of C57BL/6-Kit^{W-Sh}/Kit^{W-Sh} mice challenged with oxazolone, OXA-Sash^{-CD8} - ears of C57BL/6-Kit^{W-Sh}/Kit^{W-Sh} anti-CD8 antibody-treated mice challenged with oxazolone, OXA-WT - ears of C57BL/6-Kit^{+}/Kit^{+}

mice challenged with oxazolone, Ψ - indication when an individual Sash mouse ear became necrotic, p-value < 0.001 (***), CCHS - chronic contact hypersensitivity, OXA - oxazolone.

5.5 Effects of MCs on the numbers and function of skin TRM CD8β⁺ T cells

5.5.1 MC deficient mice show more TRM CD8β⁺ T cells in the dLNs after a single challenge with OXA

MCs can potentially modify the T cell development in secondary lymphoid organs (Kunder *et al.*, 2009, Hershko *et al.*, 2011). In order to investigate whether MCs control the generation of TRM CD8β⁺ T cells in secondary lymphoid organs, the numbers of these cells in the dLNs and in the skin were assessed at different time points after the 1ˢᵗ challenge with OXA using flow cytometry.

Five days after OXA-sensitization on the abdominal skin, unchallenged mice contained a small population of TRM CD8β⁺ T cells in the superficial cervical LNs, i.e. the LNs draining the ear skin (Fig. 29 left graph). Sash mice and WT mice exhibited similar numbers of TRM CD8β⁺ T cells in their superficial cervical LNs at this time (p-value > 0.05).

On day 4 after the OXA-challenge of ears, the numbers of TRM CD8β⁺ T cells in the dLNs of both Sash and WT mice were similar to those in unchallenged control mice (Fig. 29 left graph; n.s.).

On day 6 after the OXA-challenge of ears, the dLNs of both Sash and WT mice showed a strong increase in the numbers of TRM CD8β⁺ T cells as compared to the previous time point (Fig. 29 left graph; day 4; p-value < 0.001). At this time, the numbers of TRM CD8β⁺ T cells found in the dLNs of Sash mice were about twice as high as those in the dLNs of their WT control littermates (Fig. 29 left graph; p-value < 0.001).

On day 8 after OXA challenge, the dLNs of Sash mice were similar to those WT mice (Fig. 29 left graph; p-value > 0.05), and reduced compared with the previous time point (Fig. 29 left graph; day 6; p-value < 0.001).

Five days after OXA-sensitization on the abdominal skin, unchallenged mice did not present TRM CD8β$^+$ T cells in their ears (Fig. 29 right graph).

On day 4 after the OXA-challenge of ears, the ears of all mice present some TRM CD8β$^+$ T cells. There was no difference in the numbers of these cells between Sash mice and WT mice (Fig. 29 right graph; p-value > 0.05).

On day 6 after the OXA-challenge of ears, the ears of Sash mice showed more TRM CD8β$^+$ T cells compared with both their WT controls at this time point (Fig. 29 right graph; p-value < 0.05) and Sash mice at the previous time point (Fig. 29 right graph; *compare to* day 4; p-value < 0.05).

On day 6 after the OXA-challenge of ears, the ears of both Sash and WT mice contained more TRM CD8β$^+$ T cells than on day 6, and the ears of Sash mice had significantly more TRM CD8β$^+$ T cells than their WT controls (Fig. 29 right graph, p-value < 0.01).
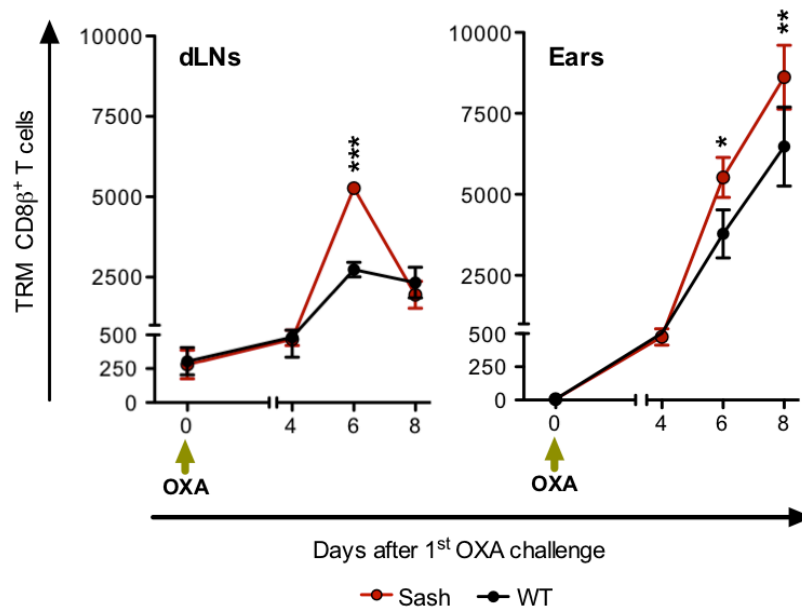
Figure 29. Sash mice exhibit more TRM CD8β$^+$ T cells in draining lymph nodes and OXA-challenged ears during the recovery phase of CHS. Mice were sensitized on the abdominal skin (day -5) and challenged on both ears (day 0). The number of TRM CD8β$^+$ T cells was evaluated in dLNs and ears on days 0, 4, 6 and 8 after the OXA challenge by flow cytometry. The graphs show the absolute numbers of TRM CD8β$^+$ T cells in different organs and different points on time. Data are shown as means of pooled values of n = 3 experiments, error bars indicate ±SEM of 9 animals per group. Statistical significance calculated with Student's t-test. *Abbreviations and legend description*: dLNS - draining lymph nodes, TRM - tissue resident memory, p-value < 0.001 (***), OXA - oxazolone,

p-value < 0.05 (*), p-value < 0.01 (**), mustard arrow indicates the day of the OXA-challenge, Sash - ears of C57BL/6-*Kit*$^{W-Sh}$/*Kit*$^{W-Sh}$ mice challenged with oxazolone, WT - ears of C57BL/6-*Kit*$^+$/*Kit*$^+$ mice challenged with oxazolone.

These results suggest that the absence of MCs promotes the accumulation of TRM CD8β+ T cells in OXA-challenged ears as early as 6 days after CHS challenge. This may be linked to the higher numbers of CD8β$^+$ T cells in the dLNs of Sash mice observed on day 6 after CHS induction.

5.5.2 MCs modulate the accumulation of TRM CD8β$^+$ T cells in the challenged ears

To test whether the increased numbers of TRM CD8β$^+$ T cells observed in dLNs of Sash mice at day 6 after the CHS induction, account for the increased accumulation of these cells on in the OXA-challenged ears, we performed adoptive transfer experiments.

Equal numbers of CD8β$^+$ T cells obtained from the dLNs and the blood of Ly5.1 mice (WT animals expressing the CD45.1 haplotype) on day 6 after the 1st challenge with OXA, were injected i.v. into either Sash or WT mice on day 6 after their 1st challenge with OXA (*see* methods section 4.8.7). Because Sash and conventional WT mice do not express the CD45.1 haplotype, this approach allows the use of anti-CD45.1 antibody to identify the transferred cells that migrate into the target organ, i.e. skin or dLNs, of recipient mice.

Two days after adoptive transfer (day 8 after the 1st challenge with OXA), the ears and dLNs of recipient animals were assessed for the numbers and phenotype of the CD45.1$^+$ donor cells by flow cytometry.

The majority of CD45.1$^+$ donor cells that had homed to the OXA-challenged ears of recipient Sash animals showed the TRM CD8β$^+$ T cell phenotype (87.8% [85 – 87]), i.e. CD103$^+$ and CD44^{high+}. This was in contrast to the CD45.1$^+$CD8β$^+$ T cells found in the dLNs of these mice, which generally did not exhibit co-expression of TRM-markers (1% [0 – 2]) (Fig. 30A).

On day 8 after the challenge with OXA, the numbers of CD45.1$^+$ TRM CD8β$^+$ donor T cells present in the ears of recipient Sash mice were 2.14 [2.37 – 2.91] fold higher than in their WT control littermates (Fig. 30B).

A   **B**

■ Ears ■ dLNs
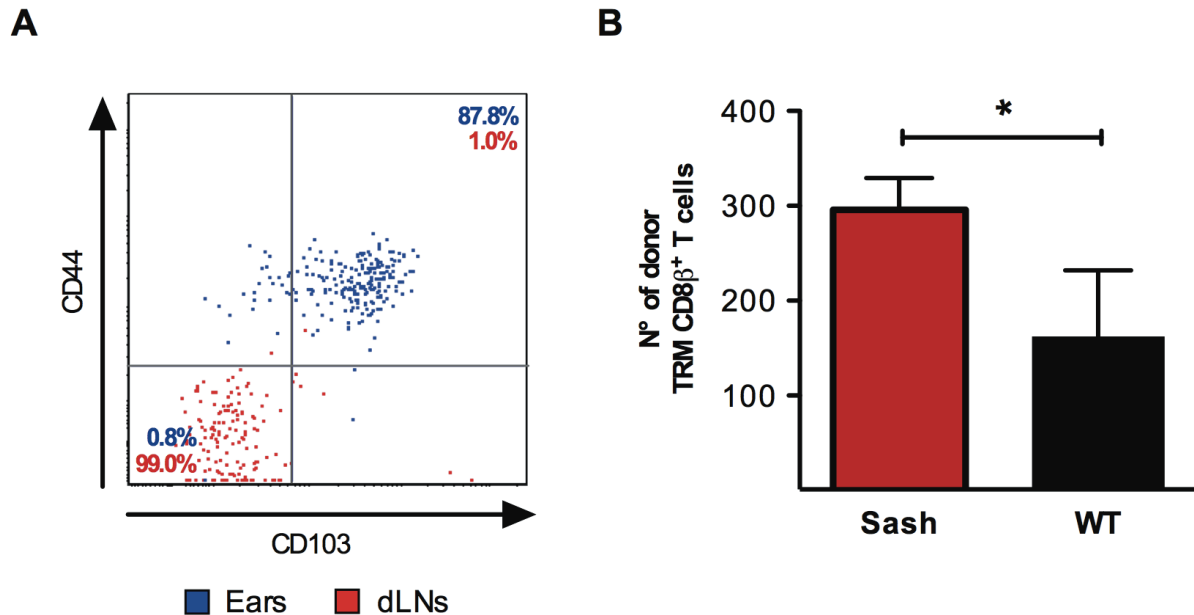
Figure 30. The ears of Sash mice display increased accumulation of intravenously engrafted TRM CD8β$^+$ T cells compared with WT control mice. Donor mice (Ly5.1) as well as recipient mice (Sash and WT) were sensitized with OXA on the abdominal skin (day -5) and challenged with the same hapten on both ears (day 0). The whole CD8β$^+$ T cell compartment contained in the blood and dLNs of donor mice was isolated (day 6 after challenge). Subsequently, the same numbers of donor CD8β$^+$ T cells were injected intravenously in the recipient WT and Sash mice (1x10^7 cells/ mouse). Two days after adoptive transfer, the ears of Sash and WT recipient mice were harvested (day 8 after challenge) and the immunophenotype and numbers of donor CD45.1$^+$ TRM CD8β$^+$ T cells were analyzed by flow cytometry. (A) Dot-plot overlay of CD45.1$^+$CD8β$^+$TCRβ$^+$ cells from dLNs (blue) and from ears (red) of Sash recipient mice showing the degree of CD103 and CD44 expression in each organ. (B) Quantification of CD45.1$^+$ TRM CD8β$^+$ T cells in the ears of Sash and WT recipient animals. Data are shown as means of pooled values of n = 3 experiments, error bars indicate ±SEM of 9 animals per group. Statistical significance calculated with Student's t-test. *Abbreviations and legend description*: dLNs - draining lymph nodes, TRM - tissue resident memory, p-value < 0.05 (*), Sash - ears of C57BL/6-*Kit^{W-sh}/Kit^{W-sh}* mice challenged with oxazolone, WT - ears of C57BL/6-*Kit^{W+}/Kit^{W+}* mice challenged with oxazolone, OXA - oxazolone.

This result suggests that MCs control the accumulation of TRM CD8β$^+$ T cells in the OXA-treated skin at least in part, through local mechanisms that are restricted to the challenged-skin site.

6 Discussion

The aim of this study was to investigate the role of MCs in a chronic contact hypersensitivity (CCHS) model for human allergic contact dermatitis (ACD) in mice. ACD patients develop skin inflammation after repeated cutaneous exposure to contact allergens (Tan *et al.,* 2014). Our understanding of the immunopathogenesis of ACD relays largely in studies of acute contact hypersensitivity (CHS) responses to experimental contact allergens (haptens) in mice. These studies have led to the distinction of three phases of contact hypersensitivity responses, i.e. sensitization, elicitation and resolution, and they have clarified the essential role of hapten-specific T cells for the elicitation of ACD inflammation upon further encounters to contact allergens/haptens (Tončić *et al.,* 2011). However, many aspects of ACD remain ill characterized, and CHS models appear to be of limited use for studying these aspects. For example; some CHS studies, but not others, have identified MCs to be the promoters of CHS inflammation (Bidermann *et al*., 2000; Dudeck *et al.,* 2011; Otzuka *et al.,* 2011), and in some other CHS studies, but not in all, MCs appear to inhibit or terminate CHS inflammation (Askenase *et al.,* 1984; Grimbaldeston *et al.,* 2007). In order to overcome these limitations in CHS and to represent the chronic phase of ACD patients, we developed the CCHS model to oxazolone (OXA). Using this model we followed for up to four months, inflammatory responses as a result of repeated OXA challenges by measuring ear swelling responses and skin signals of inflammation. This, together with the use of MC-deficient mice and mice with MCs targeted by pharmacological intervention (cromolyn), allowed us to study the role of MCs during CCHS inflammatory responses. By modifying the hapten application protocol of the original CCHS model, we explored the role of local vs. systemic MC effects during CCHS inflammation. With flow cytometry, cytokines array, skin whole mount immunofluorescence staining using confocal microscopy and adoptive transfer strategies we identified and characterized the relevance of tissue-resident memory CD8β$^+$ T cells in our CCHS model.

6.1 CCHS to OXA as a model for ACD

Contact hypersensitivity (CHS) as a model for ACD was designated to understand the immune-mechanisms involved in the sensitization phase and elicitation phase of this disease (Christensen *et al.*, 2012). CHS as a model was successful in clarifying the pivotal role of T cells in hapten-mediated inflammatory responses during acute inflammation (Honda *et al.* 2012). However, ACD patients are susceptible to develop chronic lesions, and it occur by recurrent contact to a relevant hapten in the same skin site. In this case, CHS is not a suitable model, because it consists in a single hapten challenge that results in acute inflammatory responses. Our model of chronic CHS (CCHS) shares some similarities with acute CHS models, but it differs in some key features that we consider to be important for ACD in patients. In our CCHS to OXA model, the time lapse between every challenge, i.e. 30 days, leads to MC accumulation in the skin and a role for memory T lymphocytes as it is the case of ACD patients (Bangert *et al.,* 2003, Chereches-Panta *et al.*, 2011 and Sterry *et al.,* 1990). In ACD patients, the lesions appear when a sensitized individual is exposed recurrently to a relevant hapten (Rustemeyer *et al.* 2006). In these individuals, the time intervals of hapten exposures can be either short (days) or long (months or years), which evidence the involvement of long-living hapten-specific memory T cells. In support of this idea, Sterry and coworkers, show the predominance, relevance of hapten-specific memory T cells over naive T cells in blood of patients suffering ACD (Sterry *et al.,* 1990). The skin of those patients may also involve changes in its composition. Bangert *et al.* show that in ACD patientes, a controlled exposition (patch-test) to relevant contact allergens results in a long-lasting accumulation of immune cells in this skin sites, i.e. T lymphocytes, MCs and neutrophils (Bangert *et al.,* 2003). These reports are in accordance with our findings, because in our CCHS model, MC numbers increase in the OXA-challenged skin and control the long-lasting accumulation of resident memory CD8β+ T cells.

A study carried by Hershko *et al.* reported the use of a model of chronic CHS to OXA. In this model they challenged the ears of mice with 30 µl of 0.5% OXA three times per week for up to a total of 10 challenges, whereas in our CCHS model, we challenged the mice with 20 µl of 0.6 % OXA, every 30 days for up to a total of 4 challenges. In accordance to our results, Hershko's study shows that MCs contribute to suppress OXA-induced chronic allergic dermatitis, but their mechanism differs from

ours. They show that under chronic inflammatory conditions, MCs migrate to the dLNs and to the spleen and produce IL-2, which is necessary to control the effector/regulatory CD4$^+$ T cells axis in the spleen. By doing so, MCs suppress the effector phase of OXA-induced chronic CHS (Hershko *et al.* 2011). The high frequency challenge in the experimental protocol used by Hershko *et al.* may allow the involvement of both memory and effector hapten-specific T cells, whereas our CCHS model is exclusively dependent on memory T cells. Differences in the challenging pattern in Hershko's chronic CHS model and our CCHS model, lead to dramatic consequences, which makes Hershko's model inappropriate to study the chronic phase of ACD in patients. These consequences are: (1) Their challenge protocol induces the generation of OXA specific IgE. They show that this IgE controls the accumulation of MCs in the spleen, and thus IgE mediates the MC-protective effect in this model. If patients suffering ACD would have IgE against contact allergens, the inflammatory responses should be observed immediately after hapten contact, but this is not the case. (2) The high frequency, which Hershko *et al.* uses to challenge the mice, induces strong inflammatory responses such as necrosis of dLNs (Hershko *et al.,* 2011). However, it is unlikely that such extreme symptoms appear in patients with ACD.

To induce CCHS we used the contact sensitizer oxazolone (OXA). This allergen is considered as a hapten, because it requires the interaction with proteins to induce immune responses. Other haptens, e.g. DNFB or TNCB, are also used to induce CHS, but only OXA was reported to generate hapten specific TRM T cells (Rana *et al.*, 2008 and 2009). Moreover, DNFB is able to attract virus specific CD8$^+$ T cells to the skin and induces them to become TRM T cells, but contact to DNFB does not generate DNFB-specific TRM T cells (Mackay *et al.*, 2012). Of note, CHS reactions to TNCB, DNFB and OXA are similar, but not identical. For example, 49% of the up-regulated gene expression profile after DNFB sensitization differs from that after OXA sensitization (Saito *et al.* 2013). It is likely that the capacities of OXA to generate TRM T cells are mediated by mechanisms involving nucleic acids modifications. Masayuki and collaborators in 2014 demonstrated that UV-A spectrum catalyzes the production of OXA through the oxidation of the nucleotide Guanine present in nucleic acids. In line with this, herpes simplex virus (HSV), which induces the generation of HSV-specific skin TRM CD8$^+$ T cells and provokes type IV hypersensitivity

responses, undergoes DNA oxidation during their infective phase (Valyi-Nagy *et al.,* 2000; Mackay *et al.* 2013). Hence, presentation of oxidized DNA products by antigen presenting cells in the dLNs might be implicated in the generation of skin TRM CD8β$^+$ T cells or their precursors in these secondary lymphoid organs.

It is noteworthy that oxazoles, i.e. OXA or OXA derivatives, may play a role in human Type IV hypersensitivity mediated diseases. Since these haptens can be generated by UV-A exposure (Masayuki *et al.* 2014), the DNA and RNA of individuals can serve as endogenous source of oxazoles. There are type IV hypersensitivity responses called polymorphic light eruption (PMLE), a disease that shares similarities with ACD. In PMLE, inflammatory skin reactions appear at skin sites exposed to the sun (Tutrone WD *et al.,* 2003). One can hypothesize that OXA or other oxidized DNA products can be generated by sunstroke, which induces the sensitization of PMLE individuals and the subsequent generation of hapten-specific T cells.

Despite CCHS was designed to be a suitable model to approach other chronic phase of ACD, it presented some limitations that were discovered during the development of this study. In contrast to DNFB- and TNCB-specific T cells, OXA-specific T cells can be poorly re-stimulated *in vitro* by adding the hapten to the culture media. Consequently, this limitation restricted our experimental approaches to *in vivo* and *ex vivo* experiments. Accounting the complexity of our CCHS model, *in vitro* approaches could greatly facilitate the elucidation of the molecular mechanisms involved in this model. For example, *in vitro* approaches could help to answer whether MCs interact directly or indirectly with TRM CD8β$^+$ T cells. In addition, using *in vitro* systems would facilitate the determination of MC-mediated effects on TRM CD8β$^+$ T cells, e.g. maturation, migration, apoptosis, cytokine expression, etc. Rana and coworkers reported a method to generate skin TRM CD8β$^+$ to OVA (ovalbumin) peptides in a model of chronic skin inflammation in mice (Rana *et al.* in 2011). There are commercial transgenic murine models, in which their antigen presenting cells (APC), e.g. DC, macrophages, B cells, only recognize a specific OVA peptide sequence, i.e. OT-I and OT-II mice. Additionally, This approach enables *in vitro* culturing of OVA pulsed T cells that can be easily be re-stimulated (Clarke *et al.,* 2000). Consequently, validating the OVA model of Rana *et al.* in our MC-deficient mice, and using OVA instead OXA in our CCHS model could facilitate the study of molecular aspects involving MCs and TRM CD8β$^+$ T cells interaction by using *in vitro* methods.

The poor isolation of viable TRM CD8β⁺ T cells from the skin impaired the possibility to use *in vitro* methods in this study. Differently to T cells isolated from LNs or spleen, the isolation of TRM T cells from the skin was challenging and required the use of proteases to disrupt the extracellular matrix. After isolation, the TRM CD8β⁺ T cells lacked signals from the extracellular matrix. It was purposed that these signals are determinant for the correct maturation and function of TRM CD8β⁺ T cells (Mackay *et al.* 2013). In addition, in our hands the majority of the isolated T cells showed signs of activation or death induced by the extreme strong mechanical stress generated during the isolation process. Therefore, an *in vitro* approach to study the MCs-TRM CD8b+ T cell interaction in detail was not possible in this study.

6.2 Control of CCHS inflammatory responses requires local MCs and depends on their numbers

The MC-dependent control of CCHS inflammatory responses to OXA evidences two independent aspects of the MC biology, each of which may contribute to the protective role of MCs in this model. These are: (1) the presence and (2) the accumulation of MCs in hapten-challenged skin sites.

Two of our experiments highlight the importance of local MCs for the control of CCHS inflammatory responses to OXA. (1) In MC-deficient Sash mice, the local MC reconstitution of the ear pinnae (Sash-Ears⁺ᴮᴹᶜᴹᶜˢ) was sufficient to markedly reduce CCHS inflammatory responses to OXA, i.e. reduced ear swelling and abrogation of skin necrosis. (2) Using the MCPT5-Cre x iDTR mice, we show that selective deletion of skin MCs was sufficient to lead increased CCHS inflammatory responses to OXA.

However, Sash-Ears⁺ᴮᴹᶜᴹᶜˢ mice did not completely restore normal inflammatory responses during CCHS to OXA as compared to WT control mice (*see* results section 5.1.3). This can have different reasons, but the most likely, is indeed that MC-accumulation in the OXA-challenged ears of WT mice is required to protect the skin from CCHS inflammation (Fig. 20). MC accumulation in CCHS skin is, at least in part, due to the migration and differentiation of bone marrow MC progenitors as reviewed elsewhere (Dahlin & Hallgren, 2014). Because the mutation of Kit present in Sash mice does not allow for the generation of mature MCs from bone marrow progenitors under *in vivo* conditions, Sash-Ears⁺ᴮᴹᶜᴹᶜˢ mice are not able to increase their MC

numbers by this mechanism and consequently these mice lack the protective contribution provided by the MC accumulation in the OXA-challenged skin during CCHS inflammation. The quantification of MCs in CCHS ears of Sash-Ear$^{+BMCMCs}$ mice and its comparison to CCHS ears of WT control mice could clarify whether MC accumulation represents a relevant factor for contention of CCHS inflammatory responses.

Coming back to the importance of MCs in the locality of CCHS inflammation, experiments with MCPT5-Cre x iDTR mice confirmed the contribution of local MCs for the contention of CCHS inflammation, since depletion of CTMCS was sufficient to induce increased CCHS inflammatory responses in Cre$^+$ mice as compared to their Cre$^-$ controls (Fig. 16). MCPT5 protein is expressed in connective tissue type MCs (CTMCS) but not in mucosal tissue MCs (MMCS). CTMCS populate the skin and peritoneum, whereas MMCS populate the spleen, lungs and other inner organs. Consequently, DT-treatment depletes skin and peritoneal MCs, but does not affect MCs in inner organs. Therefore, this data reinforces the role of CTMCs in this model.

Combining the data of Sash-Ear$^{+BMCMCs}$ mice and that of MCPT5-Cre x iDTR mice, we demonstrated the importance of MCs in the challenged skin area for the contention of CCHS inflammation to OXA.

Neither the data of MCPT5-Cre x iDTR mice nor that of Sash-Ear$^{+BMCMCs}$ mice discard the involvement of MMCS in CCHS inflammation to OXA. In fact, it is still possible that MMCS provide a partial protection during CCHS to OXA, because DT-treated Cre$^+$ mice exhibited a milder CCHS inflammatory response as compared to Sash mice. For example, Sash mice exhibited scaling and necrosis after CCHS to OXA, whereas DT-treated Cre$^+$ mice did not show such symptoms.

However, we favor the idea that differences between CCHS inflammatory responses in DT-treated Cre$^+$ mice and Sash mice are based on their respective numbers of local MC. This idea points, again, towards the importance of MC numbers and the MC accumulation in the skin site of hapten exposure, i.e. in CCHS ears, for the contention of CCHS inflammation. The CCHS ears of Sash mice are above 97% deficient of MCs as compared to their WT control mice, whereas in the CCHS ears of DT-treated Cre$^+$ mice, MC skin levels were only reduced by 70% as compared to Cre$^-$ control mice (Fig. 16B). This evidenced that the number of MCs present in Sash and

Cre$^+$ mice correlates negatively to the degree of CHS inflammation observed in each mouse strain. Another argument in favor of this hypothesis is provided by our experiments with cromolyn. WT mice treated with cromolyn (WT^{Cromolyn}) developed increased inflammation during the effector phase of CCHS to OXA compared with their WT control mice (WT^{Vehicle}). This response was accompanied with reduced numbers of MCs in the CCHS ears of WT^{Cromolyn} mice (43% less MCs than in control WT^{vehicle} animals) (*see* results section 5.1.6). The reduced MC numbers observed in cromolyn-treated WT mice in our settings are in consonance with those of Brower and coworkers published in 2002. They showed that continued i.p. injection with cromolyn is effective in preventing the increase in MC numbers in a model of myocarditis in rats (Brower *et al.*, 2002). In our experiments the number of MCs of WT^{Cromolyn} mice inversely correlates with the degree of CCHS inflammation, which constitutes another evidence pointing to the accumulation of MCs in OXA-challenged ears as a protective factor from CCHS inflammation.

It is important to highlight that achieving conclusions with experiments performed in MCPT5-Cre x iDTR mice or in WT^{Cromolyn} mice can be confusing, because of the limitations in these models. For example, it is noteworthy to mention that bystander effects generated by treatment with diphtheria toxin could also explain the discrepancies observed in Sash mice and DT-treated Cre$^+$ mice in regards to the CCHS responses to OXA. It is known that treatment with diphtheria toxin induces unspecific toxicity in mice. As mentioned in the review from Bennett *et al.,* increasing the dose of diphtheria toxin during the depletion of Cre-expressing cells leads to death of some animals and this is independent of the Cre expression (Bennett *et al.,* 2007). We also experienced this observation with our own MCPT5-Cre x iDTR mouse colony. The likeliest reason for this epiphenomenon is the presence of a very low affinity receptor for diphtheria toxin present in all murine cells (Palmiter, 2001). The treatment with diphtheria toxin consists in an intraperitoneal injection before and during the induction of CCHS. Therefore the release of diphtheria toxin to the bloodstream occurs shortly after injection. The majority of the immune compartment circulates between the blood and secondary lymphoid organs. Consequently, the toxic effects produced by the injected diphtheria toxin, could be especially deleterious for off-target cells of the immune system circulating in the blood at that time point. Buch and coworkers in 2005 reported that using DT-treated Cre$^+$ mice for the

depletion of specific immune populations showed no differences in off-target immune cells compared with DT-treated Cre⁻ control mice, but in this study they did not control the effect of unspecific toxicity of diphtheria toxin by comparing the absolute numbers of immune cells with control animals that were not treated with diphtheria toxin (Buch *et al.*, 2005). In conclusion, diphtheria toxin treatment for depleting MCs, could influence nonspecifically the read out of inflammation, which makes the identification of real mechanisms difficult.

To study MC-degranulation as possible mechanism of MC contribution in our CCHS model to OXA, we employed a pharmacological inhibitor of MCs, cromolyn, to block the MC activity in WT mice (WT^{Cromolyn}) during CCHS responses. We obtained analog results in WT^{Cromolyn} mice as compared to MC-deficient mice in CCHS, since WT^{Cromolyn} mice showed increased CCHS inflammatory responses as compared to WT^{Vehicle} mice, but we were not able to demonstrate that such differences were due to inhibition of MC-degranulation. In fact, our results confirm earlier study findings showing that cromolyn does not inhibit MC-degranulation in mice (Oka *et al.*, 2012). In contrast, cromolyn has been reported to inhibit MC-degranulation in rats and humans. For example, Ratner and colleagues published in 2002 the effectiveness of the nasal administration of cromolyn to inhibit MC-degranulation and subsequent symptoms in patients with rhinitis (Ratner *et al.*, 2002). Oka and coworkers demonstrated that in contrast to rat MCs, cromolyn did not inhibit degranulation of mouse MCs in two different acute MC-dependent models *in vivo*, i.e. passive cutaneous anaphylaxis and passive systemic anaphylaxis. Our results are in line with this, because we showed that contact to OXA induces degranulation and the treatment with cromolyn did not inhibit it.

On the other hand, cromolyn may not be a MC-selective inhibitor. Oka and coworkers demonstrated the possible effects of cromolyn on other cells. In this study i.p. injection of LPS in MC-deficient mice induced the production of TNFα and treatment with cromolyn, in this mice, inhibited it (Oka *et al.*, 2012). Treatment with cromolyn in Sash mice during induction of CCHS responses to OXA, could clarify whether the effects of Cromolyn in WT^{Cromolyn} mice are exerted by inhibition of MCs or of off-target cells. Some reports use cromolyn as "mouse MC-stabilizer" under chronic settings, but these studies presented poor or none morphological evidence of MC stabilization. Concluding, we could not study the contribution of MC-degranulation in our CCHS to

OXA model, because cromolyn treatment did not inhibit MC-degranulation in our mice. Cromolyn might not be a selective MC-inhibitor in mice, therefore more experiments are required e.g. cromolyn treatment of Sash mice during induction of CCHS inflammation, in order to clarify whether the effects of cromolyn in WT animals submitted to CCHS were by selective targeting of MC-functions, but not by effects in off-target cells. However, treatment with cromolyn in WT mice results in reduced MC numbers in OXA-challenged ears, which can explain why WT[Cromolyn] mice showed increased CCHS inflammatory responses to OXA. In support of this, other studies, which stated Cromolyn as MC-stabilizer for chronic mouse models, show indirect evidence of reduced MC activity, which could also be explained by reduced MC accumulation in the targeted tissue (Costa *et al.*, 2008; Kneilling *et al.*, 2007; Kobayashi *et al.*, 2002).

These results together indicate that skin MCs are required in the OXA-challenged skin to control CCHS inflammatory responses, and suggest the accumulation of MCs in the CCHS skin as a protecting factor from CCHS inflammation.

6.3 MCs provide local protection from CCHS exacerbated inflammation

The generation of hapten-specific T lymphocytes allows individuals to become systemically sensitized. Hapten-specific T lymphocytes persist in the systemic circulation of sensitized individuals. Wherever a secondary contact to the relevant hapten occurred, hapten-specific T lymphocytes migrate to the site of this contact to initiate the corresponding inflammatory responses (Bellanti, 2012). Our results show that mice recurrently exposed to OXA at different skin sites develop inflammation after each new contact to this hapten. This demonstrates that those mice were systemically sensitized with OXA. However, using the "left-belly-ears" approach we showed that independently of the systemic sensitization, OXA challenge at skin sites previously exposed to this hapten (OXA pre-exposed skin sites) induces stronger inflammation than that at areas that did not have previous OXA exposition. Furthermore, the use of MC-deficient mice in the "left-belly-ears" approach allowed us to conclude that MCs only protect from CCHS inflammation at OXA pre-exposed skin sites. These results suggested that local factors residing at OXA pre-exposed

skin sites promote stronger inflammatory responses during further contacts to this hapten and that MCs play a role in this process by limiting these local factors. MCs can also provide protection in other settings. For example in graft versus host diseases MCs activated by IL-9 potentiate the regulatory capacities of CD4$^+$ T regulatory cells which then inactivate the CD8$^+$ T cells in the engrafted organ and control their generation in the dLNs (Lu *et al.*, 2006). In addition, a recent study described the importance of MC chymase in limiting cecal ligation and puncture (CLP) inflammation by degrading TNF (Piliponsky *et al.,* 2012).

Our results demonstrate that MCs provide protection from CCHS inflammation at OXA pre-exposed skin sites (Fig. 13 after 3rd OXA challenge and Fig. 21B), but they do not support consistently that MCs confer protection from inflammation after OXA-challenge at uninvolved skin sites (Fig. 13 after 1st OXA challenge and Fig. 21A). In this regard, one discrepancy between different experimental approaches surged along the development of this study and it will be discussed now. During the "left-right-left" approach, we observed that right ears of Sash mice exhibited stronger inflammation as compared to those of WT control mice after the 2nd challenge with OXA. This effect was observed despite the right ears of this mice were uninvolved skin sites, i.e. these ears were not pre-exposed to OXA before (Fig. 13). However, this is in contrast to results obtained when the "belly-belly-ears" approach was employed. The CCHS inflammatory response after the "belly-belly-ears" approach of Sash mice was comparable to that of WT mice (Fig. 21A), which indicates no protective contribution of MCs from inflammation elicited at uninvolved skin sites. The likeliest explanation of this discrepancy observed between the "left-right-left" approach and the "belly-belly-ears" approach, is the sequence of murine grooming phases. Mice have four consecutive grooming (or self cleaning) phases, each of which is well defined by a specific encephalographic pattern. During phase III of grooming, mice lick the forepaws and subsequently clean both ears several times. The rest of the mouse body, including the belly, is groomed only during the last phase grooming phase (the IV phase) (Berridge *et al.*, 2005). According to this, when our mice are challenged with OXA on the belly, the chance of cross-contamination of one of their ears is minimal, whereas mice challenged with OXA on the left ears might cross-contaminate their right ears. The amount of hapten applied to the cross-contaminated ears should be enough to attract some hapten-specific TRM T cells,

which are the culprits of increased inflammation in our CCHS model. In fact, we observed some residual inflammation in vehicle treated ears when OXA-challenges were performed on the right ears, but never when the challenge was performed on the abdominal skin of mice. Therefore hapten cross-contamination could explain the results observed during the 2nd challenge with OXA in the "left-right-left" approach.

6.4 MCs control CCHS to OXA by modifying the immune composition of the exposed skin

MCs contain a variety of preformed mediators located within the granules, e.g. histamine, proteases, IL-2, IL-4, IL-5 and TNFα, (*see* introduction section table 1). Additionally, MCs produce leukotriene and prostaglandins coming from the metabolism of arachidonic acid, numerous chemokines and cytokines can also be produced *de novo* by these cells (*see* introduction section table 1).

Our results show that 12 hours after the induction of CCHS inflammation, the OXA pre-exposed ears of Sash mice as well as WT[Cromolyn] mice exhibited reduced levels of IL-4 in contrast to WT control mice (*see* results section 5.1.5). On the other hand, 24 hours after the induction of CCHS inflammation, the OXA pre-exposed Sash ears contained levels of IL-4 comparable to those in the ears of their WT control littermates (*see* results section 5.1.2). Therefore it is possible that MCs are the source of IL-4 at early time points, i.e. around 12h after the 3rd challenge, and that IL-4 is released by MCs via degranulation. Whether increased skin levels of IL-4 observed in WT animals subjected to CCHS at early time points are involved in the control of CCHS inflammation remains to be investigated in detail.

MC-deficient Sash mice presented enhanced levels of IFNɣ and IL-17 24 hours after the induction of CCHS inflammation. According to the literature the source of such cytokines are infiltrated T cells. Peiser in 2013 showed that CD4^{+} T cells as well as gamma-delta T cells produce IL-17 in a CHS model to DNFB. Diverse CHS models demonstrated that skin infiltrating CD8^{+} T cells are able to produce IFNɣ as well as IL-17 *in situ* (Watanabe *et al.*, 2002, He *et al.*, 2009, Peiser, 2013). We, therefore, speculated that after CCHS inflammation subsided, OXA pre-exposed skin sites contain different sub-populations of T cells compared to uninvolved skin sites. The analysis of the T cell composition of the ears revealed that: (1) Contact to OXA in

sensitized mice leads to a long-lasting accumulation of $CD4^+$ and $CD8\beta^+$ lymphocytes in OXA-challenged ears, which prevailed there even after the inflammation subsided (see Fig. 22 and Fig. 23). (2) Most of $CD8\beta^+$ T cells found in the OXA-challenged ears express the markers of tissue resident memory (TRM) lymphocytes, i.e. they are $CD103^+CD44^{high+}$ (see Fig. 24). (3) After CCHS to OXA the ears of MC-deficient mice contained more TRM $CD8\beta^+$ T cells than those of their WT littermates (see Fig. 23A and B). These results are in accordance with studies published by Rana and coworkers (Rana *et al.,* 2008, 2009 and 2011). They demonstrated that cutaneous contact to OXA or to Ovalbumine in sensitized WT mice induces an accumulation of skin TRM $CD8^+$ T cells at the challenged skin site. They also showed that re-exposure with the relevant allergen in the pre-challenged skin can induce the expression of IFNɣ by these TRM $CD8\beta^+$ T cells. This is also in line with our results (Fig. 25). The results described above points to TRM $CD8\beta^+$ T cells in OXA pre-exposed skin sites as primer candidates for driving increased CCHS inflammation. Furthermore, the finding that TRM $CD8\beta^+$ T cells are even more accumulated in the ears of MC-deficient mice after CCHS to OXA, can explain why the protective contribution of MCs was restricted to those skin sites.

The local innate immune compartment, i.e. the $CD45^+CD3^-$ cells, was also increased in the ears of MC-deficient mice after CCHS to OXA. Hence we investigated their involvement in this model. Unlike hapten-specific T cells, innate immune cells, e.g. DC, macrophages and neutrophils, can react to a wide range of stimuli and are not antigen specific (Bellanti, 2012). We, therefore, employed a hapten cross-sensitization approach with DNFB to study the contribution of the local innate immune compartment in our CCHS model. DNFB was chosen, because it induces CHS responses that are similar to those induced by OXA (Goubier *et al.*, 2013). For example, Otsuka and coworkers showed that CHS reactions to DNFB as well as to OXA are involve a sub-population of DC (Otsuka *et al.,* 2011). Tuckermann and collaborators discovered that after challenge with DNFB or with OXA, treatment with glucocorticoids inhibited CHS responses by suppressing neutrophils and macrophages at the challenged area (Tuckermann *et al.,* 2007). However, OXA-specific T cells do not cross-react with DNFB and vice versa (Moorhead, 1976, Bacci *et al.*, 1997). For our cross-sensitization approach, 25 days after the 3rd challenge with OXA, WT mice, Sash mice and Sash mice treated with anti-CD8 antibody (Sash$^-$

^{CD8}) were sensitized with DNFB on the belly. After DNFB sensitization, these mice committed two conditions that were required for this experiment: (1) They contained the local innate immune components in the challenged ears necessary to mount a CCHS reaction to OXA, and (2) as consequence of the DNFB sensitization, they developed DNFB-specific effector T cells. Five days after DNFB-sensitization, these mice were challenged with DNFB on the right ears and with OXA on the left ears. Consequently, if the increased innate immune compartment of MC-deficient mice contributed to their exacerbated CCHS inflammation to OXA, the inflammation of Sash mice should be also exacerbated after this DNFB challenge. However, this was not the case, Sash mice and WT mice developed comparable CHS inflammatory responses to DNFB (*see* Fig. 28A). Thus, this result does not support the involvement of the innate immune compartment in the exacerbated CCHS inflammation of MC-deficient mice. Additionally, it reinforces the role of OXA-specific TRM CD8β$^+$ T cells in our CCHS model.

To study the contribution of TRM CD8β$^+$ T cells in our CCHS model, we reduced the numbers of these cells in the ears of Sash mice by a treatment with anti-CD8 antibody (Sash^{-CD8}). The results of this experiment showed that Sash^{-CD8} mice, which contained similar numbers of skin TRM CD8β$^+$ T cells as their WT controls, also displayed similar CCHS inflammatory responses (*see* results section 5.4.1, Fig. 27). In order to reduce the TRM CD8β$^+$ T cells in Sash mice, we used the anti-CD8 antibody clone 2.43 in a procedure called *in vivo* antibody-mediated cell depletion (Kruisbeek AM., 2001). The antibody clone 2.43 recognizes the alpha subunit of the CD8 complex. The CD8 complex can form a homodimer of two CD8α subunits as in some DC sub-populations or a heterodimer composed of one CD8α and one CD8β subunit as in CD8$^+$ T cells, including TRM CD8β$^+$ T cells. Once the anti-CD8 antibody is injected, it binds to CD8α$^+$ cells and induces them to die by phagocytosis and by complement-mediated mechanisms (Kruisbeek AM., 2001). Consequently, anti-CD8 antibody treatment reduces the numbers of TRM CD8β$^+$ T cells as well as of other CD8α$^+$ expressing cells. To exclude whether the effects of this antibody treatment on these other CD8α$^+$ cells modifies the inflammatory responses of our CCHS model, we use the DNFB cross-sensitization approach. In this experiment, we observed that compared to Sash mice, Sash^{-CD8} mice can mount normal CHS responses to DNFB on the right ears (Fig. 28A), whereas at the same time these Sash^{-CD8} mice showed

reduced CCHS responses to OXA on the left ears (Fig. 28B). CHS reactions to DNFB are mediated by DNFB-specific CD8$^+$ T cells (Otsuka *et al.*, 2011), and CHS to DNFB require similar sub-populations of DC than for CHS reactions to OXA (Honda *et al.*, 2013). Combining these to observations, we concluded that besides of OXA-specific TRM CD8β$^+$, other CD8α$^+$ cells, which were depleted during the anti-CD8 antibody treatment, were not required for inflammatory CCHS responses to OXA. This allows us to conclude that the increased numbers of OXA-specific TRM CD8β$^+$ T cells observed in the ears of MC-deficient mice are sufficient to induce exacerbated CCHS inflammatory responses to OXA.

In order to nail down the mechanism whereby MCs control the skin accumulation of TRM CD8β$^+$ T cells in our CCHS model, it was required to know when this accumulation occurred and how MC-deficient mice accumulate more of these cells in the challenged skin. Hence, we employed two different approaches to address this: (1) Quantification of TRM CD8β$^+$ T cells in the challenged ears of Sash mice and of WT mice between 0 - 8 days after the 1st challenged with OXA (*see* results section 5.4.1). (2) An adoptive transfer approach (*see* methods section 4.8.7). For this approach we engrafted intravenously the same number of CD45.1$^+$ TRM CD8β$^+$ T cells of Ly5.1 WT donor mice, in CD45.1$^-$ Sash and WT mice 6 days after the 1st challenge with OXA. This approach allowed us to quantify the number of CD45.1$^+$ TRM CD8β$^+$ T cells that migrated inside of donor challenged ears. By using the 1st approach, we determined that as early as 4 days after the 1st challenge with OXA, the CD8β$^+$ T cells in the challenged skin showed a TRM phenotype. i.e. CD103$^+$CD44^{high+}, but a difference between Sash mice and WT mice was first observed 6 days after this challenge (Fig. 29 right bar-graph). On day 6 and 8 after challenge Sash mice showed more TRM CD8β$^+$ T cells than their WT littermates. A possible explanation for this is that MCs could control the generation of TRM CD8β$^+$ T cells in the dLNs. Examination of the dLNs of these mice showed more TRM CD8β$^+$ T cells on day 6 after OXA challenge in the dLNs of Sash mice than in their WT control mice (Fig. 29 left bar-graph). The adoptive transfer approach showed that although both strains received the same number of donor of CD45.1$^+$ TRM CD8β$^+$ T cells, the number of this cells found in the ears of recipient Sash mice was significantly higher than those found in the ears of their WT control littermates (Fig. 30). This suggests that the increased numbers of TRM CD8β$^+$ T cells observed in the

challenged ears of Sash mice does not depend on their generation in secondary lymphoid organs. A publication from Mackay and coworkers in 2013 supports our findings obtained in the adoptive transfer approach. Using HSV infection as a model, they suggest that TRM CD8$^+$ T cells are generated directly in the skin from KLRG1$^+$ precursors. These KLRG1$^+$ precursors are in fact a sub-population of antigen-specific effector T cells generated during primary stages of the HSV infection (Mackay *et al*., 2013). More experiments are necessary to clarify the origin of TRM CD8β$^+$ T cells in our model.

6.5 Integrative hypothetical view of the role of MCs in CCHS

The most important findings included in this thesis are summarized in figure 31. Our results demonstrate that OXA challenge in sensitized mice leads to long-term changes of the immune composition of the challenged skin. MCs degranulate immediately after OXA contact, and repeated OXA contacts induce the accumulation of MCs, innate immune cells and TRM T cells in OXA challenged skin (Fig. 31. Step 1 - 3). MCs are critical for the accumulation of TRM CD8β$^+$ T cells in the OXA-challenged skin (Fig. 31. Step 4). The mechanisms by which MCs do so are still under investigation, however the literature provide us with some candidate mechanisms: (1) Memory T cells require specific adhesion molecules to migrate into target organs (Gebhardt and Mackay, 2012, Mackay *et al.,* 2013) and MCs are known to induce the expression of adhesion molecules in the endothelium to recruit immune cells to the skin (Kunder *et al.*, 2011). (2) Alternatively, MCs could enhance the cutaneous recruitment of T regulatory cells to control the TRM CD8β$^+$ T cells. In support of this hypothesis, Lu and coworkers published that MCs activated by IL-9 attract CD4$^+$ T regulatory cells, which then inactivate CD8$^+$ T cells in the engrafted organ and control their generation in the dLNs in a model for graft versus host diseases (Lu *et al.*, 2006). In our model, TRM CD8β$^+$ T cells reside in the challenged skin for more than 60 days after the 1st challenge with OXA (Fig. 31. Step 5). OXA re-exposure at the same skin site induced the activation of these TRM CD8β$^+$ T cells, which resulted in the production of IFNɣ by these and by other cells (Fig. 31. Step 6 and 7). The pro-inflammatory activity of TRM CD8β$^+$ T cells during CCHS to OXA was responsible for the increased inflammation in WT mice and for the uncontrolled inflammation in MC-deficient mice (Fig. 31. Step 8). CCHS inflammation activates

MCs (Fig. 31. Step 9) and our results suggest that this activation was required to enhance the production of cutaneous IL-4 (Fig. 31. Step 10) and to inhibit the accumulation of pro-inflammatory cytokines at the challenged skin, i.e. IFNɣ, IL-17 and IL-23 (Fig. 31. Step 11). In line with this, some studies identified MC-derived anti-inflammatory mediators that could dampen CHS reactions. For example Grimbaldeston and coworkers showed that MC-derived IL-10 limits skin pathology of CHS and of chronic irradiation with ultraviolet B light (Grimbaldestone *et al.,* 2007). In this regard, the beneficial effect of IL-4 after CCHS to OXA, which was increased in WT mice compared to Sash mice and WT^{Cromolyn} mice (*see* results section 5.1.5), needs to be verified.
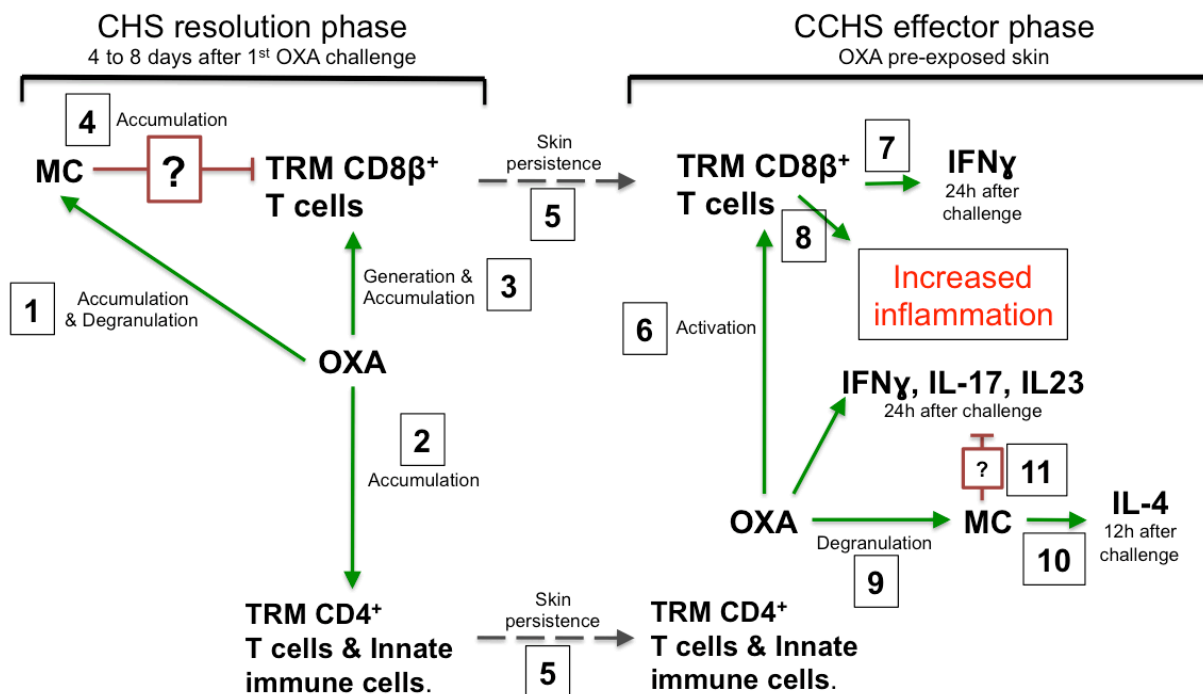
Figure 31. The role of mast cells in CCHS. Main findings of this study: During the resolution phase of CHS to OXA, challenge with OXA induces the activation and accumulation of MCs (1) as well as the generation and accumulation of TRM T cells and innate immune cells (2, 3). MCs control TRM CD8β^{+} T cell accumulation by unknown mechanisms (4). TRM T cells and innate immune cells persist in the challenged skin (5). During the effector phase of CCHS, OXA challenge leads to the activation of TRM CD8β^{+} T cells (6) followed by IFNɣ release (7), which induces inflammation (8). OXA-derived degranulation of MCs (9) results in IL-4 expression (10) and reduces IFNɣ, IL-17 and IL-23 by an unknown mechanism (11). *Abbreviations*: OXA - oxazolone, MC - mast cells, TRM - tissue resident memory, IFNɣ - interferon-gamma, IL - interleukin.

6.6 Translation of the knowledge acquired in this study to the clinical picture of human ACD

Allergic contact dermatitis (ACD) is a type IV hypersensitivity-mediated disease and is initiated by the activation of allergen-specific memory T cells to contact allergens.

Using CCHS to OXA as a model for ACD, we demonstrated that MCs importantly contribute to the control of skin CCHS inflammation by preventing the accumulation of allergen-specific TRM CD8β$^+$ T cells in the allergen-exposed skin. Our finding suggest that skin MCs help to limit inflammatory reactions in ACD patients and that MCs and MC-mediators may be novel and promising targets for prophylactic approaches to prevent the chronification of ACD. Further studies should clarify how MCs control TRM CD8β$^+$ T cells accumulation in CCHS on a molecular level.

6.7 Conclusions and perspectives

1. **Mast cells protect from exaggerated inflammation after chronic contact hypersensitivity (CCHS) to oxazolone (OXA).** Mast cell-activity diminished both, ear-swelling responses after the elicitation of CCHS inflammation and the levels of pro-inflammatory cytokines at the site of CCHS induction, i.e. IFNɣ, IL-17 and IL-23.

2. **Mast cells contribute to increase the levels of interleukin-4 (IL-4) during CCHS inflammation.** Twelve hours after the induction of CCHS inflammation, WT mice displayed more IL-4 than mast cell-deficient Sash mice and WT mice treated with the mast cell-inhibitor cromolyn. More experiments will be required to elucidate the role of IL-4 in this model.

3. **Mast cells protect from CCHS inflammation only in skin chronically exposed to OXA.** In OXA sensitized animals, skin sites that were repeatedly exposed to OXA (chronic exposition = CCHS) displayed stronger inflammation than skin sites that received a single exposition to OXA (acute exposition = CHS). Additionally, mast cell protection from inflammation was only seen at skin sites that were repeatedly (chronically) exposed to OXA.

4. **OXA-induced inflammation modifies permanently the immune composition of the skin and mast cell-activity controls this.** Exposition to OXA in sensitized mice changed the composition of the adaptive as well as the innate immune compartment of the involved skin, i.e. increased numbers of skin memory T lymphocytes as well as innate immune cells (CD45^{+}CD3^{-} cells). The numbers of mast cells were also increased after OXA exposition in the involved skin, which was associated with reduced numbers of both, pro-inflammatory OXA-specific TRM CD8β^{+} T cells and innate immune cells.

5. **Mast cells protect from CCHS inflammation by limiting the accumulation of OXA-specific TRM CD8β^{+} T cells in the challenged skin.** The CD8β^{+} T cells residing in the previously OXA challenged skin are the main producers of the pro-inflammatory cytokine IFNɣ at early time points after the elicitation of CCHS inflammation (24 hours). Sash mice showed increased numbers of TRM CD8β^{+} T cells. Reduction of these cells in Sash mice (to similar numbers of TRM CD8β^{+} T cells observed in WT mice) caused reduced CCHS inflammation to a level comparable to that of WT mice.

6. **Mast cells control the number of TRM CD8β^{+} T cells at different levels during the 1st challenge with OXA.** The mast cell-activity reduced the numbers of TRM CD8β^{+} T cells in the dLNs and in parallel controlled their accumulation in the skin. Mast cell effect on the numbers of these T cells was restricted between 6 - 8 days after the 1st challenge with OXA. The mast cell-derived signals required for controlling the accumulation of TRM CD8β^{+} T cells, as well as the final mast cell-mediator responsible for this task, will require further experiments. In this regards, a recent study about signals required by TRM CD8β^{+} T cells to growth and differentiate in the skin, points towards IL-15, TGFβ and IL-7 as important regulators (Mackay *et al.*, 2013). Experiments directed to assess the effects of mast cells over these cytokines might provide new insights to the molecular mechanism in our CCHS model.

Together, our results suggest that TRM CD8β^{+} T cells provide the skin with "*Immunologic tissue memory*" that primes this tissue to react stronger upon chronic encounters with the relevant antigen. Mast cells play a modulatory role by reducing the numbers of those cells. This idea is also supported by work done in murine

models of cutaneous viral infections. The work of Shin and coworkers in 2013 for example, evidenced the importance of TRM T cells in the protection from herpes simplex virus (HSV) infections. In this study they show that skin engrafted with HSV-specific TRM CD8$^+$ T cells displayed enhanced recovering ratio from infection as compared to non-engrafted skin sites (Shin *et al.,* 2013). "*Immunologic tissue memory*" is also observed in human pathologic conditions. For example eczematous lesions in ACD and psoriasis tend to reappear at specific body sites (Mackey *et al.,* 2012; Cheuk *et al.* 2014). However, how mast cells could interplay with the rest of the immune compartment in order to contribute to "*Immunologic tissue memory*" has not yet been investigated, but the data presented in this doctoral thesis provide the basis for further investigations of "*Immunologic tissue memory*" and therefore builds the next important step for the long-term goal of curing ACD.

7 Bibliography

Akahoshi, M., Song, C.H., Piliponsky, A.M., Metz, M., Guzzetta, A., Abrink, M., Schlenner, S.M., Feyerabend, T.B., Rodewald, H.R., Pejler, G., Tsai, M. & Galli, S.J., 2011. Mast cell chymase reduces the toxicity of Gila monster venom, scorpion venom, and vasoactive intestinal polypeptide in mice. *J Clin Invest,* 121**,** 4180-91.

Akiba, H., Satoh, M., Iwatsuki, K., Kaiserlian, D., Nicolas, J.F. & Kaneko, F., 2004. CpG immunostimulatory sequences enhance contact hypersensitivity responses in mice. *J Invest Dermatol,* 123**,** 488-93.

Alase, A. & Wittmann, M., 2012. Therapeutic strategies in allergic contact dermatitis. *Recent Pat Inflamm Allergy Drug Discov,* 6**,** 210-21.

Albanesi, C., Scarponi, C., Giustizieri, M.L. & Girolomoni, G., 2005. Keratinocytes in inflammatory skin diseases. *Curr Drug Targets Inflamm Allergy,* 4**,** 329-34.

Anderson, S.D., 2004. Single-dose agents in the prevention of exercise-induced asthma: a descriptive review. *Treat Respir Med,* 3**,** 365-79.

Anthony, R.M., Rutitzky, L.I., Urban, J.F., Stadecker, M.J. & Gause, W.C., 2007. Protective immune mechanisms in helminth infection. *Nat Rev Immunol,* 7**,** 975-87.

Arthur, J.C., Lich, J.D., Ye, Z., Allen, I.C., Gris, D., Wilson, J.E., Schneider, M., Roney, K.E., O'connor, B.P., Moore, C.B., Morrison, A., Sutterwala, F.S., Bertin, J., Koller, B.H., Liu, Z. & Ting, J.P., 2010. Cutting edge: NLRP12 controls dendritic and myeloid cell migration to affect contact hypersensitivity. *J Immunol,* 185**,** 4515-9.

Artuc, M., Steckelings, U.M. & Henz, B.M., 2002. Mast cell-fibroblast interactions: human mast cells as source and inducers of fibroblast and epithelial growth factors. *J Invest Dermatol,* 118**,** 391-5.

Askenase PW, Van Loveren H, Kraeuter-Kops S, Ron Y, Meade R, Theoharides TC, Nordlund JJ, Scovern H, Gerhson MD, Ptak W., 1983. Defective elicitation of delayed-type hypersensitivity in W/Wv and Sl/Sld mast cell-deficient mice. *J Immunol.* 131(6):2687-94.

Asherson, G.L. & Dieli, F., 1992. Immune deviation in the mouse: transfer of selective depression of the contact sensitivity and interleukin-2 response with retention of interferon-gamma production requires CD8+ T cells. *Immunology,* 76**,** 427-32.

Bacci, S., Alard, P., Dai, R., Nakamura, T. & Streilein, J.W., 1997. High and low doses of haptens dictate whether dermal or epidermal antigen-presenting cells promote contact hypersensitivity. *Eur J Immunol,* 27**,** 442-8.

Baker, D., Kimber, I., Ahmed, K. & Turk, J.L., 1991. Antigen-specific and non-specific depression of proliferative responses induced during contact sensitivity in mice. *Int J Exp Pathol,* 72**,** 55-65.

Bangert, C., Friedl, J., Stary, G., Stingl, G. & Kopp, T., 2003. Immunopathologic features of allergic contact dermatitis in humans: participation of plasmacytoid dendritic cells in the pathogenesis of the disease? *J Invest Dermatol,* 121**,** 1409-18.

Bennett CL., Clausen BE., 2007. DC ablation in mice: promises, pitfalls, and challenges. *Trends Immunol.* 28(12):525-31.

Berridge KC., Aldridge JW., Houchard KR., Zhuang X., 2005. Sequential super-stereotypy of an instinctive fixed action pattern in hyper-dopaminergic mutant mice: a model of obsessive-compulsive disorder and Tourette's. *BMC Biol.,* 14;3:4.

Bellanti, J., 2012. *Immunology. IV ed.* I Care Press*,* Maryland.

Bethin, K.E., Vogt, S.K. & Muglia, L.J., 2000. Interleukin-6 is an essential, corticotropin-releasing hormone-independent stimulator of the adrenal axis during immune system activation. *Proc Natl Acad Sci U S A,* 97**,** 9317-22.

Biedermann, T., Kneilling, M., Mailhammer, R., Maier, K., Sander, C.A., Kollias, G., Kunkel, S.L., Hultner, L. & Rocken, M., 2000. Mast cells control neutrophil recruitment during T cell-mediated delayed-type hypersensitivity reactions through tumor necrosis factor and macrophage inflammatory protein 2. *J Exp Med.,* 192**,** 1441-52.

Bienenstock, J., Befus, A.D., Pearce, F., Denburg, J. & Goodacre, R., 1982. Mast cell heterogeneity: derivation and function, with emphasis on the intestine. *J Allergy Clin Immunol,* 70**,** 407-12.

Biggs, L., Yu, C., Fedoric, B., Lopez, A.F., Galli, S.J. & Grimbaldeston, M.A., 2010. Evidence that vitamin D(3) promotes mast cell-dependent reduction of chronic UVB-induced skin pathology in mice. *J Exp Med,* 207**,** 455-63.

Botchkarev, V.A., Eichmüller, S., Peters, E.M., Pietsch, P., Johansson, O., Maurer, M. & Paus, R., 1997. A simple immunofluorescence technique for simultaneous visualization of mast cells and nerve fibers reveals selectivity and hair cycle--dependent changes in mast cell--nerve fiber contacts in murine skin. *Arch Dermatol Res,* 289**,** 292-302.

Bour, H., Peyron, E., Gaucherand, M., Garrigue, J.L., Desvignes, C., Kaiserlian, D., Revillard, J.P. & Nicolas, J.F., 1995. Major histocompatibility complex class I-restricted CD8+ T cells and class II-restricted CD4+ T cells, respectively, mediate and regulate contact sensitivity to dinitrofluorobenzene. *Eur J Immunol,* 25**,** 3006-10.

Boyman, O., Hefti, H.P., Conrad, C., Nickoloff, B.J., Suter, M. & Nestle, F.O., 2004. Spontaneous development of psoriasis in a new animal model shows an essential role for resident T cells and tumor necrosis factor-alpha. *J Exp Med,* 199**,** 731-6.

Brower GL., Chancey AL., Thanigaraj S., Matsubara BB., Janicki JS., 2002. Cause and effect relationship between myocardial mast cell number and matrix metalloproteinase activity. *Am J Physiol Heart Circ Physiol.* 283(2):H518-25.

Bryce, P.J., Miller, M.L., Miyajima, I., Tsai, M., Galli, S.J. & Oettgen, H.C., 2004. Immune sensitization in the skin is enhanced by antigen-independent effects of IgE. *Immunity,* 20**,** 381-92.

Buch, T., Heppner, F.L., Tertilt, C., Heinen, T.J., Kremer, M., Wunderlich, F.T., Jung, S. & Waisman, A., 2005. A Cre-inducible diphtheria toxin receptor mediates cell lineage ablation after toxin administration. *Nat Methods,* 2**,** 419-26.

Bursch, L.S., Wang, L., Igyarto, B., Kissenpfennig, A., Malissen, B., Kaplan, D.H. & Hogquist, K.A., 2007. Identification of a novel population of Langerin+ dendritic cells. *J Exp Med,* 204**,** 3147-56.

Caron, G., Delneste, Y., Roelandts, E., Duez, C., Bonnefoy, J.Y., Pestel, J. & Jeannin, P., 2001a. Histamine polarizes human dendritic cells into Th2 cell-promoting effector dendritic cells. *J Immunol,* 167**,** 3682-6.

Caron, G., Delneste, Y., Roelandts, E., Duez, C., Herbault, N., Magistrelli, G., Bonnefoy, J.Y., Pestel, J. & Jeannin, P., 2001b. Histamine induces CD86 expression and chemokine production by human immature dendritic cells. *J Immunol,* 166**,** 6000-6.

Cavani, A., Mei, D., Guerra, E., Corinti, S., Giani, M., Pirrotta, L., Puddu, P. & Girolomoni, G., 1998. Patients with allergic contact dermatitis to nickel and nonallergic individuals display different nickel-specific T cell responses. Evidence for the presence of effector CD8+ and regulatory CD4+ T cells. *J Invest Dermatol,* 111**,** 621-8.

Clarke SR., Barnden M., Kurts C., Carbone FR., Miller JF., Heath WR., 2000. Characterization of the ovalbumin-specific TCR transgenic line OT-I: MHC elements for positive and negative selection. *Immunol Cell Biol.* 78(2):110-7.

Chen, K., Xiang, Y., Yao, X., Liu, Y., Gong, W., Yoshimura, T. & Wang, J.M., 2011. The active contribution of Toll-like receptors to allergic airway inflammation. *Int Immunopharmacol,* 11**,** 1391-8.

Chen, R., Ning, G., Zhao, M.L., Fleming, M.G., Diaz, L.A., Werb, Z. & Liu, Z., 2001. Mast cells play a key role in neutrophil recruitment in experimental bullous pemphigoid. *J Clin Invest,* 108**,** 1151-8.

Cheng, L.E., Hartmann, K., Roers, A., Krummel, M.F. & Locksley, R.M., 2013. Perivascular mast cells dynamically probe cutaneous blood vessels to capture immunoglobulin E. *Immunity,* 38**,** 166-75.

Chereches-Panta, P., C, S., Dumitrescu, D., Marshall, M., Mirestean, I., Muresan, M., Iacob, D., Farcau, M., Ichim, G.E. & Nanulescu, M.V., 2011. Epidemiological survey 6 years apart: increased prevalence of asthma and other allergic diseases in schoolchildren aged 13-14 years in cluj-napoca, romania (based on isaac questionnaire). *Maedica (Buchar),* 6**,** 10-6.

Costa R., Marotta DM., Manjavachi MN., Fernandes ES., Lima-Garcia JF., Paszcuk AF., Quintão NL., Juliano L., Brain SD., Calixto JB., 2008. Evidence for the role of neurogenic inflammation components in trypsin-elicited scratching behaviour in mice. *Br J Pharmacol.* 154(5):1094-103.

Cheuk S., Wikén M., Blomqvist L., Nylén S., Talme T., Ståhle M., Eidsmo L., 2014. Epidermal Th22 and Tc17 cells form a localized disease memory in clinically healed psoriasis. *J Immunol.* 192(7):3111-20.

Christensen AD., Haase C., 2012. Immunological mechanisms of contact hypersensitivity in mice. *APMIS.* 120(1):1-27.

Crivellato, E., Nico, B. & Ribatti, D., 2008. Mast cells and tumour angiogenesis: new insight from experimental carcinogenesis. *Cancer Lett,* 269**,** 1-6.

Cumberbatch, M., Dearman, R.J. & Kimber, I., 1997. Langerhans cells require signals from both tumour necrosis factor-alpha and interleukin-1 beta for migration. *Immunology,* 92**,** 388-95.

Cumberbatch, M. & Kimber, I., 1995. Tumour necrosis factor-alpha is required for accumulation of dendritic cells in draining lymph nodes and for optimal contact sensitization. *Immunology,* 84**,** 31-5.

Dahlin JS., Hallgren J., 2014. Mast cell progenitors: Origin, development and migration to tissues. *Mol Immunol.* 63(1):9-17.

Denucci, C.C., Mitchell, J.S. & Shimizu, Y., 2009. Integrin function in T-cell homing to lymphoid and nonlymphoid sites: getting there and staying there. *Crit Rev Immunol,* 29**,** 87-109.

Dilulio, N.A., Engeman, T., Armstrong, D., Tannenbaum, C., Hamilton, T.A. & Fairchild, R.L., 1999. Groalpha-mediated recruitment of neutrophils is required for elicitation of contact hypersensitivity. *Eur J Immunol,* 29**,** 3485-95.

Dudeck, A., Dudeck, J., Scholten, J., Petzold, A., Surianarayanan, S., Köhler, A., Peschke, K., Vöhringer, D., Waskow, C., Krieg, T., Müller, W., Waisman, A., Hartmann, K., Gunzer, M. & Roers, A., 2011. Mast cells are key promoters of contact allergy that mediate the adjuvant effects of haptens. *Immunity,* 34**,** 973-84.

Dyring-Andersen, B., Skov, L., Løvendorf, M.B., Bzorek, M., Søndergaard, K., Lauritsen, J.P., Dabelsteen, S., Geisler, C. & Bonefeld, C.M., 2013. CD4(+) T cells producing interleukin (IL)-17, IL-22 and interferon-γ are major effector T cells in nickel allergy. *Contact Dermatitis,* 68**,** 339-47.

Ehrlich P,. 1877. Beiträge zur Kenntnis der Anilinfärbungen und ihrer Verwendung in der mikroskopischen Technik. Arch. mikr. Anat. 1877;13:263–277. *Arch. mikr. Anat.* (Leipzig), 13, 263

Ehrlich P,. 1879. Beiträge zur Kenntnis der granulierten Bindegwebszellen und der eosinophilen Leokozyten. *Arch Anat Physiol,* 3**:** 166-169.

Enerbäck, L., 1966. Mast cells in rat gastrointestinal mucosa. I. Effects of fixation. *Acta Pathol Microbiol Scand,* 66**,** 289-302.

Engeman, T., Gorbachev, A.V., Kish, D.D. & Fairchild, R.L., 2004. The intensity of neutrophil infiltration controls the number of antigen-primed CD8 T cells recruited into cutaneous antigen challenge sites. *J Leukoc Biol,* 76**,** 941-9.

Faveeuw, C., Gosset, P., Bureau, F., Angeli, V., Hirai, H., Maruyama, T., Narumiya, S., Capron, M. & Trottein, F., 2003. Prostaglandin D2 inhibits the production of interleukin-12 in murine dendritic cells through multiple signaling pathways. *Eur J Immunol,* 33**,** 889-98.

Feyerabend, T.B., Weiser, A., Tietz, A., Stassen, M., Harris, N., Kopf, M., Radermacher, P., Möller, P., Benoist, C., Mathis, D., Fehling, H.J. & Rodewald, H.R., 2011. Cre-mediated cell ablation contests mast cell contribution in models of antibody- and T cell-mediated autoimmunity. *Immunity,* 35**,** 832-44.

Friedmann, P.S. & Pickard, C., 2014. Contact hypersensitivity: quantitative aspects, susceptibility and risk factors. *Experientia. Supplementum,* 104**,** 51-71.

Galli, S.J. & Hammel, I., 1984. Unequivocal delayed hypersensitivity in mast cell-deficient and beige mice. *Science,* 226**,** 710-3.

Galli, S.J., Kalesnikoff, J., Grimbaldeston, M.A., Piliponsky, A.M., Williams, C.M. & Tsai, M., 2005. Mast cells as "tunable" effector and immunoregulatory cells: recent advances. *Annu Rev Immunol,* 23**,** 749-86.

Galli, S.J. & Tsai, M., 2008. Mast cells: versatile regulators of inflammation, tissue remodeling, host defense and homeostasis. *J Dermatol Sci,* 49**,** 7-19.

Gebhardt, T. & Mackay, L.K., 2012. Local immunity by tissue-resident CD8(+) memory T cells. *Front Immunol,* 3**,** 340.

Gelbmann, C.M., Mestermann, S., Gross, V., Köllinger, M., Schölmerich, J. & Falk, W., 1999. Strictures in Crohn's disease are characterised by an accumulation of mast cells colocalised with laminin but not with fibronectin or vitronectin. *Gut,* 45**,** 210-7.

Gell PGH., Coombs RRA.,1963. *Clinical Aspects of Immunology.* Blackwell Scientific Publications, London.

Gerritsen, M.E., 1996. Physiological and pathophysiological roles of eicosanoids in the microcirculation. *Cardiovasc Res,* 32**,** 720-32.

Gessner, A., Mohrs, K. & Mohrs, M., 2005. Mast cells, basophils, and eosinophils acquire constitutive IL-4 and IL-13 transcripts during lineage differentiation that are sufficient for rapid cytokine production. *J Immunol,* 174**,** 1063-72.

Gilfillan, A.M. & Tkaczyk, C., 2006. Integrated signalling pathways for mast-cell activation. *Nat Rev Immunol,* 6**,** 218-30.

Gillitzer, R. & Goebeler, M., 2001. Chemokines in cutaneous wound healing. *J Leukoc Biol,* 69**,** 513-21.

Gocinski, B.L. & Tigelaar, R.E., 1990. Roles of CD4+ and CD8+ T cells in murine contact sensitivity revealed by in vivo monoclonal antibody depletion. *J Immunol,* 144**,** 4121-8.

Gosset, P., Bureau, F., Angeli, V., Pichavant, M., Faveeuw, C., Tonnel, A.B. & Trottein, F., 2003. Prostaglandin D2 affects the maturation of human monocyte-derived dendritic cells: consequence on the polarization of naive Th cells. *J Immunol,* 170**,** 4943-52.

Gorbachev AV., Fairchild RL., 2001. Induction and regulation of T-cell priming for contact hypersensitivity. *Crit Rev Immunol,* 21(5):451-72

Goubier, A., Vocanson, M., Macari, C., Poyet, G., Herbelin, A., Nicolas, J.F., Dubois, B. & Kaiserlian, D., 2013. Invariant NKT cells suppress CD8(+) T-cell-mediated allergic contact dermatitis independently of regulatory CD4(+) T cells. *J Invest Dermatol,* 133**,** 980-7.

Grabbe, S. & Schwarz, T., 1996. Immunoregulatory mechanisms involved in elicitation of allergic contact hypersensitivity. *Am J Contact Dermat,* 7**,** 238-46.

Gri, G., Frossi, B., D'inca, F., Danelli, L., Betto, E., Mion, F., Sibilano, R. & Pucillo, C., 2012. Mast cell: an emerging partner in immune interaction. *Front Immunol,* 3**,** 120.

Grimbaldeston, M.A., Chen, C.C., Piliponsky, A.M., Tsai, M., Tam, S.Y. & Galli, S.J., 2005. Mast cell-deficient W-sash c-kit mutant Kit W-sh/W-sh mice as a model for investigating mast cell biology in vivo. *Am J Pathol,* 167**,** 835-48.

Grimbaldeston, M.A., Nakae, S., Kalesnikoff, J., Tsai, M. & Galli, S.J., 2007. Mast cell-derived interleukin 10 limits skin pathology in contact dermatitis and chronic irradiation with ultraviolet B. *Nat Immunol,* 8**,** 1095-104.

Guiraldelli, M.F., França, C.N., De Souza, D.A., Da Silva, E.Z., Toso, V.D., Carvalho, C.C., Jamur, M.C. & Oliver, C., 2013. Rat embryonic mast cells originate in the AGM. *PLoS One,* 8**,** e57862.

Gunzer, M., 2012. Vaccine adjuvants: Tailor-made mast-cell granules. *Nat Mater,* 11**,** 181-2.

Gurish, M.F. & Boyce, J.A., 2006. Mast cells: ontogeny, homing, and recruitment of a unique innate effector cell. *J Allergy Clin Immunol,* 117**,** 1285-91.

Hand, T.W. & Kaech, S.M., 2009. Intrinsic and extrinsic control of effector T cell survival and memory T cell development. *Immunol Res,* 45**,** 46-61.

Handa, S., Kaur, I., Gupta, T. & Jindal, R., 2012. Hand eczema: correlation of morphologic patterns, atopy, contact sensitization and disease severity. *Indian J Dermatol Venereol Leprol,* 78**,** 153-8.

Hart, P.H., Gorman, S. & Finlay-Jones, J.J., 2011. Modulation of the immune system by UV radiation: more than just the effects of vitamin D? *Nat Rev Immunol,* 11**,** 584-96.

Hart, P.H., Grimbaldeston, M.A., Swift, G.J., Jaksic, A., Noonan, F.P. & Finlay-Jones, J.J., 1998. Dermal mast cells determine susceptibility to ultraviolet B-induced systemic suppression of contact hypersensitivity responses in mice. *J Exp Med,* 187**,** 2045-53.

Harvima, I.T., 2008. Induction of matrix metalloproteinase-9 in keratinocytes by histamine. *J Invest Dermatol,* 128**,** 2748-50.

Harvima, I.T. & Nilsson, G., 2011. Mast cells as regulators of skin inflammation and immunity. *Acta Derm Venereol,* 91**,** 644-50.

Harvima, I.T. & Nilsson, G., 2012. Stress, the neuroendocrine system and mast cells: current understanding of their role in psoriasis. *Expert Rev Clin Immunol,* 8**,** 235-41.

Harvima, I.T., Nilsson, G. & Naukkarinen, A., 2010. Role of mast cells and sensory nerves in skin inflammation. *G Ital Dermatol Venereol,* 145**,** 195-204.

Hawke, S., Stevenson, P.G., Freeman, S. & Bangham, C.R., 1998. Long-term persistence of activated cytotoxic T lymphocytes after viral infection of the central nervous system. *J Exp Med,* 187**,** 1575-82.

He, D., Wu, L., Kim, H.K., Li, H., Elmets, C.A. & Xu, H., 2009. IL-17 and IFN-gamma mediate the elicitation of contact hypersensitivity responses by different mechanisms and both are required for optimal responses. *J Immunol,* 183**,** 1463-70.

He, Z.X., Huang, S.L., Zhou, Q.F. & Li, S.N., 2004. [Generation of CD34+/Sca-1+ cells from mouse embryonic stem cells with two-step differentiation in vitro]. *Zhonghua Er Ke Za Zhi,* 42**,** 830-4.

Hendrix, S., Picker, B., Liezmann, C. & Peters, E.M., 2008. Skin and hair follicle innervation in experimental models: a guide for the exact and reproducible evaluation of neuronal plasticity. *Exp Dermatol,* 17**,** 214-27.

Hershko, A.Y., Charles, N., Olivera, A., Alvarez-Errico, D. & Rivera, J., 2012. Cutting edge: persistence of increased mast cell numbers in tissues links dermatitis to enhanced airway disease in a mouse model of atopy. *J Immunol,* 188**,** 531-5.

Hershko, A.Y., Suzuki, R., Charles, N., Alvarez-Errico, D., Sargent, J.L., Laurence, A. & Rivera, J., 2011. Mast cell interleukin-2 production contributes to suppression of chronic allergic dermatitis. *Immunity,* 35**,** 562-71.

Hofmann, M. & Pircher, H., 2011. E-cadherin promotes accumulation of a unique memory CD8 T-cell population in murine salivary glands. *Proc Natl Acad Sci U S A,* 108**,** 16741-6.

Honda, T., Egawa, G., Grabbe, S. & Kabashima, K., 2013. Update of immune events in the murine contact hypersensitivity model: toward the understanding of allergic contact dermatitis. *J Invest Dermatol,* 133**,** 303-15.

Honda, T., Miyachi, Y. & Kabashima, K., 2010a. The role of regulatory T cells in contact hypersensitivity. *Recent Pat Inflamm Allergy Drug Discov,* 4**,** 85-9.

Honda, T., Nakajima, S., Egawa, G., Ogasawara, K., Malissen, B., Miyachi, Y. & Kabashima, K., 2010b. Compensatory role of Langerhans cells and langerin-positive dermal dendritic cells in the sensitization phase of murine contact hypersensitivity. *J Allergy Clin Immunol,* 125**,** 1154-1156.e2.

Ierna, M.X., Scales, H.E., Saunders, K.L. & Lawrence, C.E., 2008. Mast cell production of IL-4 and TNF may be required for protective and pathological responses in gastrointestinal helminth infection. *Mucosal Immunol,* 1**,** 147-55.

Igyarto, B.Z., Jenison, M.C., Dudda, J.C., Roers, A., Müller, W., Koni, P.A., Campbell, D.J., Shlomchik, M.J. & Kaplan, D.H., 2009. Langerhans cells suppress contact hypersensitivity responses via cognate CD4 interaction and langerhans cell-derived IL-10. *J Immunol,* 183**,** 5085-93.

Ikeda, R.K., Miller, M., Nayar, J., Walker, L., Cho, J.Y., Mcelwain, K., Mcelwain, S., Raz, E. & Broide, D.H., 2003. Accumulation of peribronchial mast cells in a mouse model of ovalbumin allergen induced chronic airway inflammation: modulation by immunostimulatory DNA sequences. *J Immunol,* 171**,** 4860-7.

Ishikawa, T., Kanda, N., Hau, C.S., Tada, Y. & Watanabe, S., 2009. Histamine induces human beta-defensin-3 production in human keratinocytes. *J Dermatol Sci,* 56**,** 121-7.

Islam, S.A. & Luster, A.D., 2012. T cell homing to epithelial barriers in allergic disease. *Nat Med,* 18**,** 705-15.

Jack, A.R., Norris, P.L. & Storrs, F.J., 2013. Allergic contact dermatitis to plant extracts in cosmetics. *Semin Cutan Med Surg,* 32**,** 140-6.

Jarboe, D.L. & Huff, T.F., 1989. The mast cell-committed progenitor. II. W/Wv mice do not make mast cell-committed progenitors and S1/S1d fibroblasts do not support development of normal mast cell-committed progenitors. *J Immunol,* 142**,** 2418-23.

Jawdat, D.M., Albert, E.J., Rowden, G., Haidl, I.D. & Marshall, J.S., 2004. IgE-mediated mast cell activation induces Langerhans cell migration in vivo. *J Immunol,* 173**,** 5275-82.

Kabashima, K., Sakata, D., Nagamachi, M., Miyachi, Y., Inaba, K. & Narumiya, S., 2003. Prostaglandin E2-EP4 signaling initiates skin immune responses by promoting migration and maturation of Langerhans cells. *Nat Med,* 9**,** 744-9.

Kaech, S.M., Wherry, E.J. & Ahmed, R., 2002. Effector and memory T-cell differentiation: implications for vaccine development. *Nat Rev Immunol, 2,* 251-62.

Kalesnikoff, J. & Galli, S.J., 2008. New developments in mast cell biology. *Nat Immunol,* 9**,** 1215-23.

Kalesnikoff, J. & Galli, S.J., 2011. Antiinflammatory and immunosuppressive functions of mast cells. *Methods Mol Biol,* 677**,** 207-20.

Kanda, N., Ishikawa, T. & Watanabe, S., 2010. Prostaglandin D2 induces the production of human beta-defensin-3 in human keratinocytes. *Biochem Pharmacol,* 79**,** 982-9.

Kanda, N. & Watanabe, S., 2003. Histamine enhances the production of nerve growth factor in human keratinocytes. *J Invest Dermatol,* 121**,** 570-7.

Kanda, N. & Watanabe, S., 2004. Histamine enhances the production of granulocyte-macrophage colony-stimulating factor via protein kinase Calpha and extracellular signal-regulated kinase in human keratinocytes. *J Invest Dermatol,* 122**,** 863-72.

Kawakami, T. & Galli, S.J., 2002. Regulation of mast-cell and basophil function and survival by IgE. *Nat Rev Immunol,* 2**,** 773-86.

Kent, D., Copley, M., Benz, C., Dykstra, B., Bowie, M. & Eaves, C., 2008. Regulation of hematopoietic stem cells by the steel factor/KIT signaling pathway. *Clin Cancer Res,* 14**,** 1926-30.

Kimber, I., Maxwell, G., Gilmour, N., Dearman, R.J., Friedmann, P.S. & Martin, S.F., 2012. Allergic contact dermatitis: a commentary on the relationship between T lymphocytes and skin sensitising potency. *Toxicology,* 291**,** 18-24.

Kimura, T., Sugaya, M., Blauvelt, A., Okochi, H. & Sato, S., 2013. Delayed wound healing due to increased interleukin-10 expression in mice with lymphatic dysfunction. *J Leukoc Biol,* 94**,** 137-45.

Kirshenbaum, A.S., Kessler, S.W., Goff, J.P. & Metcalfe, D.D., 1991. Demonstration of the origin of human mast cells from CD34+ bone marrow progenitor cells. *J Immunol,* 146**,** 1410-5.

Kissenpfennig, A., Henri, S., Dubois, B., Laplace-Builhé, C., Perrin, P., Romani, N., Tripp, C.H., Douillard, P., Leserman, L., Kaiserlian, D., Saeland, S., Davoust, J. & Malissen, B., 2005. Dynamics and function of Langerhans cells in vivo: dermal dendritic cells colonize lymph node areas distinct from slower migrating Langerhans cells. *Immunity,* 22**,** 643-54.

Kleij, H.P. & Bienenstock, J., 2005. Significance of Conversation between Mast Cells and Nerves. *Allergy Asthma Clin Immunol,* 1**,** 65-80.

Kneilling M., Hültner L., Pichler BJ., Mailhammer R., Morawietz L., Solomon S., Eichner M., Sabatino J., Biedermann T., Krenn V., Weber WA., Illges H., Haubner R., Röcken M., 2007. Targeted mast cell silencing protects against joint destruction and angiogenesis in experimental arthritis in mice. *Arthritis Rheum.* 56(6):1806-16.

Kneilling, M., Mailhammer, R., Hültner, L., Schönberger, T., Fuchs, K., Schaller, M., Bukala, D., Massberg, S., Sander, C.A., Braumüller, H., Eichner, M., Maier, K.L., Hallmann, R., Pichler, B.J., Haubner, R., Gawaz, M., Pfeffer, K., Biedermann, T. & Röcken, M., 2009. Direct crosstalk between mast cell-TNF and TNFR1-expressing endothelia mediates local tissue inflammation. *Blood,* 114**,** 1696-706.

Kobayashi Y., Okunishi H., 2002. Mast cells as a target of rheumatoid arthritis treatment. *Jpn J Pharmacol.* 90(1):7-11.

Kolb, H.J., 2013. Mast cells and GVHD: old cells with a new role. *Blood,* 122**,** 3556-7.

Kristensen, T., Vestergaard, H. & Møller, M.B., 2011. Improved detection of the KIT D816V mutation in patients with systemic mastocytosis using a quantitative and highly sensitive real-time qPCR assay. *J Mol Diagn,* 13**,** 180-8.

Kruisbeek AM., 2001. In vivo depletion of CD4- and CD8-specific T cells. *Curr Protoc Immunol.* Chapter 4:Unit 4.1.

Ku, H.O., Jeong, S.H., Kang, H.G., Pyo, H.M., Cho, J.H., Son, S.W., Yun, S.M. & Ryu, D.Y., 2009. Gene expression profiles and pathways in skin inflammation induced by three different sensitizers and an irritant. *Toxicol Lett,* 190**,** 231-7.

Kunder, C.A., St John, A.L. & Abraham, S.N., 2011. Mast cell modulation of the vascular and lymphatic endothelium. *Blood,* 118**,** 5383-93.

Kunder, C.A., St John, A.L., Li, G., Leong, K.W., Berwin, B., Staats, H.F. & Abraham, S.N., 2009. Mast cell-derived particles deliver peripheral signals to remote lymph nodes. *J Exp Med,* 206**,** 2455-67.

Lantz, C.S., Boesiger, J., Song, C.H., Mach, N., Kobayashi, T., Mulligan, R.C., Nawa, Y., Dranoff, G. & Galli, S.J., 1998. Role for interleukin-3 in mast-cell and basophil development and in immunity to parasites. *Nature,* 392**,** 90-3.

Lehtimäki, S., Savinko, T., Lahl, K., Sparwasser, T., Wolff, H., Lauerma, A., Alenius, H. & Fyhrquist, N., 2012. The temporal and spatial dynamics of Foxp3+ Treg cell-mediated suppression during contact hypersensitivity responses in a murine model. *J Invest Dermatol,* 132**,** 2744-51.

Lilla, J.N., Chen, C.C., Mukai, K., Benbarak, M.J., Franco, C.B., Kalesnikoff, J., Yu, M., Tsai, M., Piliponsky, A.M. & Galli, S.J., 2011. Reduced mast cell and basophil numbers and function in Cpa3-Cre; Mcl-1fl/fl mice. *Blood,* 118**,** 6930-8.

Lu, L.F., Lind, E.F., Gondek, D.C., Bennett, K.A., Gleeson, M.W., Pino-Lagos, K., Scott, Z.A., Coyle, A.J., Reed, J.L., Van Snick, J., Strom, T.B., Zheng, X.X. &

Noelle, R.J., 2006. Mast cells are essential intermediaries in regulatory T-cell tolerance. *Nature,* 442**,** 997-1002.

Lundequist, A. & Pejler, G., 2011. Biological implications of preformed mast cell mediators. *Cell Mol Life Sci,* 68**,** 965-75.

Lyon, M.F. & Glenister, P.H., 1982. A new allele sash (Wsh) at the W-locus and a spontaneous recessive lethal in mice. *Genet Res,* 39**,** 315-22.

Mackay, L.K., Rahimpour, A., Ma, J.Z., Collins, N., Stock, A.T., Hafon, M.L., Vega-Ramos, J., Lauzurica, P., Mueller, S.N., Stefanovic, T., Tscharke, D.C., Heath, W.R., Inouye, M., Carbone, F.R. & Gebhardt, T., 2013. The developmental pathway for CD103(+)CD8+ tissue-resident memory T cells of skin. *Nat Immunol,* 14**,** 1294-301.

Mackay, L.K., Stock, A.T., Ma, J.Z., Jones, C.M., Kent, S.J., Mueller, S.N., Heath, W.R., Carbone, F.R. & Gebhardt, T., 2012. Long-lived epithelial immunity by tissue-resident memory T (TRM) cells in the absence of persisting local antigen presentation. *Proc Natl Acad Sci U S A,* 109**,** 7037-42.

Mal'tsev, D.V., Kazmirchuk, V.E. & Tsarik, V.V., 2012. [The revised Gell and Coombs classification: a new reading of old truths in the context of immunodeficiencies theory]. *Lik Sprava***,** 28-44.

Marichal, T., Starkl, P., Reber, L.L., Kalesnikoff, J., Oettgen, H.C., Tsai, M., Metz, M. & Galli, S.J., 2013. A beneficial role for immunoglobulin E in host defense against honeybee venom. *Immunity,* 39**,** 963-75.

Marshall, J.S., 2004. Mast-cell responses to pathogens. *Nat Rev Immunol,* 4**,** 787-99.

Martin, S.F., 2012. Allergic contact dermatitis: xenoinflammation of the skin. *Curr Opin Immunol,* 24**,** 720-9.

Martin, S.F. & Jakob, T., 2008. From innate to adaptive immune responses in contact hypersensitivity. *Curr Opin Allergy Clin Immunol,* 8**,** 289-93.

Masayuki M., Katsuhito K., Takanori O., Masayo S., Takanobu K. and Hiroshi M. 2014. Analysis of Guanine Oxidation Products in Double-Stranded DNA and Proposed Guanine Oxidation Pathways in Single-Stranded, Double-Stranded or Quadruplex DNA. *Biomolecules. 4*, 140-159.

Masopust, D., Jiang, J., Shen, H. & Lefrançois, L., 2001. Direct analysis of the dynamics of the intestinal mucosa CD8 T cell response to systemic virus infection. *J Immunol,* 166**,** 2348-56.

Matthaei, K.I., 2007. Genetically manipulated mice: a powerful tool with unsuspected caveats. *J Physiol,* 582**,** 481-8.

Mayer, T.C., 1970. A comparison of pigment cell development in albino, steel, and dominant-spotting mutant mouse embryos. *Dev Biol,* 23**,** 297-309.

Mazzoni, A., Siraganian, R.P., Leifer, C.A. & Segal, D.M., 2006. Dendritic cell modulation by mast cells controls the Th1/Th2 balance in responding T cells. *J Immunol,* 177**,** 3577-81.

Merad, M., Fong, L., Bogenberger, J. & Engleman, E.G., 2000. Differentiation of myeloid dendritic cells into CD8alpha-positive dendritic cells in vivo. *Blood,* 96**,** 1865-72.

Mekori YA., Galli SJ., 1985. Undiminished immunologic tolerance to contact sensitivity in mast cell-deficient W/Wv and Sl/Sld mice. *J Immunol* 135:879–885

Metz M, Maurer M., 2007. Mast cells-key effector cells in immune responses. *Trends Immunol*. 28(5):234-41.

Meulenbroeks C., van Weelden H., Schwartz C., Voehringer D., Redegeld FA., Rutten VP., Willemse T., Sijts AJ., Zaiss DM., 2014. Basophil-Derived Amphiregulin Is Essential for UVB Irradiation-Induced Immune Suppression. *J Invest Dermatol.* jid.2014.329.

Michel, A., Schüler, A., Friedrich, P., Döner, F., Bopp, T., Radsak, M., Hoffmann, M., Relle, M., Distler, U., Kuharev, J., Tenzer, S., Feyerabend, T.B., Rodewald, H.R., Schild, H., Schmitt, E., Becker, M. & Stassen, M., 2013. Mast cell-deficient Kit(W-sh) "Sash" mutant mice display aberrant myelopoiesis leading to the accumulation of splenocytes that act as myeloid-derived suppressor cells. *J Immunol,* 190**,** 5534-44.

Moed, H., Von Blomberg, M., Bruynzeel, D.P., Scheper, R., Gibbs, S. & Rustemeyer, T., 2005. Improved detection of allergen-specific T-cell responses in allergic contact dermatitis through the addition of 'cytokine cocktails'. *Exp Dermatol,* 14**,** 634-40.

Moorhead, J.W., 1976. Tolerance and contact sensitivity to DNFB in mice. VI. Inhibition of afferent sensitivity by suppressor T cells in adoptive tolerance. *J Immunol,* 117**,** 802-6.

Mori, T., Kabashima, K., Fukamachi, S., Kuroda, E., Sakabe, J., Kobayashi, M., Nakajima, S., Nakano, K., Tanaka, Y., Matsushita, S., Nakamura, M. & Tokura, Y., 2013. D1-like dopamine receptors antagonist inhibits cutaneous immune reactions mediated by Th2 and mast cells. *J Dermatol Sci,* 71**,** 37-44.

Nagle, D.L., Kozak, C.A., Mano, H., Chapman, V.M. & Bućan, M., 1995. Physical mapping of the Tec and Gabrb1 loci reveals that the Wsh mutation on mouse chromosome 5 is associated with an inversion. *Hum Mol Genet,* 4**,** 2073-9.

Nakae, S., Suto, H., Berry, G.J. & Galli, S.J., 2007. Mast cell-derived TNF can promote Th17 cell-dependent neutrophil recruitment in ovalbumin-challenged OTII mice. *Blood,* 109**,** 3640-8.

Nakae, S., Suto, H., Iikura, M., Kakurai, M., Sedgwick, J.D., Tsai, M. & Galli, S.J., 2006. Mast cells enhance T cell activation: importance of mast cell costimulatory molecules and secreted TNF. *J Immunol,* 176**,** 2238-48.

Nakahata, T. & Toru, H., 2002. Cytokines regulate development of human mast cells from hematopoietic progenitors. *Int J Hematol,* 75**,** 350-6.

Naukkarinen, A., Harvima, I., Paukkonen, K., Aalto, M.L. & Horsmanheimo, M., 1993. Immunohistochemical analysis of sensory nerves and neuropeptides, and their contacts with mast cells in developing and mature psoriatic lesions. *Arch Dermatol Res,* 285**,** 341-6.

Nestle, F.O., Di Meglio, P., Qin, J.Z. & Nickoloff, B.J., 2009. Skin immune sentinels in health and disease. *Nat Rev Immunol,* 9**,** 679-91.

Nigrovic, P.A., Gray, D.H., Jones, T., Hallgren, J., Kuo, F.C., Chaletzky, B., Gurish, M., Mathis, D., Benoist, C. & Lee, D.M., 2008. Genetic inversion in mast cell-deficient (Wsh) mice interrupts corin and manifests as hematopoietic and cardiac aberrancy. *Am J Pathol,* 173**,** 1693-701.

Noordegraaf, M., Flacher, V., Stoitzner, P. & Clausen, B.E., 2010. Functional redundancy of Langerhans cells and Langerin+ dermal dendritic cells in contact hypersensitivity. *J Invest Dermatol,* 130**,** 2752-9.

Norman, M.U., Hwang, J., Hulliger, S., Bonder, C.S., Yamanouchi, J., Santamaria, P. & Kubes, P., 2008. Mast cells regulate the magnitude and the cytokine microenvironment of the contact hypersensitivity response. *Am J Pathol,* 172**,** 1638-49.

Nosbaum, A., Vocanson, M., Rozieres, A., Hennino, A. & Nicolas, J.F., 2009. Allergic and irritant contact dermatitis. *Eur J Dermatol,* 19**,** 325-32.

Oka, T., Kalesnikoff, J., Starkl, P., Tsai, M. & Galli, S.J., 2012. Evidence questioning cromolyn's effectiveness and selectivity as a 'mast cell stabilizer' in mice. *Lab Invest,* 92**,** 1472-82.

Okayama, Y., 2005. Mast cell-derived cytokine expression induced via Fc receptors and Toll-like receptors. *Chem Immunol Allergy,* 87**,** 101-10.

Okazaki, F., Kanzaki, H., Fujii, K., Arata, J., Akiba, H., Tsujii, K. & Iwatsuki, K., 2002. Initial recruitment of interferon-gamma-producing CD8+ effector cells, followed

by infiltration of CD4+ cells in 2,4,6-trinitro-1-chlorobenzene (TNCB)-induced murine contact hypersensitivity reactions. *J Dermatol,* 29**,** 699-708.

Ord, T., Ord, D., Kuuse, S. & Plaas, M., 2012. Trib3 is regulated by IL-3 and affects bone marrow-derived mast cell survival and function. *Cell Immunol,* 280**,** 68-75.

Otsuka, A., Kubo, M., Honda, T., Egawa, G., Nakajima, S., Tanizaki, H., Kim, B., Matsuoka, S., Watanabe, T., Nakae, S., Miyachi, Y. & Kabashima, K., 2011. Requirement of interaction between mast cells and skin dendritic cells to establish contact hypersensitivity. *PLoS One,* 6**,** e25538.

Palmiter, R., 2001. Interrogation by toxin. *Nat Biotechnol,* 19**,** 731-2.

Peine, M., Rausch, S., Helmstetter, C., Fröhlich, A., Hegazy, A.N., Kühl, A.A., Grevelding, C.G., Höfer, T., Hartmann, S. & Löhning, M., 2013. Stable T-bet(+)GATA-3(+) Th1/Th2 hybrid cells arise in vivo, can develop directly from naive precursors, and limit immunopathologic inflammation. *PLoS Biol,* 11**,** e1001633.

Peiser, M., 2013. Role of Th17 cells in skin inflammation of allergic contact dermatitis. *Clin Dev Immunol,* 2013**,** 261037.

Peiser, M., Tralau, T., Heidler, J., Api, A.M., Arts, J.H., Basketter, D.A., English, J., Diepgen, T.L., Fuhlbrigge, R.C., Gaspari, A.A., Johansen, J.D., Karlberg, A.T., Kimber, I., Lepoittevin, J.P., Liebsch, M., Maibach, H.I., Martin, S.F., Merk, H.F., Platzek, T., Rustemeyer, T., Schnuch, A., Vandebriel, R.J., White, I.R. & Luch, A., 2012. Allergic contact dermatitis: epidemiology, molecular mechanisms, in vitro methods and regulatory aspects. Current knowledge assembled at an international workshop at BfR, Germany. *Cell Mol Life Sci,* 69**,** 763-81.

Pejler, G., Abrink, M., Ringvall, M. & Wernersson, S., 2007. Mast cell proteases. *Adv Immunol,* 95**,** 167-255.

Pichler WJ,. 2004. Immune mechanism of drug hypersensitivity. *Immunol Allergy Clin North Am.* 24(3):373-97, v-vi.

Piliponsky AM., Chen CC., Rios EJ., Treuting PM., Lahiri A., Abrink M., Pejler G., Tsai M., Galli SJ., 2012. The chymase mouse mast cell protease 4 degrades TNF, limits inflammation, and promotes survival in a model of sepsis. *Am J Pathol.* 181(3):875-86.

Rana, S., Byrne SN., MacDonald LJ., Chan CY., Halliday GM., 2008. Ultraviolet B suppresses immunity by inhibiting effector and memory T cells. *Am J Pathol.*;172(4):993-1004.

Rana S., Rogers LJ., Halliday GM., 2009. Immunosuppressive ultraviolet-A radiation inhibits the development of skin memory CD8 T cells. *Photochem Photobiol Sci.* 9(1):25-30.

Rana S., Rogers LJ., Halliday GM., 2011. Systemic low-dose UVB inhibits CD8 T cells and skin inflammation by alternative and novel mechanisms. *Am J Pathol.* 178(6):2783-91.

Ratner, P.H., Ehrlich, P.M., Fineman, S.M., Meltzer, E.O. & Skoner, D.P., 2002. Use of intranasal cromolyn sodium for allergic rhinitis. *Mayo Clin Proc,* 77**,** 350-4.

Razin, E., Cordon-Cardo, C. & Good, R.A., 1981. Growth of a pure population of mouse mast cells in vitro with conditioned medium derived from concanavalin A-stimulated splenocytes. *Proc Natl Acad Sci U S A,* 78**,** 2559-61.

Reber, L., Da Silva, C.A. & Frossard, N., 2006. Stem cell factor and its receptor c-Kit as targets for inflammatory diseases. *Eur J Pharmacol,* 533**,** 327-40.

Reber LL., Marichal T., Galli SJ., 2012. New models for analyzing mast cell functions in vivo. *Trends Immunol.* 33(12):613-25.

Reber, LL., Marichal, T., Mukai, K., Kita, Y., Tokuoka, S.M., Roers, A., Hartmann, K., Karasuyama, H., Nadeau, K.C., Tsai, M. & Galli, S.J., 2013. Selective ablation

of mast cells or basophils reduces peanut-induced anaphylaxis in mice. *J Allergy Clin Immunol,* 132**,** 881-8.e1-11.

Ring, S., Enk, A.H. & Mahnke, K., 2011. Regulatory T cells from IL-10-deficient mice fail to suppress contact hypersensitivity reactions due to lack of adenosine production. *J Invest Dermatol,* 131**,** 1494-502.

Romani, N., Clausen, B.E. & Stoitzner, P., 2010. Langerhans cells and more: langerin-expressing dendritic cell subsets in the skin. *Immunol Rev,* 234**,** 120-41.

Rothenberg, M.E., 2010. Innate sensing of nickel. *Nat Immunol,* 11**,** 781-2.

Rustemeyer T., van Hoogstraten IMW., von Blomberg BM., Scheper RJ., 2006. Mechanisms in Allergic Contact Dermatitis. In: Frosch PJ, Menné T, Lepoittevin J-P, editors. Contact Dermatitis. *Springer; p. 11-43.*

Ruoss, S.J., Gold, W.M. & Caughey, G.H., 1991. Mast cell exocytosis: evidence that granule proteoglycan processing is not coupled to degranulation. *Biochem Biophys Res Commun,* 179**,** 140-6.

Saint-Mezard, P., Berard, F., Dubois, B., Kaiserlian, D. & Nicolas, J.F., 2004. The role of CD4+ and CD8+ T cells in contact hypersensitivity and allergic contact dermatitis. *Eur J Dermatol,* 14**,** 131-8.

Saito K, Nukada Y, Takenouchi O, Miyazawa M, Sakaguchi H, Nishiyama N., 2013. Development of a new in vitro skin sensitization assay (Epidermal Sensitization Assay; EpiSensA) using reconstructed human epidermis. *Toxicol In Vitro.* 2213-24.

Sandig, H. & Bulfone-Paus, S., 2012. TLR signaling in mast cells: common and unique features. *Front Immunol,* 3**,** 185.

Santone, D.J., Shahani, R., Rubin, B.B., Romaschin, A.D. & Lindsay, T.F., 2008. Mast cell stabilization improves cardiac contractile function following

hemorrhagic shock and resuscitation. *Am J Physiol Heart Circ Physiol,* 294**,** H2456-64.

Sawaguchi, M., Tanaka, S., Nakatani, Y., Harada, Y., Mukai, K., Matsunaga, Y., Ishiwata, K., Oboki, K., Kambayashi, T., Watanabe, N., Karasuyama, H., Nakae, S., Inoue, H. & Kubo, M., 2012. Role of mast cells and basophils in IgE responses and in allergic airway hyperresponsiveness. *J Immunol,* 188**,** 1809-18.

Schnuch, A., Szliska, C., Uter, W. & Ivdk, 2009. [Facial allergic contact dermatitis. Data from the IVDK and review of literature]. *Hautarzt,* 60**,** 13-21.

Scholten, J., Hartmann, K., Gerbaulet, A., Krieg, T., Müller, W., Testa, G. & Roers, A., 2008. Mast cell-specific Cre/loxP-mediated recombination in vivo. *Transgenic Res,* 17**,** 307-15.

Seier, A.M., Renkl, A.C., Schulz, G., Uebele, T., Sindrilaru, A., Iben, S., Liaw, L., Kon, S., Uede, T. & Weiss, J.M., 2010. Antigen-specific induction of osteopontin contributes to the chronification of allergic contact dermatitis. *Am J Pathol,* 176**,** 246-58.

Shin, H. & Iwasaki, A., 2013. Tissue-resident memory T cells. *Immunol Rev,* 255**,** 165-81.

Skotnicki-Grant, 2008. *Allergic contact dermatitis versus irritant contact dermatitis.*

Smith, L., 2011. Good planning and serendipity: exploiting the Cre/Lox system in the testis. *Reproduction,* 141**,** 151-61.

Sterry W., Bruhn S., Künne N., Lichtenberg B., Weber-Matthiesen K., Brasch J., Mielke V., 1990. Dominance of memory over naive T cells in contact dermatitis is due to differential tissue immigration. *Br J Dermatol.* 123(1):59-64.

St John, A.L., Chan, C.Y., Staats, H.F., Leong, K.W. & Abraham, S.N., 2012. Synthetic mast-cell granules as adjuvants to promote and polarize immunity in lymph nodes. *Nat Mater,* 11**,** 250-7.

Suto, H., Nakae, S., Kakurai, M., Sedgwick, J.D., Tsai, M. & Galli, S.J., 2006. Mast cell-associated TNF promotes dendritic cell migration. *J Immunol,* 176**,** 4102-12.

Takeshita, K., Sakai, K., Bacon, K.B. & Gantner, F., 2003. Critical role of histamine H4 receptor in leukotriene B4 production and mast cell-dependent neutrophil recruitment induced by zymosan in vivo. *J Pharmacol Exp Ther,* 307**,** 1072-8.

Tan CH., Rasool S., Johnston GA., 2014. Contact dermatitis: allergic and irritant. *Clin Dermatol.* 32(1):116-24.

Theoharides, T.C., Alysandratos, K.D., Angelidou, A., Delivanis, D.A., Sismanopoulos, N., Zhang, B., Asadi, S., Vasiadi, M., Weng, Z., Miniati, A. & Kalogeromitros, D., 2012. Mast cells and inflammation. *Biochim Biophys Acta,* 1822**,** 21-33.

Thierse, H.J., Gamerdinger, K., Junkes, C., Guerreiro, N. & Weltzien, H.U., 2005. T cell receptor (TCR) interaction with haptens: metal ions as non-classical haptens. *Toxicology,* 209**,** 101-7.

Tončić RJ., Lipozenčić J., Martinac I., Gregurić S., 2011. Immunology of allergic contact dermatitis. *Acta Dermatovenerol Croat.*19(1):51-68.

Toru, H., Eguchi, M., Matsumoto, R., Yanagida, M., Yata, J. & Nakahata, T., 1998. Interleukin-4 promotes the development of tryptase and chymase double-positive human mast cells accompanied by cell maturation. *Blood,* 91**,** 187-95.

Tuckermann JP., Kleiman A., Moriggl R., Spanbroek R., Neumann A., Illing A., Clausen BE., Stride B., Förster I., Habenicht AJ., Reichardt HM., Tronche F., Schmid W., Schütz G., 2007. Macrophages and neutrophils are the targets for

immune suppression by glucocorticoids in contact allergy. *J Clin Invest.* 117(5):1381-90.

Tutrone WD., Spann CT., Scheinfeld N., Deleo VA. 2003. Polymorphic light eruption. *Dermatol Ther.* 16(1):28-39.

Ulrich, P., Grenet, O., Bluemel, J., Vohr, H.W., Wiemann, C., Grundler, O. & Suter, W., 2001. Cytokine expression profiles during murine contact allergy: T helper 2 cytokines are expressed irrespective of the type of contact allergen. *Arch Toxicol,* 75**,** 470-9.

Urb, M. & Sheppard, D.C., 2012. The role of mast cells in the defence against pathogens. *PLoS Pathog,* 8**,** e1002619.

Van Loveren, H. & Askenase, P.W., 1984. Delayed-type hypersensitivity is mediated by a sequence of two different T cell activities. *J Immunol,* 133**,** 2397-401.

Valyi-Nagy T., Olson SJ., Valyi-Nagy K., Montine TJ., Dermody TS. 2000. Herpes simplex virus type 1 latency in the murine nervous system is associated with oxidative damage to neurons. *Virology.* 278(2):309-21.

Varadaradjalou, S., Féger, F., Thieblemont, N., Hamouda, N.B., Pleau, J.M., Dy, M. & Arock, M., 2003. Toll-like receptor 2 (TLR2) and TLR4 differentially activate human mast cells. *Eur J Immunol,* 33**,** 899-906.

Verjans, G.M., Hintzen, R.Q., Van Dun, J.M., Poot, A., Milikan, J.C., Laman, J.D., Langerak, A.W., Kinchington, P.R. & Osterhaus, A.D., 2007. Selective retention of herpes simplex virus-specific T cells in latently infected human trigeminal ganglia. *Proc Natl Acad Sci U S A,* 104**,** 3496-501.

Vincent, L., Vang, D., Nguyen, J., Gupta, M., Luk, K., Ericson, M.E., Simone, D.A. & Gupta, K., 2013. Mast cell activation contributes to sickle cell pathobiology and pain in mice. *Blood,* 122**,** 1853-62.

Wakim, L.M., Woodward-Davis, A. & Bevan, M.J., 2010. Memory T cells persisting within the brain after local infection show functional adaptations to their tissue of residence. *Proc Natl Acad Sci U S A,* 107**,** 17872-9.

Wang, B., Fujisawa, H., Zhuang, L., Freed, I., Howell, B.G., Shahid, S., Shivji, G.M., Mak, T.W. & Sauder, D.N., 2000. CD4+ Th1 and CD8+ type 1 cytotoxic T cells both play a crucial role in the full development of contact hypersensitivity. *J Immunol,* 165**,** 6783-90.

Wang, H.W., Tedla, N., Lloyd, A.R., Wakefield, D. & Mcneil, P.H., 1998. Mast cell activation and migration to lymph nodes during induction of an immune response in mice. *J Clin Invest,* 102**,** 1617-26.

Wang, Y. & Thorlacius, H., 2005. Mast cell-derived tumour necrosis factor-alpha mediates macrophage inflammatory protein-2-induced recruitment of neutrophils in mice. *Br J Pharmacol,* 145**,** 1062-8.

Waskow, C., Bartels, S., Schlenner, S.M., Costa, C. & Rodewald, H.R., 2007. Kit is essential for PMA-inflammation-induced mast-cell accumulation in the skin. *Blood,* 109**,** 5363-70.

Watanabe, H., Unger, M., Tuvel, B., Wang, B. & Sauder, D.N., 2002. Contact hypersensitivity: the mechanism of immune responses and T cell balance. *J Interferon Cytokine Res,* 22**,** 407-12.

Wong DJ., Chang HY., 2008-2009. Skin tissue engineering. *StemBook [Internet].*

Wolverton W., Gada S., 2013. Systemic contact dermatitis to ethanol. *J Allergy Clin Immunol Pract.*1(2):195-6.

Wu, K.N., Emmons, R.V., Lisanti, M.P., Farber, J.L. & Witkiewicz, A.K., 2009. Foxp3-expressing T regulatory cells and mast cells in acute graft-versus-host disease of the skin. *Cell Cycle,* 8**,** 3593-7.

Xu, H., Diiulio, N.A. & Fairchild, R.L., 1996. T cell populations primed by hapten sensitization in contact sensitivity are distinguished by polarized patterns of cytokine production: interferon gamma-producing (Tc1) effector CD8+ T cells and interleukin (II) 4/Il-10-producing (Th2) negative regulatory CD4+ T cells. *J Exp Med,* 183**,** 1001-12.

Xu, Z.X., Yang, Y.Z., Feng, D.M., Wang, S., Tang, Y.L., He, F., Xia, Y. & Li, F., 2008. Oxidized high-density lipoprotein promotes maturation and migration of bone marrow derived dendritic cells from C57BL/6J mice. *Chin Med Sci J,* 23**,** 224-9.

Yagi, R., Tanaka, S., Motomura, Y. & Kubo, M., 2007. Regulation of the Il4 gene is independently controlled by proximal and distal 3' enhancers in mast cells and basophils. *Mol Cell Biol,* 27**,** 8087-97.

Yang, M.Q., Ma, Y.Y., Tao, S.F., Ding, J., Rao, L.H., Jiang, H. & Li, J.Y., 2014. Mast cell degranulation promotes ischemia-reperfusion injury in rat liver. *J Surg Res,* 186**,** 170-8.

Yawalkar, N., Hunger, R.E., Buri, C., Schmid, S., Egli, F., Brand, C.U., Mueller, C., Pichler, W.J. & Braathen, L.R., 2001. A comparative study of the expression of cytotoxic proteins in allergic contact dermatitis and psoriasis: spongiotic skin lesions in allergic contact dermatitis are highly infiltrated by T cells expressing perforin and granzyme B. *Am J Pathol,* 158**,** 803-8.

Yokozeki, H., Watanabe, K., Igawa, K., Miyazaki, Y., Katayama, I. & Nishioka, K., 2001. Gammadelta T cells assist alphabeta T cells in the adoptive transfer of contact hypersensitivity to para-phenylenediamine. *Clin Exp Immunol,* 125**,** 351-9.

Yokozeki, H., Wu, M.H., Sumi, K., Igawa, K., Miyazaki, Y., Katayama, I., Takeda, K., Akira, S. & Nishioka, K., 2003. Th2 cytokines, IgE and mast cells play a crucial role in the induction of para-phenylenediamine-induced contact hypersensitivity in mice. *Clin Exp Immunol,* 132**,** 385-92.

Ziegler, S.F. & Artis, D., 2010. Sensing the outside world: TSLP regulates barrier immunity. *Nat Immunol,* 11**,** 289-9

8 Abbreviations and important definitions

Abbreviations and explanations of relevant terms are provided below (Table 12).

Table 12. List of abbreviations and relevant terms

Abbreviations and terms	Description
ACD	Allergic contact dermatitis. It is a chronic inflammatory skin disease.
$\alpha\beta$T cells	Also called conventional T cells. Represent the majority of T cells in the draining lymph nodes. Are functionally different than NKT cells or $\gamma\delta$T cells.
$\alpha_E\beta7$	Integrin class, involved in tissue migration and attachment. It is composed of the CD103 sub unit and the betha-7 subunit.
AUC	Area under the curve. It is a mathematical method that calculates the area under a curve of responses occurred over-time. Here, it is used to perform statistical comparisons of inflammatory responses displayed after haptens challenge.
Avidin-TR staining	Chemical staining of the granular content of mast cells and basophils
Bio	Biotin. A protein used for histologic staining. It binds strongly to Avidin.
BMCMC	Bone marrow derived culture mast cells. Mast cells obtained after weeks of culture the bone marrow cells in presence of IL-3 (mouse) or IL4 (in humans).
BSA	Bovine serum albumin. High molecular weight protein used as blocking reagent during histology or to supplement buffers for culture cells.
c-Kit	c-Kit is the gene responsible for the production of CD117 (KIT), which is the natural receptor for SCF, The most important growth factor for mast cells.
CCHS	Chronic contact hypersensitivity. Experimental murine model to induce sensitization to haptens by chronic hapten applications, and leading time intervals for recovering between episodes of hapten contact.
CCL	Family of chemokines
CD	Cluster differentiation complex. Is a system to organize proteins that has been recognized by specific antibodies, e.g. CD103, CD4, Etc..
CHS	Contact hypersensitivity. Experimental murine model to induce sensitization to haptens by a single hapten challenge.
Cpa3	Carboxypeptidase 3
Cre	Also called Cre recombinase. Protein that recognize the LoxP sequence in the genome and cuts the genomic region surrounded by LoxP sequences.
CTMC	Connective tissue type mast cells
CXC	Family of chemokines
CXCL	CXC ligands

DAPI staining	Nuclear stain
DC	Dendritic cell/s
dDC	dermal dendritic cells
dLN	draining lymph nodes
DNFB	1-fluoro-2,4-dinitrobenzene
DT	Diphtheria toxin
DTH	Delayed type hypersensitivity. A type of hypersensitivity response characterized by a delayed inflammatory response after contact to the antigen.
DTR	Diphtheria toxin receptor
ELISA	Enzyme-Linked ImmunoSorbent Assay
FACS	Fluorescence-activated cell sorting
Fc-Block	A mixture of FcgRI and FcgRII used to block unspecific binding in FACS and immunohistochemistry
FceR1	Fc epsilon receptor 1. It is expressed in mast cells and basophils and binds the IgE by the Fc part.
FCS	Fetal calf serum. Supplement for culture eukaryote cells.
FGF	Fibroblast growth factor
FI	Fluorescence intensity.
FITC	Fluorescein isothiocyanate is a fluorochrome used for FACS and histology. FITC isomer I is also a hapten and induces CHS responses if applied topically in the skin.
FSC	Forward scatter. It is a FACS parameter that indicates the size of the cell or particle analyzed.
i.d.	Intradermal
i.p.	Intraperitoneal
ICAM-1	Adhesion molecule involved in tissue recruitment and attachment
IFNγ	Interferon gamma. It is a cytotoxic cytokine, highly produced by Th1 cells, Tc1 cells and macrophages. In this study, it is used as marker of active inflammation.
IgE	Immunoglobuline E. It is the principal immunoglobuline mediated allergic responses in mammals. It binds the FceR in Mast cells and basophils.
IL	Interleukin. It is a family of proteins that are known to be secreted by immune cells and other cells and have effects in cells expressing its receptor.
Inflammasome	It is a complex of proteins assembled upon inflammatory stimulation. The activation of the inflammasome involves the production of Alarmins, e.g. IL-1β and IL-33.
iNK	Invariable NK T cells
Kit^{w}/Kit^{w-v}	Kit-dependent mast cell-deficient mouse strain
LaGeSo	Landesamtes für Gesundheit und Soziales Berlin
LC	Langerhans cells
LL37	Antibacterial peptide
LN	Lymph nodes
Lox-P	Nucleotide sequence that is recognize by Cre

LPS	Lipopolysaccharide
LTB	Leukotriene B
LTC	Leukotriene C
Ly5.1 strain	Genetically modified mice that express the CD45.2 isoform. Normal C57BL/6 mice that expresses the CD45.1 isoform.
Mas-TRECK	Mast cell-deficient mouse strain
MC	Mast cell/s
Mcl-1	Myeloid leukemia cell differentiation protein. Antitumor protein. It is important for the development of mast cells.
MCP	Mast cell protease
MCPT5	Mast cell protease 5
Mcpt5-Cre x R-DTA	Cre-dependent mast cell-deficient mouse strain
MDSC	Myeloid derived suppressor cells
MHC	Mayor histocompatibility complex
MMC	Mucosal mast cells
mMCP	murine mast cell protease
NF-kB	Transcription factor
NiSO4	Nickel sulfate
OXA	Oxazolone
PBS	Phosphate Buffer Saline
PFA	Paraformaldehyde
PGD	Prostaglandin D
PGE	Prostaglandin E
Ras	Metabolic pathway and transcription factor
RIPA buffer	Radio-Immunoprecipitation Assay buffer. Digestion buffer
ROS	Reactive oxigen species
RPM	Round per minute
Sash *or* Kit^{W-sh}/Kit^{W-sh}	Mast cell-deficient mouse strain
SCF	Stem cell factor
SD	Standard deviation
Selectins	Adhesion molecules
SEM	Standard error of the mean
SSC	Side scatter. It is a FACS parameter that indicates the granularity of complexity of the cell or particle analyzed.
Strept	Streptavidin. It is a protein used in histology and FACS. It binds strongly to Biotin.
TBS	Tris-buffered saline. Buffer used here to do histology
Tc	T cytotoxic cell types. It is a variation of CD8+ T cells that can produce type 1 (Tc1) or type 2 (Tc2) cytokines
TCRβ	T cell receptor beta subunit
TGFβ	Tissue growth factor beta
Th (t helper)	T helper cell types. It is a variation of CD4+ T cells that can produce type 1 (Tc1) or type 2 (Tc2) cytokines
TLR	Toll-like receptor
TNCB	Trinitrochlorobenzene
TNFα	Tumor necrosis factor alpha

TRECK	Toxin Receptor-mediated Conditional cell Knock out
Treg	T regulatory cells
TRM	Tissue resident memory. It is a new subset of memory T cells, characterized by hosting organs such as the skin and gut, and resides there for long periods of time, expressing the CD103 molecule.
TSLP	Thymic stromal lymphopoietin. It is a pro-inflammatory cytokine. It acts by enhancing the antigen presenting capacities of T cells.
VEGF	Vascular endothelial growth factor
Vehi	Vehicle. In this study two vehicles were used. Acetone, as vehicle for OXA, Saline as a vehicle for cromolyn.
VIP	Vasoactive intestinal peptide
Z-stack	It is a type of tridimensional representation, generated by the assembly of dimensional pictures that were taken in different levels of the Z-axis.

CURRICULUM VITAE:

For reasons of data protection, the curriculum vitae is not published in the electronic version

CURRICULUM VITAE:

For reasons of data protection, the curriculum vitae is not published in the electronic version

LIST PUBLICATIONS:

1. Basophils and Mast Cells: Methods and Protocols. Mast cell mediated reactions *in vivo*. **Vladimir Andrey Giménez Rivera**, Martin Metz, Frank Siebenhaar. Springer ISBN 978-1-4939-1178-8 31 August 2014.

2. Association screening in the epidermal differentiation complex (EDC) identifies an SPRR3 repeat number variant as a risk factor for eczema. Ingo Marenholz*, **Vladimir Andrey Gimenez-Rivera***, Anja Bauerfeind, Jorge Esparza-Gordillo, (7 authors more). ** These authors contributed equally to this work.* J Invest Dermatol. Aprl 2011.

3. Nerve Growth Factor Partially Recovers Inflamed Skin from Stress-Induced Worsening in Allergic Inflammation. Peters EM, Liezmann C, Spatz K, Daniltchenko M, Joachim R, **Gimenez-Rivera A**, (5 authors more). J Invest Dermatol. Nov 2010.